Dissertation

Impact of gait patterns, bony morphology, and derotation osteotomy on knee joint loads in patients with patellofemoral instability

submitted by

Bernhard Guggenberger, BSc MSc

for the Academic Degree of

Doctor of Medical Sciences

(Dr. scient. med.)

at the

Medical University of Graz

Department of Orthopaedics and Trauma

Section Paediatric Orthopaedics

Under the Supervision of

Priv.-Doz. Dr. med. Martin Svehlik, PhD

2025

Statutory Declaration

I hereby declare that this thesis is my own original work and that I have fully acknowledged by name all of those individuals and organizations that have contributed to the research for this thesis. Due acknowledgement has been made in the text to all other material used. Throughout this thesis and in all related publications I followed the “Guidelines of the Medical University of Graz on Good Scientific Practice“.

04.02.2025, Graz

Disclosures

Parts of this thesis have been published in:

> (1) Guggenberger B, Horsak B, Habersack A, Kruse A, Smith CR, Kainz H, et al. Patient-specific gait pattern in individuals with patellofemoral instability reduces knee joint loads. Sci Rep. 2024 Nov 18;14(1):28520.
> doi: 10.1038/s41598-024-79021-x

Furthermore, parts of this thesis are under revision or prepared for submission:

Under revision at Wiley Journal of Orthopaedic Research:

> Guggenberger B, Koller W, Habersack A, Kraus T, Sperl M, Svehlik M, Kainz H. Impact of femoral and tibial torsion on patellofemoral loading in individuals with patellofemoral instability.

In preparation for submission:

> Guggenberger B, Kainz H, Kraus T, Svehlik M. Femoral derotation osteotomy medially shifts patellofemoral loading in individuals with patellofemoral instability: insights from a simulation-based study.

The following co-authors have contributed to the original research presented as part of this thesis:

> Andreas Habersack, Medical University of Graz, Department of Orthopaedics and Trauma; University of Graz, Institute of Human Movement Science, Sport and Health
>
> Brian Horsak, St. Pölten University of Applied Sciences, Center for Digital Health and Social Innovation
>
> Hans Kainz, University of Vienna, Neuromechanics Research Group, Department of Biomechanics, Kinesiology and Computer Science in Sport, Centre for Sport Science and University Sports

Tanja Kraus, Medical University of Graz, Department of Orthopaedics and Trauma

Annika Kruse, University of Graz, Institute of human movement sciences, sport and health

Willi Koller, University of Vienna, Neuromechanics Research Group, Department of Biomechanics, Kinesiology and Computer Science in Sport, Centre for Sport Science and University Sports

Colin R. Smith, Steadman Philippon Research Institute, Department of Biomedical Engineering

Matthias Sperl, Medical University of Graz, Department of Orthopaedics and Trauma

Martin Svehlik, Medical University of Graz, Department of Orthopaedics and Trauma

All co-authors explicitly agreed to the use and reproduction of the published und non-published data, text excerpts, figures and tables. Written statements are submitted together with the thesis.

During the preparation of this thesis “ChatGPT 4” and “DeepL Write” were used in order to improve grammar, readability and writing style of the texts.

Acknowledgements

As a doctoral student, I was financially supported by the Medical University of Graz throughout the doctoral school “Musculoskeletal System & Oral Health” and the Department of Orthopaedics and Trauma.

Additionally, I want to thank everyone who supported me in the process of completing this dissertation.

I want to thank my main supervisor, Priv.-Doz. Dr. med. Martin Svehlik and supervisor Assoc.-Prof. Priv.-Doz. Mag. Hans Kainz, MSc PhD for their extensive support throughout my whole academic journey. I want to thank my co-supervisor FH-Prof. Priv.-Doz. Dr. Brian Horsak, who supported me intensively, especially in getting familiar with modelling, simulations and the COMAK routine. Further, I want to thank Ass.-Prof. Priv.-Doz. Dr. med. Tanja and Univ.-Prof. Dr. Markus Tilp for their consistent support. Thanks to my colleagues Andreas Habersack and Willi Koller, for their support in many questions.

The last years were intensive, and the doctoral study took a great amount of time. I want to thank my family and especially my wife Judith Guggenberger for their support. Your understanding and support helped me a lot to finish my studies.

Table of Contents

Abbreviations

A-P	anterior-posterior
BW	body weight
CDI	Caton-Deschamps index
COMAK	Concurrent Optimization of Muscle Activation and Kinematics
FDO	Femoral derotation osteotomy
GRF	ground reaction force
M-L	medio-lateral
Max	maximum
MR	Magnetic resonance
MSK	musculoskeletal
N/BW	Newton/body weight
PF	patellofemoral
PFI	patellofemoral instability
RMS	root mean square
SD	standard deviation
vert	vertical

List of Figures

List of Tables

Zusammenfassung

Die Patella ist von zentraler Bedeutung für die Kraftübertragung der Kniegelenksextensoren. Eine bestmögliche Funktion setzt eine präzise Positionierung innerhalb der Trochlea voraus, wobei die Stabilität der Patella durch eine Kombination aus ligamentären Strukturen, knöchernen Elementen und neuromuskulären Faktoren sichergestellt wird. Instabilitäten in diesem System können, besonders bei jungen, aktiven Personen, zu Luxationen und funktionellen Beeinträchtigungen führen. Die komplexe Ätiologie erschwert dabei die in-vivo Analyse gelenksstabilisierender Faktoren. Fortschritte in computergestützter Modellierung haben die Untersuchung dieser Faktoren mittels muskuloskelettaler Simulationen erleichtert. Obwohl die Auswirkungen verschiedener morphologischer Parameter auf die Stabilität des patellofemoralen Gelenks bereits erforscht wurden, bleibt der Einfluss eines veränderten Gangmusters und anderer morphologischer Faktoren, wie der Torsion der unteren Extremität, weitgehend ungeklärt. Ziel dieser Dissertation ist es, diese Forschungslücken zu schließen. Hierzu wurden drei Studien durchgeführt, die sich mit den Auswirkungen von (i) Gangmustern, (ii) Torsionen der unteren Extremität und (iii) femoralen Derotationsosteotomien auf die Belastung des patellofemoralen Gelenks auseinandersetzten.

Die erste Studie widmete sich der Untersuchung der Auswirkungen patientenspezifischer Gangmuster auf die Gelenkbelastung bei Personen mit einer patellofemoralen Instabilität. Zu diesem Zweck wurden muskuloskelettale Simulationen basierend auf 3D Ganganalysedaten von 21 Personen mit patellofemoraler Instabilität und 17 Kontrollpersonen mittels eines Modells mit 12 Freiheitsgraden im Kniegelenk durchgeführt. Die Ergebnisse zeigten, dass die Gruppe mit patellofemoraler Instabilität trotz gleicher Ganggeschwindigkeit mit reduzierter Knieflexion ging, was zu reduzierten Beuge- und Abduktionsmomenten im Vergleich zur Kontrollgruppe führte. Dieses veränderte Gangmuster erforderte eine geringere Kraft des Quadrizeps, was wiederum zu geringeren Gelenkskräften im tibiofemoralen und patellofemoralen Gelenk führte.

Die zweite Studie widmete sich dem Einfluss der knöchernen Torsionen der unteren Extremität auf die Belastung des patellofemoralen Gelenks. Zu diesem Zweck wurden, basierend auf den Daten von 40 Personen mit patellofemoraler Instabilität, muskuloskelettale Simulationen durchgeführt. Für alle Probandinnen und Probanden wurden drei Modelle erstellt: ein Modell mit generischer Femurversion und Tibiatorsion, ein Modell mit personalisierter Femurversion und Tibiatorsion und ein Modell mit personalisierter Femurversion. Die Analyse ergab eine signifikante Korrelation zwischen Tibiatorsion und den medio-lateralen patellofemoralen Kräften, während die Femurversion keine signifikante Korrelation zu diesen Kräften aufwies. Bei Vernachlässigung der individuellen Tibiatorsion, wie üblicherweise in Studien praktiziert,

zeigte die Femurversion jedoch eine moderate Korrelation mit lateralisierenden Patellakräften. Dies unterstreicht die Relevanz Tibiatorsion und Femurversion gemeinsam zu evaluieren.
In der dritten Studie wurden die Auswirkungen der femoralen Derotationsosteotomie auf die patellofemorale Stabilität und Belastung analysiert. Zu diesem Zweck wurden retrospektive Ganganalyse- und Magnetresonanzdaten Daten von 16 Personen mit patellofemoraler Instabilität und einer Femurversion größer 30 Grad verwendet, um muskuloskelettale Simulationen durchzuführen. Für jede Person wurden zwei Modelle vorbereitet: eines mit der präoperativen Femurversion und Tibiatorsion und ein weiteres, das postoperative Bedingungen mit einer angepassten Femurversion auf 12 Grad simulierte. Die Ergebnisse der Studie zeigten, dass die Derotationsosteotomie bei 14 der 16 Personen zu einer Medialisierung der patellofemoralen Kräfte führte, was potenziell die patellofemorale Stabilität erhöht. In zwei Fällen konnte keine Verbesserung festgestellt werden, was auf deren spezifische Gangmuster zurückgeführt wurde, die eine dynamische Belastung der Patella vermieden.
Zusammenfassend erweitern die Ergebnisse dieser Arbeit unser Verständnis patellofemoraler Instabilität, indem sie die Bedeutung personenspezifischer Faktoren wie Gangmuster und Torsion der unteren Extremitäten hervorheben. Es konnte gezeigt werden, dass eine umfassende biomechanische Analyse, die sowohl statische morphologische Faktoren als auch dynamische Aspekte der Bewegung umfasst, entscheidend ist, um die Biomechanik des patellofemoralen Gelenks zu beurteilen und wirksame Behandlungsstrategien zu entwickeln. Der Einsatz personalisierter muskuloskelettaler Modellierung stellt einen vielversprechenden Ansatz dar, um die Ursachen patellofemoraler Instabilität besser zu verstehen und Behandlungsergebnisse zu optimieren.

Abstract

The patella plays a critical role in enhancing power transmission within the extensor system of the lower extremity. Best possible functionality necessitates precise alignment of the patella within the trochlear groove. Patellofemoral stability is supported by ligaments, bony structures and neuromuscular factors. Instability in this system can lead to dislocations and impairments, particularly affecting young, active individuals. The complex etiology of patellofemoral instability complicates the in vivo assessment of confounding factors affecting joint stability. Recent advancements in computational models have facilitated the study of these factors through musculoskeletal simulations. Although the impact of several morphological parameters on the stability of the patellofemoral joint has been explored, substantial gaps remain in understanding the specific influences of altered gait patterns and other morphological variations, such as lower limb torsion. This thesis aims to address these gaps. Three studies were conducted to examine the impacts of (i) gait pattern, (ii) lower limb torsion and (iii) femoral derotation osteotomies on patellofemoral joint loading.

The first study addressed the impact of patient-specific gait patterns on joint loading in individuals with patellofemoral instability. Utilizing a model with twelve degrees of freedom in the knee joint, musculoskeletal simulations based on three-dimensional motion capture data from 21 individuals with patellofemoral instability and 17 healthy controls were performed. Findings indicated that the patellofemoral instability group walked with a less flexed knee joint, exhibiting reduced knee flexion and abduction moments compared to the control group despite similar gait velocity. This altered gait pattern required less quadriceps muscle force, which in turn resulted in lower tibiofemoral and patellofemoral joint contact forces.

The second study examined the influence of lower limb torsion on patellofemoral joint loading. Musculoskeletal simulations were conducted using data from 40 individuals with patellofemoral instability. Three models for each participant were created: one with generic lower limb torsion, one with personalized torsion of both the femur and tibia, and one with isolated personalization of femoral version. The analysis revealed that tibial torsion was significantly correlated with differences in medio-lateral patellofemoral forces, whereas the femoral version showed no significant correlation to these forces. However, when individual tibial torsion was neglected, as usually practiced in studies, femoral version exhibited a moderate correlation with lateralizing forces on the patella. This underlines the relevance of evaluating tibial torsion and femoral torsion conjointly.

The third study investigated the effects of femoral derotation osteotomy on patellofemoral stability and loading. Retrospective data from 16 participants with recurrent patellofemoral instability and femoral version higher than 30 degrees, were used to personalize in-silico musculoskeletal models based on gait analysis and magnetic resonance data. Two models

were prepared for each participant: one with the pre-surgery femoral version and tibial torsion, and another simulating post-surgery conditions with an adjusted femoral version to 12 degrees. The results showed that the derotation osteotomy significantly shifted the medio-lateral patellofemoral joint contact force to the medial side in 14 of 16 participants, which potentially leads to increased patellofemoral stability. However, two cases showed no improvement, which was attributed to specific gait patterns that avoided dynamic patella loading.

In conclusion, these studies collectively advance our understanding of patellofemoral instability by highlighting the significance of patient-specific factors such as gait patterns and lower limb torsion. They demonstrated that a comprehensive biomechanical analysis, which includes both static morphological factors and dynamic aspects of movement, is essential for accurately assessing the biomechanical environment of the patellofemoral joint and for devising effective treatment strategies. The use of personalized musculoskeletal modelling is a promising approach to better understand the causes of patellofemoral instability and optimize treatment outcomes.

1 Introduction

The patella plays a crucial role in the extensor system of the lower extremity, enhancing power transmission through an improved lever arm (2,3). Optimal functionality in power transmission requires precise alignment of the patella within the trochlear groove throughout the knee's range of motion. This so-called patellofemoral stability is maintained through a combination of ligaments, bony structures, and neuromuscular factors (4). A deficiency in any of these components can lead to an instability of the patellofemoral joint, characterized by the partial or complete displacement of the patella from the trochlear groove under displacing forces (5). Patella instability and associated dislocations have an incidence ranging from 23 to 69 per 100,000 population (6–8) and predominantly affect young, active females during physical activity (9,10). Symptoms commonly include a sensation of instability and/or anterior knee pain, which can significantly impair function and restrict participation in sports and exercise (11). Prolonged patellofemoral instability may also result in altered gait patterns and recurrent patellar dislocations (6).

The etiology of patellar instability is multifaceted, encompassing factors, such as an insufficiency of medial patellofemoral ligament, lateralized tibial tuberosity, patella alta or baja, trochlear and patellar dysplasia, axial deviation or torsional deformities of the lower extremities (e.g. genu valgum, femoral anteversion, external tibial torsion etc.) as well as vastus medialis insufficiency/dysplasia (5). The relative significance of these variables and their impact on gait patterns remains unclear. Additionally, current methodologies do not permit the in vivo assessment of these factors' effects on the patellofemoral joint, such as altered contact pressures on the patellar cartilage or lateralizing forces on the patella during functional movement, in a non-invasive manner.

Over recent decades, the deployment of computational physics-based models that represent the musculoskeletal system has gained widespread prominence across various domains of clinically oriented research, particularly in studies of the locomotor apparatus (12–14). These musculoskeletal models provide a mathematical representation of the human musculoskeletal system, delineating its segments, joints, and muscles, along with functional aspects such as joint movements, muscle geometry, and force generation capacities (15,16). The application of musculoskeletal modelling and simulation techniques facilitates the analysis of musculoskeletal biomarkers, including muscle and joint contact loads (17,18).

Several simulation-based studies have explored the influence of different morphological factors (19–22) and surgical intervention strategies (23,24) on the loading dynamics within the patellofemoral joint and the patellofemoral stability. Currently, there remain certain morphological factors, such as lower limb alignment, which have not yet been thoroughly investigated in cohorts with patellofemoral instability. Additionally, the majority of these studies

have neglected patient-specific movement patterns, instead relying on gait patterns derived from healthy individuals (19–21,25). Given that individuals with patellofemoral instability often modify their gait as a compensatory strategy (26), such alterations could significantly affect the patellofemoral joint loads. Therefore, this work aims to address these limitations by examining how specific gait patterns and lower limb torsions influence the stability of the patellofemoral joint.

1.1 Knee joint

The knee joint is the largest joint in the human body (27). It is optimized to forces acting upon and through the joint, whereby the complex interaction of bony and ligamentous structures plays an important role (28). While encapsulated within a shared joint capsule, the knee joint can anatomically be separated into two distinct joints: the tibiofemoral and the patellofemoral joint (27). The tibiofemoral joint is classified as a trochoginglymos, which is a type of gliding hinge joint that primarily allows flexion and extension movements (28). In flexion, additionally rotational movements are possible (27). The patellofemoral joint guides the movement of the patella, the largest sesamoid bone in the human body (29). The primary functions of the patella are to enhance the lever arm of the quadriceps muscle and to offer protection to the tibiofemoral joint (4).

1.1.1 Anatomy of the tibiofemoral and patellofemoral joint

The tibiofemoral joint consists of the articulation between the femur and the tibia (Figure 1) (27). The articulating surface of the femur is constituted by the femoral condyles, while the articulating surface of the tibia is formed by the tibial plateau (30). The menisci are critical in compensating for the incongruence of these joint surfaces, thereby augmenting the contact area within the joint (31,32). The stability of the tibiofemoral joint is passively maintained by several ligaments, including the medial and lateral collateral ligaments, as well as the anterior and posterior cruciate ligaments (33).

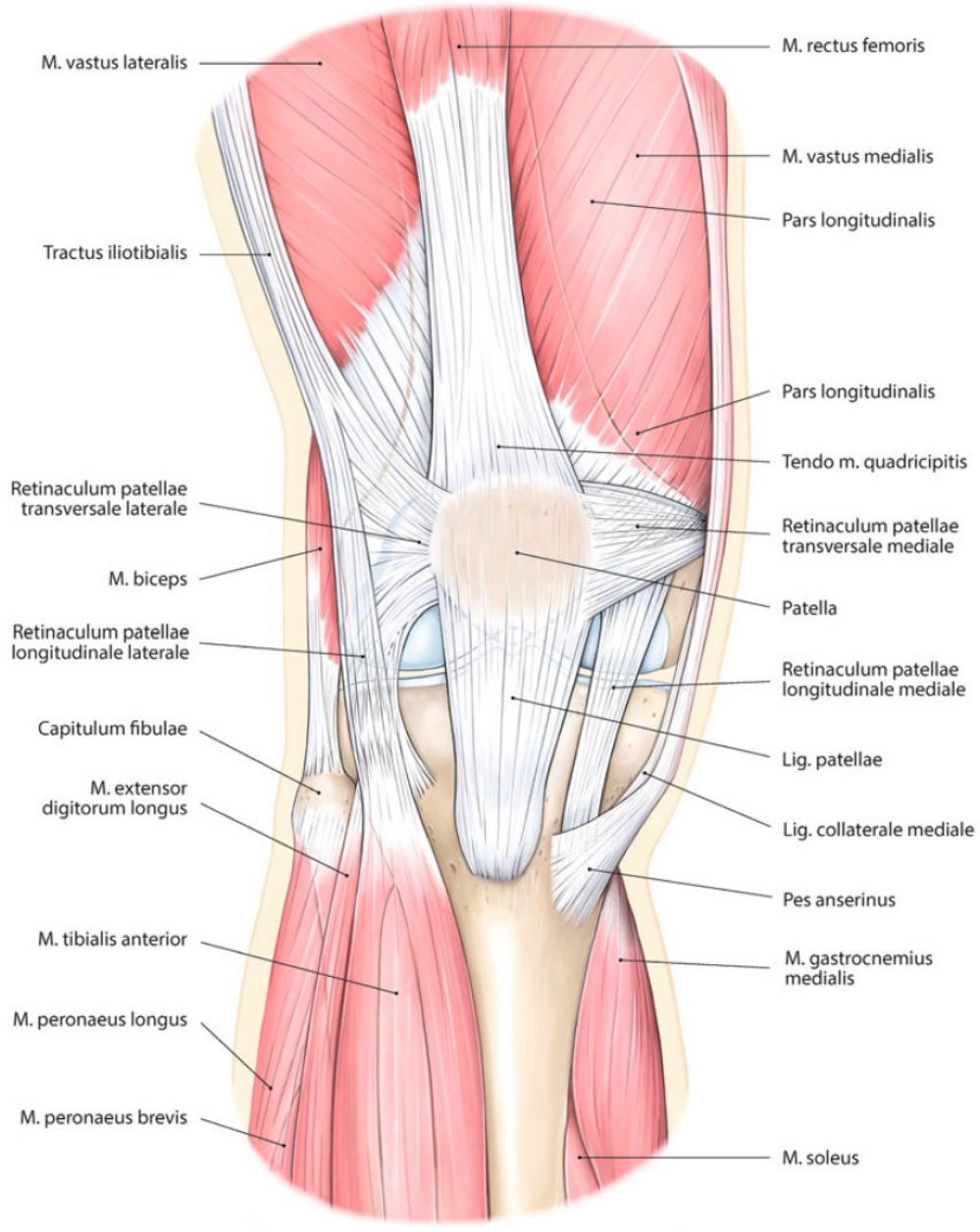

Figure 1: Anatomy of the knee joint. Knee seen from anterior. Figure reproduced from (34) with the permission of Springer Nature. © 2016 Jagodzinski, Friederich and Müller.

The patellofemoral joint comprises the trochlear groove of the femur and the patella as its bony components (29,35). Positioned between the femoral condyles, the trochlear groove is characterized by a vertical sulcus, which facilitates the guidance of the patella during knee flexion and extension (29,30). The morphology of the trochlear groove varies among individuals; variations such as a shallower trochlear groove or discrepancies in the height of the femoral condyles can diminish the guidance provided to the patella, potentially impacting its stability (36).

The patella articulates within the patellofemoral joint via its posterior surface (3,30). The articular surface of the patella, known as the facies articularis patellae, possesses the thickest

cartilage in the human body, with a thickness reaching up to 7 mm in its central region (3). The upper two-thirds of the patella's surface is covered in cartilage, whereas the lower third, termed the apex patellae, is covered by the ligamentum patellae (27,30). A vertical ridge, situated approximately in the center of the articular surface, divides it into a medial and lateral facet (27,29). Additionally, an extra articular surface, often referred to as the Odd facet, is located on the outer aspect of the medial facet (29).

The patellofemoral joint is stabilized by several ligaments. The ligaments located on the medial side can be separated into three layers. The superficial layer consists of the retinaculum patellae. The mid layer includes the medial patellofemoral ligament and the superficial part of the medial collateral ligament. The profound layer incorporates the joint capsula, the profound layer of the medial collateral ligament as well as the meniscopatellar ligament (11,35,37,37). The ligaments on the lateral side include the retinaculum patellae, the lateral patellofemoral ligament, the patellotibial ligament, parts of the tractus iliotibialis and the lateral collateral ligament (35).

The musculus quadriceps femoris is of paramount importance to the patellofemoral joint, as it is directly connected to the patella (27,29,30). The quadriceps muscle is composed of four distinct heads: the vastus medialis, vastus lateralis, vastus intermedius, and the rectus femoris (30). The three vasti originate from the ventral surface of the femur, while the rectus femoris, a biarticular muscle, originates from the spina iliaca anterior superior (27). The four heads of the quadriceps converge to form the quadriceps tendon a few centimeter above the patella (27,30). The quadriceps tendon extends to form the retinaculum patellae and attaches to the proximal part of the patella (27). The ligamentum patellae can be considered as an extension of the of quadriceps tendon and connects the apex patellae with the tibial tuberosity (27,30). Due to the patella being embedded within the tendon of the quadriceps muscle, this muscle exerts a significant influence on the patella's tracking within the trochlear groove (38).

1.1.2 Biomechanics of the tibiofemoral and patellofemoral joint

During flexion and extension movements in the tibiofemoral joint, the articulating surfaces execute a combination of rolling and gliding motions (28). The translational component of this movement results in either a dorsal displacement of the femur or a ventral displacement of the tibia during flexion, contingent upon which joint partner remains stationary (27). The ratio between rolling and translational movement is dictated and regulated by the anterior and posterior cruciate ligaments (28,33). These ligaments constrain the translational movement and maintain the correct alignment of the femur and tibia throughout flexion and extension (28). Additionally, the cruciate ligaments play a role in determining the shape of the femoral condyles (33). The medial and lateral collateral ligaments provide stability in the frontal and

transverse planes. At full extension, the tibiofemoral joint undergoes a terminal rotation of approximately 5 degrees, manifesting as an external rotation of the tibia, induced by the tension in the anterior cruciate ligament (27,33). When the knee is flexed, the collateral ligaments are relaxed and thereby allowing a certain level of rotational movement around the tibial axis.(27).

A relevant structure in terms of pressure distribution in the tibiofemoral joint are the medial and lateral menisci (33). The inherent incongruence between the tibial plateau and the femoral condyles would typically result in a limited contact area within the joint. By augmenting this contact area, the menisci effectively distribute the load over a larger surface, thereby mitigating high stress on small regions of cartilage (32). Without this increased contact area, peak pressures could precipitate cartilage degradation (31).

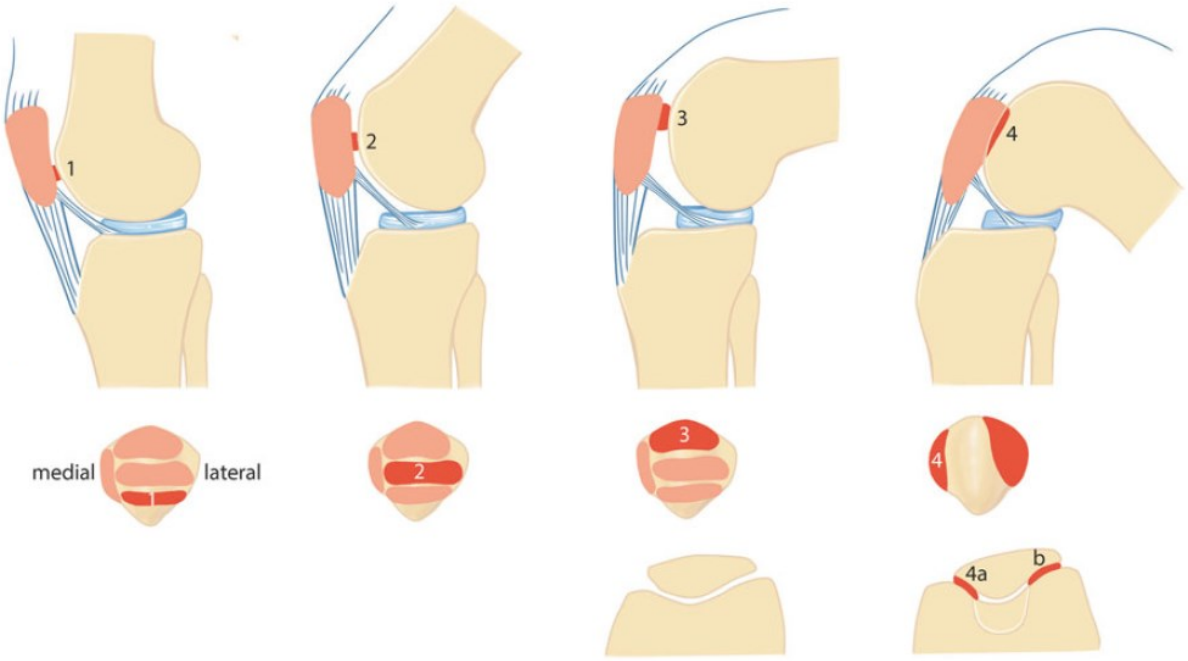

Figure 2: Contact area of the patella cartilage during knee flexion. The images present the contact area of the patellofemoral joint in progressive knee flexion (from extension on the left side to deep flexion on the right side). The first row of subfigures shows the knee joint in sagittal plane. The second row of subfigures shows the patella from dorsal. The third row of the figure shows the patellofemoral joint in transversal plane. Numbers 1 to 4 describe the patella cartilage contact area in certain flexion positions (highlighted areas). In deep flexion, the medial and lateral patella cartilage is in contact with the trochlea (4a and 4b). Figure reproduced from (34) with the permission of Springer Nature. © 2016 Jagodzinski, Friederich and Müller.

During the flexion and extension movements of the tibiofemoral joint, the patella undergoes a vertical displacement of several centimeters within the trochlear groove (34). The contact between the patella and the femur varies depending on the patella's position, with different portions of the patella's articular surface engaging with the femur (Figure 2) (4). In full extension, the contact is minimal, with only a small distal region of the patella in contact with the femur. In conditions such as hyperextension or with an increased height of the patella

(patella alta), it is possible that there is no contact between the joint surfaces (34). As flexion in the tibiofemoral joint increases, the contact area on the patella shifts from the distal to the proximal end. Upon reaching a flexion angle of approximately 90 to 120 degrees, the quadriceps tendon also makes contact with the trochlear groove. At a flexion range of 130 to 135 degrees, the Odd facet of the patella comes into contact with the femur (34,35).

The forces exerted on the patella in the sagittal plane are highly dependent of the current flexion angle of the tibiofemoral joint (39). Whereas there is low contact pressure on the patella cartilage in extension during quadriceps contraction, the pressure significantly increases with a more flexed position of the tibiofemoral joint (40). This increase in pressure is attributed to the reduction in the angle between the force vectors of the quadriceps tendon and the ligamentum patellae, resulting in a greater cumulative force impacting the patella cartilage (Figure 3) (41,42).

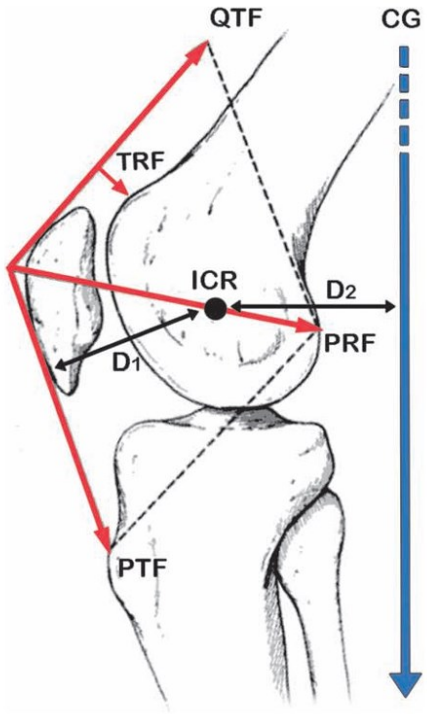

Figure 3: Force acting on the patella in sagittal plane. The patellofemoral reaction force (PRF) is defined as the resultant vector deriving from the quadriceps tendon strain force (QTF) and the patellar tendon strain force (PTF). Additionally, the tendo-femoral reaction force (TRF), which represents the force interaction between the quadriceps tendon and the trochlea, is also depicted. The center of gravity is denoted as CG, and the instant center of rotation is represented as ICR. D_1 is the normative distance between the ICR and the force PTF. D_2 is the normative distance between the ICR and the weight force. Figure reproduced from (42). © 2011 Schindler and Scott. The figure was published in an open-access article distributed under the terms of the Budapest Open Access Initiative (https://www.budapestopenaccessinitiative.org/).

In the frontal plane, the forces exerted by the quadriceps muscle and the patellar ligament have the potential to laterally or medially displace the patella (11). The magnitude and direction of these forces depend on the angle between their respective force vectors, known as the Q-

angle (4). The Q-angle is defined by two hypothetical lines: one extending from the spina iliaca anterior superior through the center of the patella, and the other from the center of the patella to the center of the tibial tuberosity (Figure 4) (43). Typically, this angle predisposes the patella to lateral displacement. Normative values for the Q-angle are approximately 15-17 degrees in females and 10-13 degrees in males (35). An increased lateralizing force leads to an heighten of the contact pressure on the lateral facet (44,45). In cases where the facet is flat or the trochlea is shallow, an increase in lateralizing force may compromise the stability of the patellofemoral joint.

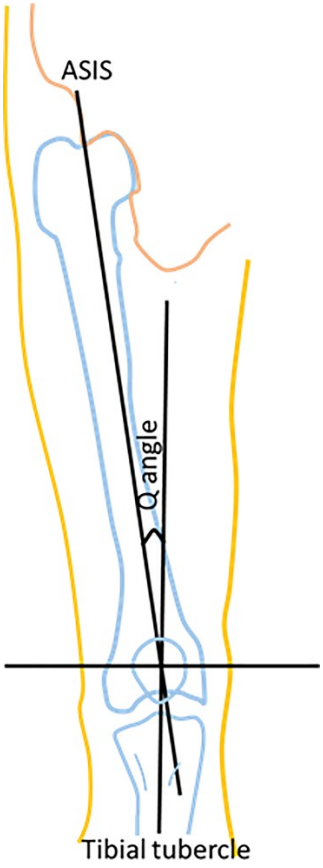

Figure 4: Q-angle. The Q-angle is the angle between a line through the center of the patella to the spina iliaca anterior superior (ASIS) and a line through the center of the patella and the tibial tubercle. Reproduced from (46).

1.2 Patellofemoral instability

Optimal functioning of the patellofemoral joint necessitates accurate guidance of the patella within the trochlear groove, as this ensures effective load transfer from the quadriceps tendon to the patellar ligament. Patellofemoral stability is maintained by a variety of structural and neuromuscular factors, whereas a lack in guidance of the patella in the trochlea groove is

called patellofemoral instability (5). Patellofemoral instability is a prevalent knee condition among adolescents and children, often leading to patellar dislocations (7). The incidence of such dislocations ranges from 23 to 69 per 100,000 population (6–8).

1.2.1 Etiology and Symptoms

In clinical practice, patellar instability and dislocations are predominantly evaluated through the analysis of medical history and clinical examination (7). To further investigate the stability of the patellofemoral joint, specific tests have been developed, including the J-sign and the Apprehension test (47). Additionally, different scales such as the Fulkerson Knee Instability scale (41) or the Kujala Anterior Knee Pain scale (48) are employed to assess the stability of the knee. Moreover, it is advisable to utilize radiographic or magnetic resonance (MR) imaging techniques to examine factors that may influence the stability of the patellofemoral joint (7).

Patellofemoral instability predominantly affects young, active females (9,10). Insufficient stability in the patellofemoral joint may manifest a spectrum of symptoms, from sensations of instability to anterior knee pain (6). Additionally, chronic patellofemoral instability can lead to decreased levels of physical activity and sports participation (11). Over the long term, patellofemoral instability has been recognized as a contributory risk factor for the development of patellofemoral osteoarthritis (8).

Another consequence of patellofemoral instability are patella dislocations, characterized by complete displacement of the patella from the trochlea groove. Patella dislocations typically happen to the lateral side and often occur spontaneously during physical activity (6,7).

The precise pathomechanism of patella dislocations remains incompletely understood. However, it is generally acknowledged that patella dislocations frequently occur when the knee is flexed up to 30 degrees, the tibia is externally rotated, and the quadriceps muscle is contracted (49). Additionally, one study indicated that approximately 80 % of dislocation cases involve a combined movement of valgus, flexion, and external rotation of the knee joint under load (50).

Patella dislocations result in acute pain, functional impairment, and potentially cartilage damage (51). In some cases flake fractures may occur as a consequence of patellar dislocation (11). If left untreated, patella dislocations can restrict participation in strenuous activities and may contribute to long-term cartilage degradation. Moreover, individuals experiencing recurrent patellofemoral instability and patella dislocations often alter their movement patterns, such as gait, to compensate for their instability (26).

1.2.2 Gait pattern of individuals with patellofemoral instability

As patellofemoral instability is apparent under dynamic movement, studying patellofemoral instability under dynamic conditions is essential. In the domain of functional analysis, the analysis of gait is of paramount importance due to its integral role as a fundamental movement pattern essential for daily activities (52). One of the benefits of analyzing gait patterns is their comparability across a wide range of healthy individuals, which establishes a uniform baseline (53). This baseline facilitates the examination of deviations attributable to diseases and the strategies individuals employ to manage their conditions (52,54).

The dynamic process of walking can be dissected into successive gait cycles. A single gait cycle is defined by the contact of one foot with the ground, continuing until the subsequent contact of the same foot (52). Each cycle is further delineated into two phases: the stance phase and the swing phase (54). The stance phase pertains to the period during which the foot remains in contact with the ground, whereas the swing phase occurs when the foot is not in contact with the ground. The stance phase is further divided into two double supported phases, the loading response phase at the beginning and the pre swing phase at the end of the stance phase (53), interspersed by a period of single support (52).

Currently, optoelectronic motion capturing represents the gold standard in three-dimensional gait analysis and is extensively utilized in both clinical and research settings (54). This method employs a combination of infrared cameras and markers. Markers are placed on the participant using a predefined configuration known as a marker set (55). Some markers are affixed to anatomical landmarks to identify specific body parts and bone segment alignment, while others facilitate the tracking of the segments (54–57). During the data collection process, the cameras emit infrared light, which is reflected by the markers and subsequently captured by the cameras (54). By calibrating the cameras to allocate their positions within three-dimensional space, it becomes feasible to determine the spatial coordinates of a marker when it is detected by at least two cameras (58). Reconstructing captured marker data and reassembling the marker set, enables to reconstruct subject specific kinematic patterns (54,55). Frequently, this marker tracking is supplemented by the use of force plates embedded in the ground, which measure ground reaction forces (54,57). The integration of marker data with ground reaction forces enables the calculation of external joint moments and power, providing a comprehensive analysis of gait mechanics (54).

Several studies have examined the gait patterns of individuals with patellofemoral instability, identifying deviations from those observed in typically developing children and adolescents (Figure 5) (26). These studies reveal that individuals with this condition exhibit a variety of gait patterns, complicating the understanding of compensatory strategies employed. Moreover, discrepancies existed among the findings of different studies. Generally, it has been observed

that individuals with patellofemoral instability tend to exhibit reduced gait velocity, cadence, and stride length (59,60). Furthermore, there is a tendency to decrease the duration of single stance time, consequently increasing the duration of double-supported stance phases (59).

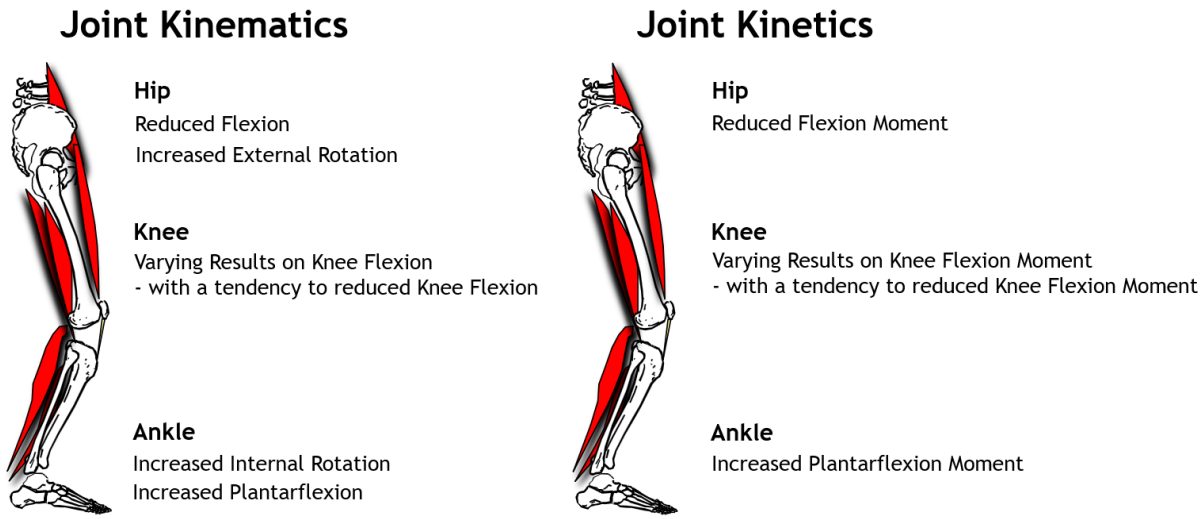

Figure 5: Differences in gait pattern compared to typically developing individuals. A summary of the most important differences in joint kinematics (left side) and joint kinetics (right side) between individuals with patellofemoral instability and typically developing controls presented in the literature. This figure was created by the author of this thesis.

Regarding hip kinematics, research indicates that individuals with patellofemoral instability demonstrate an increased external rotation of the hip (61) and reduced hip flexion (59). Consistent with these findings of reduced hip flexion, one study reported decreased hip flexion moments (59). However, the results concerning hip abduction moments are inconsistent. One study reported increased hip abduction moments (61), while another observed reduced moments (62).

Research comparing individuals with patellofemoral instability to a control group has demonstrated increased internal rotation and abduction in knee kinematics (61,62). Results regarding knee motion in the sagittal plane are mixed. Some studies noted reduced knee flexion throughout the gait cycle (59,61), with one study identifying hyperextension during the stance phase (60). In contrast, other studies found no differences compared to a control group (62), or reported slight flexion with an avoidance of knee joint extension (63).

Subjects with patellofemoral instability exhibit an increased knee abduction moment compared to controls (61). Regarding the knee flexion moment, findings are similarly inconsistent as for sagittal knee kinematics. Compared to a control group, variations range from reduced knee extension moments (56,58) to no significant differences (62), to increased extension moments in some individuals with patellofemoral instability (64).

Individuals with patellofemoral instability walk with an internal rotation of the foot and increased external rotation of the tibia, compared to a control group (61). During the loading response phase, these individuals display increased plantar flexion and associated plantar flexion moments (59).

The analysis of gait patterns in individuals with patellofemoral instability yields inconsistent results, prompting further investigation into how different morphologic factors influencing patellofemoral stability affect gait pattern. A particular study exploring the potential relationship between internal rotation of the hip and femoral anteversion in this population found no significant correlations between these parameters (61). Additionally, another study conducted by the same research group identified no significant associations between three different gait patterns and radiographic measurements in individuals with patellofemoral instability (64). It is important to note, however, that these conclusions were based on retrospective data analysis, indicating a deficiency in prospective studies on this matter (61,64). To date, there remains no established link between gait patterns and radiographic factors that may influence patellofemoral stability. Furthermore, none of these studies did assess the influence of gait pattern on joint loads in individuals with patellofemoral instability.

1.2.3 Factors influencing patellofemoral stability

The stability of the patellofemoral joint is influenced by a multitude of factors. These encompass active structures such as the quadriceps muscle, passive structures including ligaments, and bony structures that impact the patellofemoral joint (5–7). Furthermore, the alignment of the lower limb plays a significant role in the stability of the patellofemoral joint (4,5,7).

1.2.3.1 Active structures

The quadriceps muscle exerts a substantial muscular influence on the patellofemoral joint (38). Especially the vastus medialis and vastus lateralis are seen to directly impact the guidance of the patella (11). Research has demonstrated that in knee joint flexion up to 20 degrees, a reduction in tension within the vastus medialis muscle can decrease lateral patella stability by approximately 30 % (65). Conversely, isolated contraction of the vastus lateralis results in the lateral displacement of the patella (66). Analysis of the force vectors of the vastus medialis and lateralis in the frontal plane reveals that these forces tend to balance each other in an extended knee posture, resulting in a force that is parallel to the femoral shaft (43,67). This leads, coupled with the position of the tibial tuberosity to a marginally lateralizing force during knee extension (38). Thus, a weakness or reduced muscle activation of the vastus medialis may lead to an increased lateralizing force on the patella, potentially causing a lateral

shift (68). Furthermore, the vastus medialis exhibits the most rapid strength degradation of the quadriceps, when the lower extremity is immobilized (69). This resulting strength degradation could potentially exacerbate recurrent patellofemoral instability and lead to further dislocations (11).

1.2.3.2 Passive structures

In the context of passive stabilization, the patella is dependent on ligamentous structures (11). The general laxity of these ligaments is posited as a potential risk factor for patellofemoral instability, although comprehensive investigations into this association remain incomplete (11,70–72).

The medial patellofemoral ligament is identified as the most critical passive structure for maintaining the stability of the patellofemoral joint (11,73). Particularly between 0 and 30 degrees of knee flexion, the medial patellofemoral ligament plays a crucial role in counteracting the lateralization of the patella, compensating for up to 60 % of lateralizing forces (74), whereas it exhibits the highest loading at about 20 degrees flexion (65). Notably, during initial incidents of patellar dislocation, the medial patellofemoral ligament is ruptured in approximately 90 % of cases (74,75). Given the significant role of the medial patellofemoral ligament as a passive stabilizer, a rupture of this ligament could exacerbate the instability of the patellofemoral joint following an initial dislocation.

In addition to the medial patellofemoral ligament, the meniscopatellar ligament contributes modestly to patellar stabilization, compensating approximately 13 % to 22 % of the lateralizing forces exerted on the patella (74,76,77). The patellotibial ligament and the medial retinaculum are not considered to have significant roles in stabilizing the patella (74,76).

The role of the lateral retinaculum in patellofemoral stability is controversial discussed (11). A potential adverse effect identified is that a constricted lateral retinaculum may cause the patella to tilt, potentially impeding its proper alignment within the trochlear groove (78,79). Contrarily, some studies have indicated that the lateral retinaculum may exert a stabilizing influence on the patella, contributing to its alignment in both medial and lateral directions (74,80–82).

1.2.3.3 Bony structures

On the femoral side, the morphology of the trochlea significantly influences the patellofemoral joint (36,83). A dysplastic trochlea can predispose individuals to patella dislocations (65) and is frequently observed in patients experiencing patellofemoral instability (84). Specifically, a trochlea that is excessively flat, characterized by a trochlear sulcus angle exceeding 145 degrees, or even presenting a convex shape, detrimentally affects the guidance of the patella

(36). Dejour et al. (36) developed a classification scale which separates the shape of the trochlea in four groups, considering the severity of trochlea dysplasia. Furthermore, the positioning of the trochlea on the femur is crucial for patellofemoral stability, with findings indicating that the trochlea is often located more medially in individuals with patellofemoral instability compared to controls (85).

Another relevant bony structure that impacts patellofemoral stability is the shape of the patella (86,87). A dysplastic patella may exhibit alterations in the shape of the cartilage surface and the distribution of the medial and lateral facet surfaces (86). In cases of severe dysplasia, the medial facet is notably smaller and more vertically oriented (88,89).

1.2.3.4 Tibial tuberosity

The positioning of the tibial tuberosity relative to the knee joint is critical for the stability of the patellofemoral joint (83). Its position directly influences the Q-angle, which indicates the direction in which the patella is drawn by the quadriceps muscle (4,35,90). Consequently, a lateral displacement of the tibial tuberosity results in the patella being increasingly pulled laterally by the ligamentum patellae and the quadriceps muscle (35). A lateralized tibial tuberosity, relative to the center of the trochlear groove, is associated with occurrences of patella dislocations (83). A study demonstrated that in 56 % of individuals with patella dislocations the distance between trochlea groove and tibial tuberosity was increased (83).

1.2.3.5 Position of the patella

The stability of the patellofemoral joint is significantly influenced by the relative height of the patella to the trochlea, as this affects the patella's guidance within the trochlear groove (5,6,91). A condition where the patella is positioned higher than normal in relation to the trochlear groove is termed patella alta (92). The etiology of patella alta remains uncertain, though there is speculation in the literature about potential associations with quadriceps dysplasia (83). In cases of patella alta, the patella engages with the trochlear groove later during knee flexion, resulting in diminished bony guidance and increased stress on both active and passive stabilizers of the joint (40,78,93). Physiologically, the contact area between the cartilage of the patella and the trochlear groove expands as knee flexion increases (40). Consequently, patella alta results in a reduced cartilage contact area at comparable degrees of knee flexion relative to a knee with a normally positioned patella. This diminished contact area, under consistent loading forces, leads to elevated pressure on the cartilage (94).

1.2.3.6 Lower limb alignment

Abnormal skeletal alignments within the lower limb can detrimentally impact the stability of the patellofemoral joint (5). Such misalignments include excessive femoral version (6), tibial torsion, as well as deviations observed in the frontal plane, such as genu valgum (95). Genu valgum can alter the Q-angle, potentially increasing the lateralizing force acting on the patella (35). Moreover, excessive femoral anteversion is associated with increased pressure on the lateral facet of the patella (44,45) and increased lateralization of the patella (96). Beside femoral anteversion, tibial torsion is also recognized to influence the stability of the patellofemoral joint. Studies using cadaver models have indicated that increased external rotation of the tibia may augment the lateralizing force on the patella (44,97).

1.2.4 Radiographic measurements to classify patellofemoral joint morphology

Radiographic measurements allow an assessment of the initial morphological conditions of individuals with suspected patellofemoral instability (6,7). Specifically, MR imaging enables a comprehensive analysis of knee joint morphology using various parameters (5,6).

One critical factor for patellofemoral stability that can be assessed via MR imaging is the shape of the trochlear groove (98). Given the trochlear groove's essential role in guiding the patella, it is prudent to assess its morphology (35,99). Several methods exist for describing its shape, primarily based on angle measurements and shape classification (36,83,98). The trochlear sulcus angle (Figure 6A), defined as the angle between the tangents of the medial and lateral femoral condyles forming the sulcus, serves as an indicator of the trochlea groove's shape (100). A trochlear sulcus angle exceeding 145 degrees indicates a flattening of the trochlea, a condition termed trochlear dysplasia (36,83). Another measurement technique involves determining the depth of the trochlear groove (Figure 6B) by measuring the average height of the medial and lateral femoral condyles and calculating the difference to the groove's deepest point (98). A study identified a significant decreased trochlear depth between individuals with patellofemoral instability, averaging 3.1 mm, and a control group, which averaged 5.2 mm in depth (99). The Dejour classification system is another method used to categorize trochlear shapes into four subclasses (A, B, C, D), where class A indicates a minor deformity and class D represents severe trochlear dysplasia (36,83). Class A is characterized by a shallow trochlea with a sulcus angle of at least 145 degrees, class B by a flat trochlea, class C by a lateral convexity with medial hypoplasia, and class D by a cliff-like formation instead of the proximal-lateral femoral condyle (101).

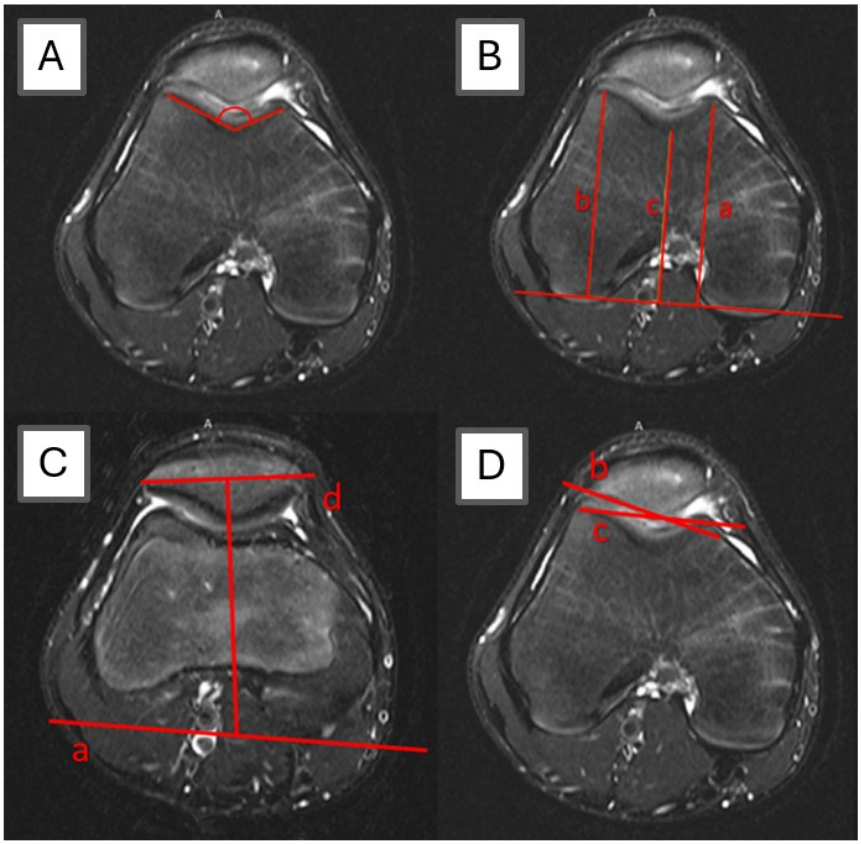

Figure 6: Magnetic resonance image measurements of the patellofemoral morphology. A) Trochlea sulcus angle. Angle between the medial and lateral face of the trochlea sulcus. B) Trochlea sulcus depth. Calculated by the mean of distance a and b subtracted by c. C) Patella tilt. Angle between the tangent along the dorsal femoral condyles (a) and the longest diameter of the patella (d). Patella tilt is calculated as the angle between those two lines. D) Fulkerson angle. Angle between the tangent along the proximal femoral condyles (c) and the lateral patella facet (d).

In addition to the shape of the trochlea, the morphology of the patella, particularly the medial and lateral facets, plays a crucial role in patellofemoral stability (86,102). The configuration of the medial articular surface can be quantified by the medial facet angle of cartilage, which is defined as the angle formed between a transverse line across the longest diameter of the patella and the tangent along the medial patella cartilage facet (87). Similarly, the lateral facet angle is measured by determining the angle between the same transverse line and the tangent along the lateral patella cartilage facet (87).

Patella tilt is another relevant determinant of patellofemoral stability (Figure 6C). It can be assessed using the inclination angle between the dorsal femoral condyles and the transverse line through the longest diameter of the patella (103). Alternatively, the Fulkerson angle (Figure 6D) can be employed to measure patella tilt, which quantifies the angle between the lateral patella facet and the distal femoral condyle (104). Angles that open to the lateral side are considered normal, while angles of 0 degrees or those opening medially are regarded as abnormal (104,105).

To assess the position of the patella relative to the femur, both lateral and vertical displacements can be measured (5,78,104). Lateral displacement is quantified by measuring the shortest distance between the lateral edge of the lateral femoral condyle and the lateral edge of the patella (104). A study identified a mean lateral displacement of 12.1 mm in individuals with patellofemoral instability, in contrast to a mean 0.2 mm displacement observed in a control group (106). For assessing vertical displacement, the Caton-Deschamps index (CDI) can be employed (Figure 7A). This index calculates the ratio of the distance from the apex of the patella to the anterior-superior edge of the tibial plateau relative to the vertical diameter of the patella (107). Normal patella height according to the CDI ranges from 0.8 to 1.2. Values exceeding a ratio of 1.2 are indicated as patella alta (108,109).

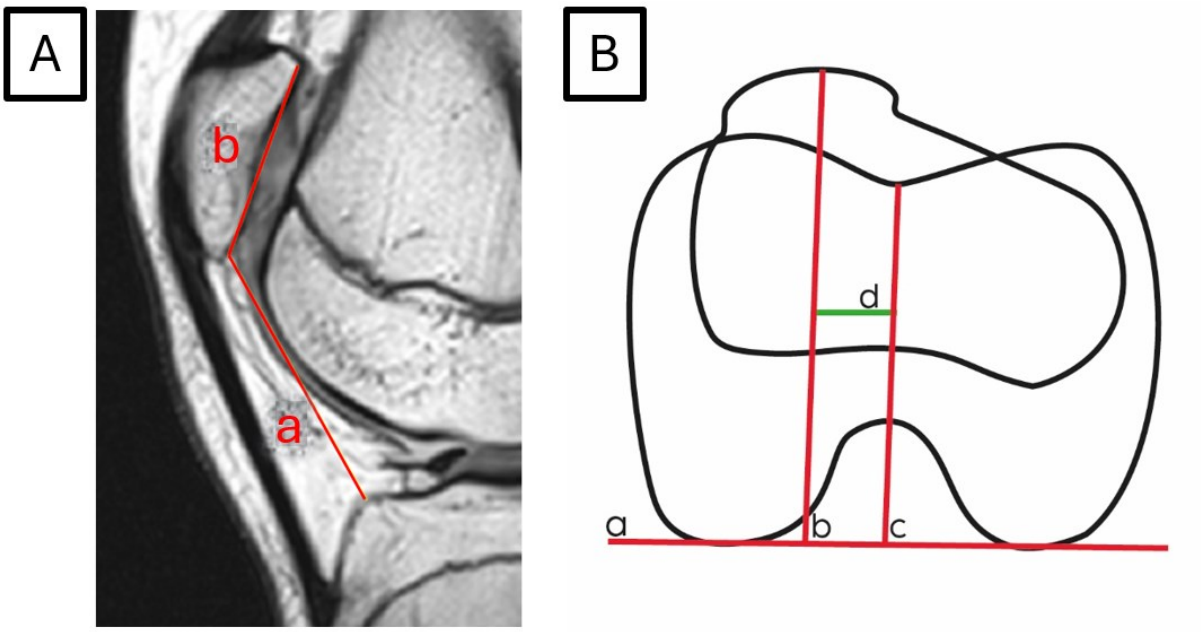

Figure 7: Magnetic resonance image measurements of the patella position. A) Caton-Deschamps index. Caton-Deschamps index is calculated by dividing the distance between the apex patellae and the proximal prominence of the tibial plateau (a) by the height of the patella (b). B) Distance between the tibial tubercle and the trochlea groove (d). Two supporting lines are drawn to the tibial tubercle (b) and the center of the trochlea groove (c) perpendicular to the tangent between the dorsal femoral condyles (a). The parameter is measured as the distance between those two helping lines (indicated by the green line; d). © 2024 Jakob Holzer. Reproduced with the permission of the copyright holder.

To ascertain a potential negative impact of the position of the tibia relative to the femur on patellofemoral stability, the distance between the tibial tuberosity and the trochlea groove can be measured (Figure 7B) (11). This measurement is conducted using two overlapping cross-sectional images to determine the distance from the tibial tuberosity to the center of the trochlea groove, with lateral displacement identified as a risk factor for patellofemoral instability (99).

The overlay of MR-based cross-sectional images at different levels of a body segment facilitates the measurement of torsions in the lower limb (110–112). Femoral version can be calculated by overlaying cross-sectional images of the femoral neck and the femoral condyles (110). It is defined as the angle between the longitudinal axis of the femoral neck and the tangent line at the dorsal femoral condyles (110,112). Normative values for femoral anteversion, which depend on the measurement technique, typically range from 7 to 24 degrees (113). Similarly, tibial torsion is determined by superimposing cross-sectional images of the tibial plateau and the lateral malleolus (110). Tibial torsion is defined as the angle between the tangent at the dorsal tibial plateau and a line extending through the middle of the tibiofibular joint surface to the middle of the lateral malleolus (110,112). An external tibial torsion exceeding 30 degrees is considered excessive and deviates from normal values (114).

1.2.5 Treatment of patellofemoral instability

Patellofemoral instability and associated patella dislocations can be managed either conservatively or through surgical intervention (5–7). Studies demonstrated favorable outcomes in patient-related outcome measures following both conservative and surgical treatments following the first dislocation (115–117). Individuals with patellofemoral instability who underwent either conservative or surgical treatment reported improvements in pain and functional levels (116,117). However, higher rates of redislocation were observed following conservative treatment compared to surgical interventions (115–117). Based on the positive findings regarding pain and function, conservative treatment is generally recommended initially after the first incidence of patella dislocation, except in cases involving osteochondral fractures (11) or severe pathologic laxity (5). Should conservative treatment fail, surgical intervention is recommended (5).

1.2.5.1 Conservative Treatment

Conservative treatment for patellofemoral instability and patella dislocations primarily focuses on pain management, initial immobilization, and physiotherapy (6,7). Within a general framework, conservative treatment should be planned and structured at the individual's needs and any present risk factors should be considered during treatment planning (11).

The initial phase of conservative treatment typically involves immobilizing the affected knee joint through the use of orthoses, posterior splints, or plaster casts (7,118). Immediate immobilization is crucial as it aids in the healing of the passive medial structures (70,119) and supports preventing redislocations (120). A study indicated that immediate mobilization of the knee joint after a dislocation could triple the risk of redislocation (120). Immobilization also facilitates pain relief and is generally recommended for approximately 2-3 weeks at a knee

flexion angle of 15 to 20 degrees (11). During this initial period, the focus should be on reducing pain, managing joint effusions, restoring range of motion, and promoting quadriceps activation (43).

Following the initial treatment phase, subsequent weeks should concentrate on enhancing the functionality of the knee joint (10,70,119). The primary objective during this period is to progressively increase the load on the knee joint and achieve full range of motion (10,70,119). During this phase, training may include closed kinetic chain exercises (70), which are particularly functional and beneficial for stimulating activity in the vastus medialis (121,122). Additionally, proprioceptive training (i.e. vibrating plates) may be beneficial in this phase by aiding in the restoration of functional stability in the knee joint (6,123).

After approximately 5 to 6 weeks, if feasible, patients may begin ergometer training and gradually resume running activities (124). Upon completion of the rehabilitation process, it is advisable to persist with coordinative and muscle strength training one to two times a week to mitigate the risk of patellar redislocation (11).

1.2.5.2 Surgical Treatment

The objective of surgical intervention for patellofemoral instability is to ensure optimal patellar tracking by rectifying abnormal morphological features and thereby preventing redislocations (6). Surgical strategies addressing patellofemoral instability are directed at different morphological structures known to affect the stability of the patellofemoral joint (5,6,11). Consequently, comprehensive imaging assessments are essential to identify potential abnormal morphologies (5). A range of isolated or combined surgical procedures is employed to enhance the stability of the patellofemoral joint, including reconstruction of the medial patellofemoral ligament, lateral release, medialization of the tibial tuberosity, and trochleaplasty (5–7,11). Furthermore, postoperative rehabilitation is a relevant factor for successful surgical treatment. Hence, surgical interventions should be complemented by a well-structured postoperative rehabilitation program (7).

A critical surgical focus is the restoration of medial constraints, particularly the medial patellofemoral ligament (5). This structure plays a significant role as a passive stabilizer and is often ruptured in the majority of patellar dislocations (74,75). Several techniques have been developed to restore the functionality of the medial patellofemoral ligament. These include different anchoring methods and grafts, such as the semitendinosus tendon, segments of the patellar tendon, or synthetic materials like polyester to reconstruct the medial patellofemoral ligament (11). The reconstruction of this ligament is of crucial importance as it substantially decreases the risk of subsequent redislocations (7).

The surgical procedure lateral release is designed to mitigate the lateralizing pull exerted by passive lateral structures through the dissection of the lateral retinaculum (11). However, biomechanical studies have reported that this procedure does not confer any beneficial effect and may even increase the overall instability of the patellofemoral joint (80,125). Consequently, lateral release is not recommended as a standalone treatment technique (5) and is contraindicated in cases of acute dislocations (7). In specific circumstances, such as those involving increased negative patella tilt (126) or chronic instability, lateral release may be considered, but only in conjunction with other surgical interventions (7,11).

A transfer of the tibial tuberosity may be employed to diminish the lateralizing traction exerted by the quadriceps on the patella (127). Given that the position of the tibial tuberosity influences the Q-angle (11), repositioning the tibial tuberosity medially can reduce the lateralizing forces within the patellofemoral joint (128), by correcting the extensor apparatus (7). This adjustment of the extensor apparatus aids in correcting maltracking of the patella and aligning it more effectively within the trochlear groove (7). In cases where an increased Q-angle or lateralization of the tibial tubercle procedure is considered as main factor for patellofemoral instability, medialization of the tibial tubercle according to Grammont (129) can be considered. In instances of patella alta, distalization of the tibial tuberosity is a viable surgical option (130). Additionally, this procedure can be augmented by tenodesing the patella tendon to effectively shorten it (131). Overall, distalization of the tibial tubercle is recognized as an effective method for preventing recurrent patella dislocations in individuals diagnosed with patella alta (130). Often done is a combination of distalization and medialization of the tibial tuberosity, as described by Elmslie and Trillat (132).

Trochleaplasty is infrequently indicated (5) and is typically reserved for revision surgeries or in cases involving specifically selected patients (7). The primary objective of trochleaplasty is to modify the shape of the distal femur, mainly by lowering the central part of the trochlea (11). It is important to note that post-operative complications such as knee rigidity often occur following this procedure (7). Additionally, trochleaplasty carries a significant risk of cartilage damage and may permanently alter knee joint kinematics, both of which can elevate the likelihood of early onset osteoarthritis (7,133).

If a torsional deviation of the lower limb is present and adversely affecting the stability of the patellofemoral joint, derotation osteotomies may be considered to correct torsional alignment (6,134,135). Derotation osteotomies can be performed on either the femur or the tibia and are aimed at adjusting excessive torsional angles to within normative values (6,136). In certain cases involving malalignment syndrome, a combination of femoral anteversion and tibial torsion abnormalities, combined femoral and tibial derotation osteotomy may be considered (137).

1.3 Musculoskeletal Modelling

Musculoskeletal modelling is a well-established methodology that provides unprecedented insights into the neuromechanical dynamics of the human body. Musculoskeletal simulations enable researchers to examine the behavior of the musculoskeletal system without the necessity for complex and invasive experiments on living organisms (16). The primary focus of musculoskeletal simulations is to explore the interactions between joint movement, muscle forces, and joint loadings (16,138).

In the medical domain, musculoskeletal simulations are utilized in several disciplines, including traumatology, neurology, and orthopedics. In orthopedics, musculoskeletal simulations are used to investigate the causes of injuries and diseases of the musculoskeletal system (138). Simulations can also be used for treatment planning to reduce the risk of complications and improve outcome (139). Additionally, musculoskeletal simulations are applied in the fields of sports science and sports orthopedics. In these areas, they are instrumental in enhancing the performance and training regimens of athletes, as well as in mitigating the risk of injuries (140).

There are three principal factors that significantly influence movement-dependent joint loads: the execution of the movement, muscle coordination, and musculoskeletal geometry (16,141). Musculoskeletal simulations, which are predicated on the integration of biomechanical and neurophysiological modeling, incorporate these critical factors (16,138). The models employed describe the geometry and properties of bones, muscles, and joints (142,143). Information regarding movement is often sourced from motion capturing data (138). Subsequent simulations are designed to emulate the functioning of the motor nervous system (16). These simulations are utilized to analyze movements, muscle dynamics, and the forces and moments exerted on bones and joints (138).

In the domain of simulation methodologies, a distinction is made between 'inverse' and 'forward' simulations. Forward simulations aim to compute the resultant movement based on a musculoskeletal model and an optimization approach, which mimics the central nervous system (138). Consequently, forward simulations are designed to reconstruct the neurophysiological and biomechanical functions to investigate how a subject would move within predefined constraints and objectives (144). For the performance of forward simulations, no experimental movement data is needed. This approach can be used to investigate how certain impairments, e.g. spasticity in CP affects gait pattern (145). Conversely, inverse simulations estimate muscle forces and joint reaction loads occurring during a pre-captured movement (16). These simulations calculate the kinematics of body parts as well as the forces and moments acting on anatomical structures (138). Movement

sequences characterized by high reproducibility, such as walking, are frequently analyzed using both forward and inverse musculoskeletal simulations (138,146–148).

One possibility to perform such musculoskeletal simulations is, by using OpenSim. OpenSim is an open-source software tool developed at the Stanford University, to conduct a broad range of musculoskeletal simulations. OpenSim can be used for rehabilitative and orthopedic studies, as well as for the development of new medical devices, like orthoses. Additionally, it is possible to simulate the outcomes of different surgical treatments in terms of what-if simulations. OpenSim encompasses the conduction of forward and inverse simulations with its toolboxes. It provides a graphical user interface and easy to use application programming interfaces for MATLAB and Python (16,138,149,150). Beside OpenSim, other software packages (e.g. AnyBody (15)) are available for musculoskeletal simulations. However, these are not freely available and were not used in this thesis.

1.3.1 Models and Personalization

A musculoskeletal model constitutes a mathematical framework designed to simulate the dynamic interplay among the muscles, bones, and joints within the human body. It comprises a set of differential equations that mathematically describe the movements and forces acting on bones and joints (138).

Musculoskeletal models are created by recording the geometry of the body parts to be modelled, such as the spine or joints. This is usually done using cadaver studies and MR scans (142,143,147). It is feasible to construct models that encompass multiple joints, thereby facilitating more comprehensive simulations that may include entire limbs or the full musculoskeletal system (148). Furthermore, areas of particular interest, such as specific joints, can be modeled with enhanced details (151,152). The integration of mechanical characteristics, encompassing bones, muscles, ligaments, and joints, into the model is a critical step (Figure 8) (152). This integration is grounded in empirical evidence gathered from clinical observations, in vivo experiments, cadaveric studies and MR scans (142,143,152). Should a suitable model already exist for a particular line of inquiry, it may be advantageous to utilize these pre-existing models. This approach can significantly expedite the time-consuming processes of model development and validation. Such models, often referred to as generic models, typically incorporate adjustments for individual variations, including a patient’s height, weight, and the proportions of body segments, through a process known as model scaling (16). Additionally, these generic frameworks offer the potential for further personalization, for instance, through the modification of osseous geometries, the trajectories of muscle fibers, or the maximum forces that muscles can exert (153).

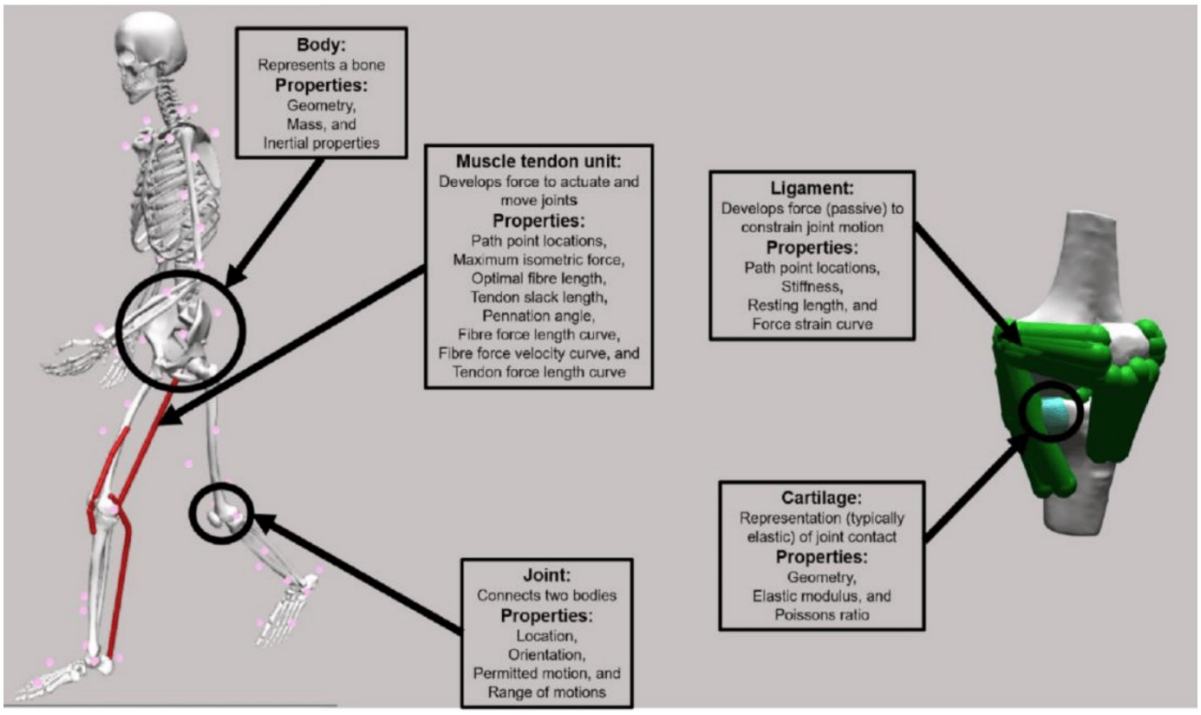

Figure 8: Example of a musculoskeletal model detailing each model component. The left side shows a generic model, presenting bones, a marker set (pink dots) and a small selection of muscles (red lines). The right side represents an example for a more complex model of the knee joint incorporating ligaments (green lines) and cartilage surfaces. Reproduced from (139). © 2020 Killen et al.. The figure was published in an open-access article distributed under the terms of the Creative Commons CC BY license 4.0 (http://creativecommons.org/licenses/by/4.0/).

One possibility of further personalization of musculoskeletal models involves the incorporation of person-specific geometric characteristics of the lower limb bones. Recent advancements in computational tools have facilitated an easy and fast adaptation of femoral version, femoral neckshaft angle and tibial torsion (154–156). Using the Torsion Tool for OpenSim, these angular adjustments can be readily implemented within a MATLAB script, thereby enabling the generation of personalized models tailored to individual anatomical variations (155,157). The Torsion Tool uniformly alters femoral version and tibial torsion along the shaft of the corresponding bone (155). All muscle attachment points are maintained at their original locations on the corresponding bones. When these modified bones are incorporated into the models, the knee and hip joints are preserved in their neutral positions. However, the foot progression angle and the position of the trochanter major are altered relative to the hip joint (Figure 9).

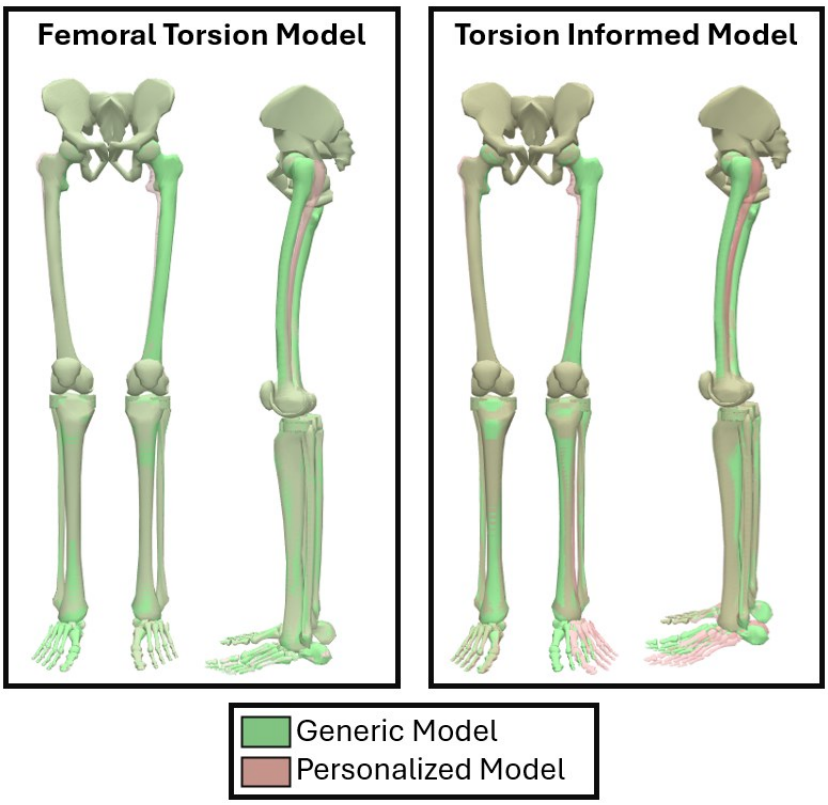

Figure 9: Alignment of the femur and tibia before and after personalization. This figure presents how the Torsion Tool changes the shape and alignment of the femur and tibia (red) compared to the generic torsion model (green). The left side represents the personalization for the femoral torsion model, while the right side represents the personalization for the torsion informed model. The personalized models represent one participant with 36° femoral version and 38° tibial torsion.

1.3.1.1 Rajagopal model

One widely used model for musculoskeletal simulations in OpenSim is the Rajagopal model (Figure 10a) (143). It incorporates overall 37 degrees of freedom for joint kinematics. Further, it includes 80 muscle-tendon units at the lower limb, characterized by Hill-type muscle models (158). For the upper body 17 ideal torque actuators are implemented in the Rajagopal model (143). The development and validation of this model's muscle-tendon properties were underpinned by the analysis of data derived from 21 cadaver samples, which was augmented through MR scans of 24 young and healthy individuals. Initially the model was validated for walking and running (143).

For the assessment of joint reaction loads, particularly within the medial and lateral compartments of the tibiofemoral joint as well as the patellofemoral joint, the Lerner knee model (151) can be integrated into the Rajagopal model (159). The Lerner model is distinctively designed with separate compartments for the medial and lateral tibiofemoral joints, thereby facilitating precise estimations of joint reaction forces exerted on both the medial and lateral femoral condyles and tibial plateau. Additionally, the Lerner model provides

methodologies for estimating patellofemoral joint reaction loads, which are influenced by the forces exerted by the quadriceps muscle and the patella tendon (151).

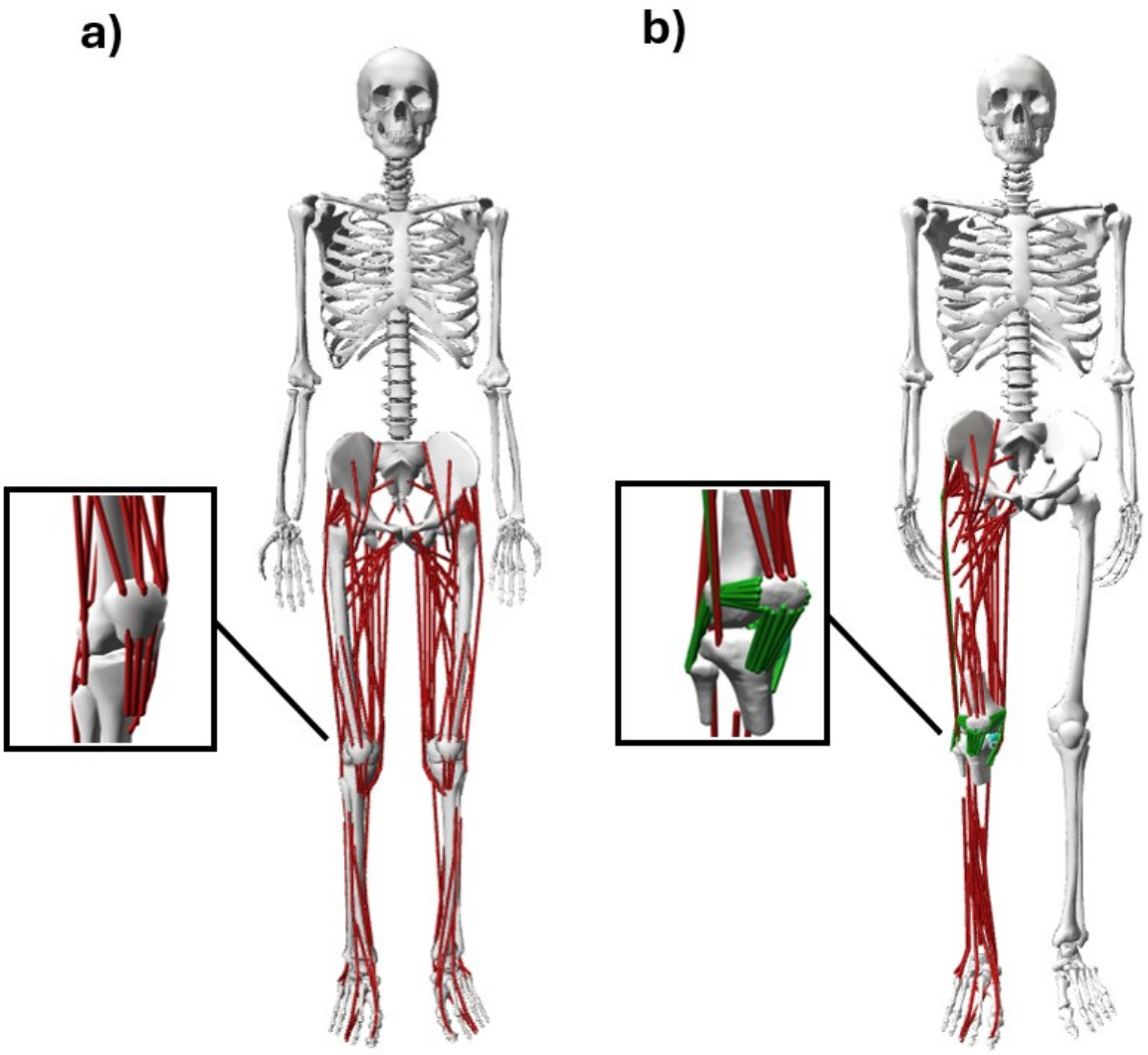

Figure 10: Musculoskeletal models for OpenSim. a) representation of the Rajagopal model. b) representation of the Lenhart model. The red lines denote the defined muscles and green lines the defined ligaments. This figure was created by the author of this thesis.

1.3.1.2 Lenhart model

For specific tasks more complex representation of specific joints can be useful in musculoskeletal models (29). Lenhart et al. (152) developed a complex knee joint, which they incorporated into a generic musculoskeletal framework designed for use in OpenSim (Figure 10b) (142). The base model features a hip joint with three degrees of freedom configured as a ball and socket joint and an ankle joint with a single degree of freedom. Additionally, it includes 44 muscle-tendon units on one lower limb, each defined according to Hill-type models (142). The knee joint of the Lenhart model comprises a six degrees of freedom tibiofemoral and six degrees of freedom patellofemoral joint (152). The model also includes 14 ligament

bundles that were reconstructed from MR scans, encompassing structures such as the medial patellofemoral ligament and both the anterior and posterior cruciate ligaments. The cartilaginous surfaces of the patellofemoral and tibiofemoral joints were similarly reconstructed using data from MR scans (152). Personalized ligaments and joint geometry allow the calculation of secondary patellofemoral and tibiofemoral kinematics, which is not measurable with standard three-dimensional motion capturing techniques (160,161). Specifically, this includes both linear and rotational movements of the patella across the frontal, sagittal, and transversal axes. Additionally, the defined cartilage surfaces, when used in conjunction with the Concurrent Optimization of Muscle Activation and Kinematics (COMAK) routine, facilitate the calculation of cartilage contact pressures based on an elastic foundation model (162–164).

1.3.2 Common simulation workflow in OpenSim

In the execution of inverse musculoskeletal simulations using OpenSim, adherence to a workflow comprising multiple stages is essential (16). Initially, a predefined or previously personalized model is scaled to align with the anthropometric and physiological characteristics of the individual under investigation. This scaling process adjusts for factors such as body size, segment dimensions and weights, muscle properties (e.g. maximum isometric muscle force), and the placement of markers on the model (153,165). Scaling of body size and segment dimensions within musculoskeletal simulations is conducted using a static pose derived from motion capturing data or segment lengths determined in radiographic measurements. During the scaling setup, the dimensions of each body segment are associated with specific markers. The body weight is adjusted to align with the weight distribution of the pre-scaling model and the actual weight of the participant (153,165). Typically, maximum isometric force of muscles are scaled in accordance with either the body weight or the size of the participants (165–167). Accurate scaling is crucial for reliable simulation results (168).

Subsequently, inverse kinematics is employed to derive the joint coordinates (OpenSim nominates joint angles as coordinates) from experimental marker data (169). This involves performing a least squares fit for each frame to align the experimental markers with the corresponding model markers, with provisions to adjust the weighting of markers based on the reliability of experimental marker position data (16). This adjustment allows for the reduction in the influence of markers likely to exhibit significant soft tissue artifacts.

$$\min_{q} \left[\sum_{i \in markers} w_i \left\| x_i^{exp} - x_i(q) \right\|^2 + \sum_{j \in unprescribed\ coords} \omega_j \left(q_j^{exp} - q_j \right)^2 \right] \quad (1)$$
$$q_j = q_j^{exp}\ for\ all\ prescribed\ coordinates\ j$$

Equation 1 describes how coordinates are calculated by inverse kinematics, where q is the vector of generalized coordinates that is solved. x_i^{exp} is the experimental position of the marker i. $x_i(q)$ is the position of the model marker i. q_j^{exp} is the experimental value for the coordinate j. Finally, w_i and ω_i describe the predefined marker and coordinate weights respectively. If a coordinate is predescribed (e.g. by locking the joint) it follows the calculation $q_j = q_j^{exp}$ (170).
In the next step, inverse dynamics, external joint moments are calculated based on the joint coordinates and ground reaction force data (171). This procedure is executed analogously to the conventional three-dimensional gait analysis (54).
A critical phase in musculoskeletal simulations is the estimation of muscle activation and forces, which follows the calculation of external joint moments (16,171). Given the redundancy in the human musculoskeletal system, where multiple muscles can perform the same movement, a direct calculation of muscle activation and forces is not possible. Instead, different algorithms (e.g. static optimization) are applied to distribute forces across synergistic muscles (16,172). Several mathematical approaches are available to estimate muscle activation and forces, taking into account muscle-specific properties such as optimal fiber length, maximum isometric force, and muscle fiber composition (16,172,173). These methodologies range from those aimed at reducing metabolic cost (174) to more sophisticated approaches that also incorporate electromyography data (175).
In the final step, the outcomes from the preceding simulation phases facilitate the calculation of joint reaction loads based on Newtonian mechanics (171,176). The external loads and moments, the muscle forces and the distal joint reaction loads are used as parameters for this calculation, while the force directions and segment accelerations are influenced by the kinematics (176). The joint forces are calculated in a recursive procedure starting at the ankle joint and moving progressively proximal (171,176). Since one of the main input parameters for calculating the joint reaction loads are the muscle forces, these seem to have a major influence on the calculated joint forces (177).
After performing musculoskeletal simulations, it is essential to validate the simulation results. The plausibility of the results can be checked by comparing them to cadaver studies (44,96), in vivo measurements (178), or previous simulations (19,20,23,179).

1.3.2.1 Static Optimization

Static optimization is a method to quantify muscle activations and forces based on the external moments applied to each joint during specific time frames (170,180). The method aims to

minimize a cost function (e.g. sum of squared muscle activations), thereby optimizing the activation pattern of muscles for each time frame of a pre-captured motion (141,174,180). As a prerequisite, static optimization utilizes the outputs from inverse kinematics and inverse dynamics, and focuses on optimizing the muscle-activation-to-force condition:

$$\sum_{m=1}^{n} [a_m f(F_m^0, l_m, v_m)] r_{mj} = \tau_j \quad (2)$$

while minimizing the cost function:

$$J = \sum_{m=1}^{n} (a_m)^p \quad (3)$$

In the specified equations 2 and 3 n describes the number of muscles in the model. Further, a_m is the activation level of a specific muscle m at a time frame. F_m^0 is the maximum isometric force, l_m it's length, v_m the shortening velocity and $f(F_m^0, l_m, v_m)$ the force-length-velocity surface of the muscle m. The variable r_{mj} is the moment arm around the joint axis j and τ_j is the generalized torque acting on the joint axis j. Finally, p is a factor which can be individually adapted to the goal of the optimization (e.g. minimizing the sum of squared muscle activations by setting p to 2) (170). When employing static optimization, it is imperative to acknowledge that this method presupposes an inextensible tendon and does not account for parallel elastic elements in muscles (170,174).

The efficacy of static optimization can vary significantly depending on the specific movement being analyzed. The success of this method is contingent upon the objectives of the movement and the defined cost term within the static optimization process. For activities such as walking, static optimization has demonstrated reliability and efficiency in computation time (180). However, its accuracy may be compromised in scenarios where the dynamics of muscle activation play a critical role or when a suitable time-independent performance criterion cannot be clearly established (180). For instance, in activities like dancing, approaches informed by electromyography have yielded superior results compared to static optimization (173). Furthermore, static optimization aims to minimize co-contraction and thus might not lead to realistic results in participants with neurological impairments (181).

1.3.2.2 Concurrent optimization of muscle activation and kinematics

An alternative method for estimating muscle activation and forces is the COMAK routine, developed by Smith et al. (182,183). This method was developed to utilize musculoskeletal

simulations with more complex models incorporating additional degrees of freedom and implemented ligaments. The COMAK routine employs a computed muscle control algorithm, functioning as a feedforward-feedback controller, which facilitates the concurrent computation of muscle activation, ligament forces, and cartilage contact pressures (184,185). It concurrently solves secondary kinematics, (tibiofemoral ab-/adduction and internal/external rotation as well as six degrees of freedom in the patellofemoral joint), by minimizing the weighted sum of squared muscle activations and contact energy based on bony morphology, ligament properties and tibiofemoral flexion/extension (182,184). In a subsequent step these outcomes can be utilized in combination with inverse kinematics and dynamics results to calculate joint reaction loads (176). Additionally, the incorporation of a solver for elastic foundation models within the COMAK routine allows for the computation of cartilage contact pressures (162–164). Elastic foundation models define cartilage as elastic tissue and bones as rigid bodies. Surface meshes are used to represent the geometry of the cartilage surface. These cartilage geometries can overlap and penetrate each other. The pressure is then calculated for each point of the surface mesh, from the mechanical properties as well as the thickness of the cartilage and the superposition (162). Previous research has demonstrated the capability of the COMAK routine to calculate differences in knee joint contact forces within different morphologic properties in an experimental context (19,23).

1.4 Biomechanic studies to investigate patellofemoral instability

Several biomechanical investigations have been undertaken to explore the influence of various morphological factors on patellofemoral instability. These studies have employed cadaveric specimens as physical models to provide empirical insights (74,76,186–188), while using musculoskeletal modeling as mathematical frameworks to simulate and analyze biomechanical dynamics (20–23,25,189).

1.4.1 Cadaver studies

Cadaver studies provide a valuable method for examining the mechanics of the patellofemoral joint, as they facilitate the dissection and isolated analysis of specific structures, allowing for precise measurement of their mechanical properties (74,76,186–188). However, these models face limitations in replicating physiological muscle activations and external loading conditions. Additionally, cadaver studies do not account for dynamic functional movements or the interconnected activation patterns of muscles typically observed in vivo. Another significant limitation is that specimens often originate from older individuals, which poses challenges in researching pathologies that are predominantly relevant to younger demographics (29).

1.4.1.1 Quadriceps muscle

Elias et al. (186) examined the influence of the vastus medialis obliquus on the pressure dynamics within the patellofemoral cartilage. The methodology involved the utilization of ten cadaveric knees, which were subjected to flexion angles of 40, 60, and 80 degrees. During these conditions, forces mimicking the action of the vastus medialis and other components of the quadriceps muscle group were applied. The distribution of joint pressures was quantitatively assessed using a thin film sensor. The findings from the study indicated that an augmentation in the force exerted by the vastus medialis resulted in a notable reduction in lateral pressure and a corresponding increase in medial pressure across all tested positions of knee flexion (186).

In an in vitro investigation Lorenz et al. (190) explored the impact of asymmetric quadriceps force on patellar tracking. The study utilized seven knee specimens, which were assessed using a knee simulator during weight-bearing knee flexion scenarios. Three distinct force distributions within the quadriceps muscle group were applied: predominantly lateral, predominantly medial and equal distributed forces. The results demonstrated that predominantly lateral loading induced a tilt and a rotation of the patella around the anteroposterior axis. However, this loading condition had only a marginal effect on the mediolateral shift of the patella (190).

Stephen et al. (191) investigated the effects of diminished tension in the vastus medialis muscle on patellar tracking, stability, and contact pressure within the patellofemoral joint. The experimental setup included nine fresh-frozen dissected cadaveric knees mounted in a rig, where the quadriceps and iliotibial band were subjected to a load of 205 N. The findings revealed that a reduction in the force exerted by the vastus medialis led to a significant increase in patellar tilt and translation. Additionally, there was a decrease in medial patellofemoral contact pressure, which contributed to an overall reduction in patellar stability (191).

1.4.1.2 Medial patellofemoral ligament

Conlan et al. (76) employed a cadaveric model to assess the role of medial soft-tissue structures in restraining lateral displacement of the patella. Utilizing 25 fresh-frozen knee specimens, the study systematically evaluated and ranked various soft tissue structures based on their significance in lateral restraint. The findings indicated that the medial patellofemoral ligament was the most critical structure for restraining lateral displacement (53 % of the restraining effect). This was followed by the patellomeniscal ligament (22 % of the restraining

effect). Conversely, the patellotibial ligament was deemed insignificant for lateral patellar restraint (76).

Desio et al. (74) conducted an examination of the restraining capabilities of soft tissue structures on medial and lateral displacement of the patella. The study utilized nine fresh-frozen cadaveric knees, positioning them at 20 degrees of flexion and applying a lateral force of 200N to the patella. The results indicated that the medial patellofemoral ligament exhibited the most significant restraining effect (60 %). This was followed by the medial patellomeniscal ligament (13 %). Notably, the lateral retinaculum also played a role (10 %). However, the medial patellotibial ligament and the superficial fibers of the medial retinaculum were determined to be functionally insignificant for patellofemoral stability (74).

1.4.1.3 Patella alta

Singerman et al. (192) conducted a study to explore the influence of patella height on patellofemoral contact force and its point of application. They simulated rising from a chair in seven cadaver knee specimens while measuring contact force with a force transducer. An increase in patella height resulted in a delayed onset and reduced magnitude of patellofemoral contact force. This delayed engagement between the lateral facet of the patella and the femoral condyles suggests that increased patella height may be a contributing factor to patellofemoral instability (192).

1.4.1.4 Shape of the trochlea

Van Haver et al. (187) assessed the impact of trochlear dysplasia on patellofemoral biomechanics. They altered the native trochlea in four cadaveric knees with various custom-made trochlear implants to simulate trochlear dysplasia. The biomechanical properties of these modified joints were evaluated under different conditions, including open-chain and closed-chain loading, as well as a patellar stability test. The results indicated that knees with trochlear dysplasia exhibited increased internal rotation, lateral tilt, and lateral translation, alongside increased contact pressure and a decreased contact area, when compared to those with a native trochlear shape. Additionally, reduced patellar stability was observed in the dysplastic trochleas. Among the dysplasia implants, those categorized as Dejour type D demonstrated the most significant deviations from the norm (187).

1.4.1.5 Position of the tibial tuberosity

Kuroda et al. (188) investigated the effect of tibial tuberosity positioning on the stability of the patellofemoral joint through simulated tibial tubercle transfers. The research utilized six fresh-frozen cadaveric knees, measuring static patellofemoral joint contact pressures both before

and after medialization of the tibial tubercle, employing a closed-kinetic chain test protocol. All specimens exhibited a normal Q-angle. Findings from the study revealed that medialization of the tibial tuberosity significantly increased medial patellofemoral contact pressure and also increased pressure within the medial tibiofemoral compartment. Consequently, the results suggest that tibial tubercle medialization should be approached with caution in patients who present a normal Q-angle (188).

Ostermeier et al. (193) tested two different surgical techniques for stabilizing the patella against lateral displacement. First surgery was a medialization of the tibial tubercle. The second surgery incorporated an additional reconstruction of the medial patellofemoral ligament. They prepared five cadaver knee specimens with a normal Q-angle and simulated isokinetic extension motions, while applying a lateralizing force of 100 N at the patella. The outcomes demonstrated that tibial tubercle medialization had no significant impact on the stability of the patellofemoral joint. Conversely, the additional reconstruction of the medial patellofemoral ligament resulted in a notable stabilizing effect on the patella, indicating its effectiveness in enhancing patellar stability (193).

1.4.1.6 Lower limb alignment

Worlicek et al. (194) evaluated the impact of varus and valgus alignment of the knee joint on patellar kinematics. They investigated patellar kinematics involving 10 lower extremity cadaver specimens which were analyzed during passive knee flexion and extension under three conditions: neutral position, valgus stress, and varus stress. The findings indicated that valgus stress resulted in an increased lateral tilt of the patella. However, neither valgus nor varus stress significantly affected the medio-lateral shift of the patella (194).

Lee et al. (45) explored the impact of fixed rotational deformities of the femur on patellofemoral contact pressure. The study involved an unspecified number of cadaver knees, upon which a quadriceps force of 200 N was applied across various knee positions featuring different femoral rotations. The results demonstrated that internal rotation of the femur resulted in an increase in peak lateral patellofemoral contact pressure (45).

Kaiser et al. (96) studied whether internal femoral torsion could be considered as a risk factor for patellofemoral instability. They utilized eight fresh-frozen cadaver knees to assess patella motion and pressure under conditions of 0, 10, and 20 degrees increased internal torsion of the femur, both with the native medial patellofemoral ligament and with the medial patellofemoral ligament transected. The findings indicated that increased internal torsion of the femur resulted in elevated lateral patellofemoral contact pressure. Specifically, with an intact medial patellofemoral ligament, 20 degrees increase in internal femoral torsion was identified as a risk factor for patellofemoral instability. Conversely, with an insufficient medial

patellofemoral ligament, even 10 degrees increase in internal femoral torsion was considered a risk factor (96).

Hefzy et al. (97) examined the impact of tibial rotation on patellar motion and patellofemoral contact areas under physiological loading conditions. The study involved four human cadaver knees, which were positioned in a tracking device to simulate movement and measure patellar motions. The results indicated that external tibial rotation resulted in an increase in lateral contact areas across the entire range of knee flexion. Additionally, external tibial rotation was associated with a lateral shift and lateral tilt of the patella (97).

1.4.2 Computational studies

Computational methods such as musculoskeletal simulations and finite element models are valuable tools to examine the effects of morphology and joint kinematics on the loading dynamics of specific joints (17,195–201). Besides other traumas such as ruptures of the anterior and posterior cruciate ligaments (202–204), musculoskeletal modeling and finite element models have also been employed to investigate diverse factors that influence patellofemoral stability (19,20,23–25).

1.4.2.1 Patella alta and position of the tibial tuberosity

Yin et al. (24) developed finite-element models for 10 individuals diagnosed with patella alta, to investigate the influence of tibial tubercle distalization and patella tendon tendonesis on the knee kinetics. The findings from these simulations indicated that performing distalization alone resulted in lower cartilage stress when compared to a combined approach of distalization and tendon tenodesis. Furthermore, an Insall-Salvati ratio of 0.95 (ratio of the patella tendon length to the vertical diameter of the patella) was identified as the optimal level for distalization, beyond which no additional benefits were observed (24).

1.4.2.2 Shape of the femoral trochlea and the patella

Jafari et al. (205) employed a two-dimensional computational transverse plane model of the knee joint with deformable articular surfaces to assess the impact of femoral groove geometry on the stability of the patellofemoral joint. The anatomical data utilized for this model were derived from transverse plane MR scans of a normally flexed knee at 20 degrees, supplemented with information from existing literature. The results demonstrated that modifying the sulcus angle from 139 to 169 degrees induced a lateral shift and tilt of less than 3 mm and 4 degrees, respectively. However, a significantly greater shift and tilt (7 mm and 18 degrees, respectively) were simulated when the quadriceps force was slightly increased and

following the release of the medial retinaculum. This combination of factors may contribute to dislocation disorders (205).

Clouthier et al. (19) developed a statistical shape model to create different configurations of the tibiofemoral and patellofemoral joints. To achieve this, they utilized MR data from 14 asymptomatic knees, which enabled the generation of 37 unique knee models based on -3 to +3 standard deviations of six principal components. Musculoskeletal modeling analyses of these different geometries revealed that a shallow trochlea leads a lateralization and increased tilt of the patella, as well as an increased loading of the medial patellofemoral ligament. Furthermore, a shallow trochlea leads to higher peak pressure on the lateral facet with a more lateralized center of pressure compared to a physiological trochlea shape (19).

Wheatley et al. (20) conducted a musculoskeletal modelling study to examine the impact of different axial patella shapes on the biomechanics of the patellofemoral joint. To facilitate this investigation, a statistical shape model was employed to generate a range of patella shapes and heights. These morphologies were integrated into a musculoskeletal model featuring a knee joint with twelve degrees of freedom. The findings indicated that variations in patella morphology and height influenced biomechanical outcomes, specifically demonstrating increased patella ligament forces associated with greater patella heights and a higher quadriceps tendon force to patella ligament force ratio in cases where the patella had a sharper apex (20).

1.4.2.3 Shape of the femoral trochlea and position of the tibial tubercle

Clouthier et al. (23) utilized statistical shape modeling and musculoskeletal simulations to explore the effects of patellofemoral geometry and tibial tubercle location on patellofemoral biomechanics. Employing a Monte Carlo approach, the researchers randomly generated 750 knee geometries featuring variations in trochlea grooves and tibial tubercle positions. The findings indicated that shallow trochlea geometries were particularly sensitive to medialization of the tubercle, leading to significant alterations in lateral position and increased contact pressure. Additionally, knees with a deep trochlea geometry exhibited more pronounced increases in medial cartilage contact pressure following medialization (23).

In another study, Clouthier et al. (25) investigated the impact of trochlea groove depth and simulated tibial tubercle osteotomy using a combination of statistical shape modeling and a Monte Carlo approach to generate 750 musculoskeletal models. To assess patellofemoral stability, a 200 N lateral force was applied to the patella during early stance, and the resultant lateral displacement was measured. The results demonstrated that knees with a shallow trochlea groove experienced increased instability following either medial or lateral displacement of the tibial tubercle. Moreover, a greater transfer of the tibial tubercle

emphasized the increased importance of the medial patellofemoral ligament in maintaining patellofemoral stability. These findings underscore the significance of considering joint geometry in surgical planning (25).

1.4.2.4 Femoral anteversion

Besier et al. (21) employed finite element models of the patellofemoral joint, constructed using MR images from 16 individuals, to explore the effect of femoral version on patellofemoral loading. The subjects performed squats both in an open MR scanner and a gait laboratory. The study found that cartilage stress was more sensitive to external femoral version, although there was considerable variability among individuals. These individual differences should be considered when devising treatment strategies aimed at reducing cartilage load through alterations in femoral version (21).

Wheatley et al. (22) conducted a study to examine the impact of femoral anteversion on the loading of the patellofemoral joint, utilizing musculoskeletal modeling. They created models featuring varying degrees of femoral version. Additionally, based on the gait pattern of a single healthy participant, they generated slightly varied gait patterns using a Monte Carlo algorithm to modify muscle activations. The findings indicated a correlation between femoral version and patellofemoral joint loading, particularly affecting the ratio between lateralizing forces and the resultant force on the patellofemoral joint. Specifically, an increase in femoral anteversion was associated with an increase in lateralizing force (22).

Passmore et al. (189) conducted a study on knee joint loadings in a cohort of 12 children and adolescents diagnosed with an idiopathic torsional deformity of the femur. Utilizing musculoskeletal simulations, the research revealed that an increased femoral anteversion could significantly elevate lateralizing forces within the patellofemoral joint (189).

1.5 Summary of gap of knowledge / Research questions

Numerous studies employed musculoskeletal modeling to investigate variables affecting patellofemoral instability (19–25,205). A shared limitation among these studies is their omission of subject-specific gait patterns in individuals with patellofemoral instability. Moreover, none of these investigations have assessed the impact of overall lower limb torsion and related treatment strategies on the patellofemoral joint loading and stability of the patellofemoral joint in a cohort of patients with patellofemoral instability. In light of these gaps, this work focused on the following research questions.

1.5.1 Research question 1: Impact of gait patterns on patellofemoral joint loadings

The first research question aimed to examine the impact of individual gait patterns on knee joint loading among individuals with patellofemoral instability. The hypothesis suggested that these individuals might modify their gait patterns as a strategic adaptation to reduce the risk of patella dislocations. This was hypothesized to be achieved through gait modification that led to alterations in the patellofemoral joint reaction forces.

The paper related to this research question has been published in Nature Portfolio Scientific Reports: Guggenberger B, Horsak B, Habersack A, Kruse A, Smith CR, Kainz H, et al. Patient-specific gait pattern in individuals with patellofemoral instability reduces knee joint loads. Sci Rep. 2024 Nov 18;14(1):28520. (1).

1.5.2 Research question 2: Impact of femoral and tibial torsion on patellofemoral joint loading

The second research question aimed to investigate the influence of lower limb torsion on patellofemoral joint loading in individuals experiencing patellofemoral instability. The hypothesis posited that internal femoral version and external tibial torsion are associated with an increase in lateralizing joint reaction forces within the patellofemoral joint. A secondary objective aimed to investigate how neglecting tibial torsion, as done in previous cadaver (96) and musculoskeletal simulation studies (22,189), affects the findings.

The manuscript related to this research question is under review at Wiley Journal of Orthopaedic Research: Guggenberger B, Koller W, Habersack A, Kraus T, Sperl M, Svehlik M, Kainz H. Impact of femoral and tibial torsion on patellofemoral loading in individuals with patellofemoral instability.

1.5.3 Research question 3: Impact of femoral derotation osteotomy on the patellofemoral joint loading

The third research question focused on the effects of femoral derotation osteotomy (FDO) on patellofemoral joint loading in individuals with patellofemoral instability. The hypothesis was that the FDO will result in a reduction of medio-lateral patellofemoral joint loading.

The manuscript related to this research question is currently under preparation for submission to The Joint and Bone Surgery Journal: Guggenberger B, Kainz H, Kraus T, Svehlik M. Femoral derotation osteotomy medially shifts patellofemoral loading in individuals with patellofemoral instability: insights from a simulation-based study.

2 Methods

2.1 General Methods

To address the research questions of this thesis, musculoskeletal simulations were performed with a retrospective data set incorporating three-dimensional motion capturing data and MR images retrieved from the clinical databases at the Medical University of Graz. The specific inclusion criteria varied across the performed studies addressing the research questions. The ethical review board at the Medical University of Graz (IRB00002556, 34-181 ex 21/22) granted approval for this research.

Optoelectronic three-dimensional gait analysis data were acquired using a ten-camera infrared-based motion capture system (Vicon Motion Systems, Oxford, UK) with a sampling rate of 120 Hz. Data collection was facilitated through the utilization of either the lower-body plug-in gait marker set (55,57) or the lower-body part of the modified Cleveland marker set (56). Those two marker sets only differ in their thigh and shank marker configurations. Both sets incorporate one marker at the sacrum, one marker on each spina iliaca anterior superior, lateral femoral condyle, lateral malleolus, head of the second metatarsal caput and calcaneus. Furthermore, the plug-in gait marker set incorporates one marker on the thigh and shank, whereas the modified version of the Cleveland marker set uses a cluster of three markers on each thigh and shank segment (Figure 11). Different marker sets were used due to a change in the gait lab routine in 2018. Marker sets were mixed in the study cohorts as the use of an inverse kinematics approach in musculoskeletal simulations is robust against variations in marker sets when calculating joint kinematics. Hence, differences in the marker set should only lead to neglectable differences in the simulation outcomes (1,169).

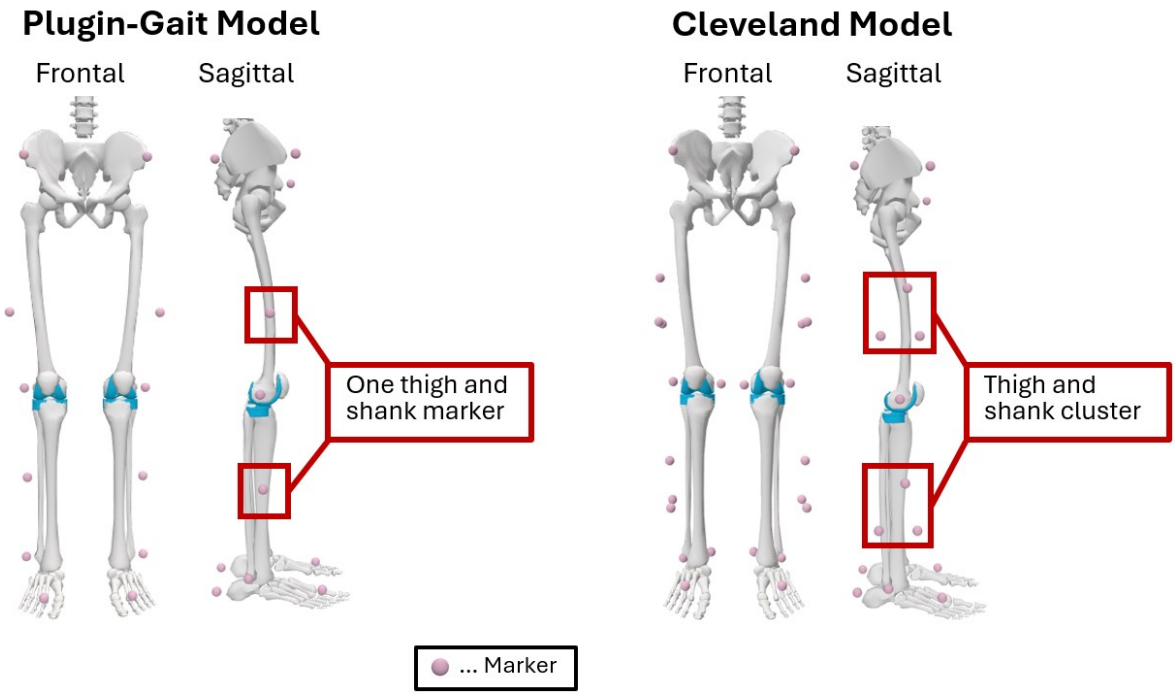

Figure 11: Three-dimensional motion capturing marker sets. Each pink dot represents one marker. The plugin-gait marker set (left) incorporates one marker on each thigh and shank. The modified Cleveland model (right) uses a marker cluster on each thigh and shank. This figure was created by the author of this thesis.

The centers of the hip joints were determined using a modified version of the Harrington equation (206) with the pelvis width obtained from the marker data as an input (207). Hip joint centers were used to scale the length of the femur individually for each participant. Ground reaction forces were recorded synchronously with kinematic trajectories using four force plates, which operated at a sampling rate of 1080Hz (Advanced Mechanical Technology Inc., Watertown, MA, USA). The threshold for force plate activation was set at 15 N of vertical force, and gait events were automatically detected for each trial. Trials in which full foot contact on one force plate did not occur were excluded from analysis.

Where available, knee MR scans were used to determine radiographic measurements to classify patellofemoral joint morphology. Furthermore, rotational MR scans were utilized to measure femoral version and tibial torsion. The femoral version was quantified based on methodologies outlined by Schneider et al. (110) and Guenther et al. (111). Measurement of tibial torsion was conducted in accordance with the technique described by Rosskopf et al. (112).

2.2 Methods study 1: Impact of gait patterns on patellofemoral joint loadings

The methods described in this chapter are based on the study Guggenberger et al. (1).To investigate the first research question musculoskeletal simulations were performed with a retrospective data set to explore the effects of gait patterns on knee joint loading, and patellofemoral contact pressure, by comparing individuals diagnosed with patellofemoral instability and a control group comprising typically developing subjects.

2.2.1 Participants and retrospective data

The inclusion criteria contained an age range of 10 to 18 years and a diagnosis of unilateral recurrent patellofemoral instability, characterized by a minimum of three patellar dislocations. Individuals presenting additional lower limb injuries or neurological disorders were excluded from participation. Over the decade spanning 2010 to 2020, a total of 256 individuals with patellofemoral instability received treatment at the pediatric orthopedic center of the Medical University of Graz. Of these, 45 patients who had experienced three or more patellar dislocations were referred to gait analysis. From this subset, 24 patients were subsequently excluded due to reasons including bilateral involvement (N = 16), other knee injuries (N = 3), neurological conditions (N = 1), or suboptimal data quality (N = 4). Consequently, the study incorporated three-dimensional gait analysis data, specifically marker trajectories and ground reaction forces, from 21 individuals diagnosed with unilateral recurrent patellofemoral instability.

The control group comprised 17 typically developing adolescents. Inclusion criteria for the control group mandated an age range of 10 to 18 years and the absence of any injuries to the lower extremities. Efforts were made to ensure that the sex and age distribution within the control group match closely with those of the participants in the patellofemoral instability group. Gait analysis data of the patellofemoral instability group were available captured with the plug-in gait marker set (55,57), whereas the control group's gait analysis data were available captured with the modified Cleveland marker set (56).

2.2.2 Musculoskeletal simulation

A generic musculoskeletal OpenSim model developed by Lenhart et al. (152) was scaled to the anthropometric dimensions of each participant utilizing three-dimensional motion capture data (208). This model incorporated 14 ligament bundles, a tibiofemoral and patellofemoral joint each with six degrees of freedom, as well as cartilage surfaces for those joints (152). The maximum isometric muscle forces of the musculoskeletal models were scaled in proportion to

the square of each participant's body height (scaling factor = participant's squared body height / generic model's squared body height) (167).

Due to the limited number of markers placed on the foot segment in both marker sets, the metatarsophalangeal and subtalar joints were locked in all musculoskeletal models. This is a common practice that has been used in previous studies (17,209). Notably, all models facilitated ankle plantar- and dorsiflexion.

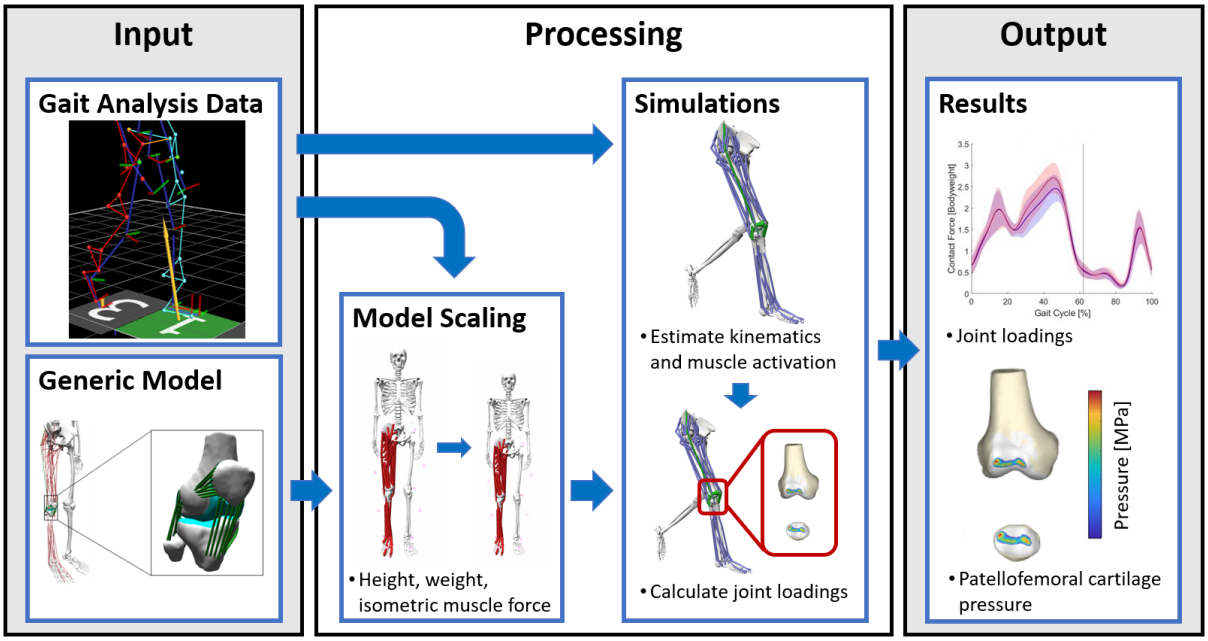

Figure 12: Schematic simulation workflow. Initial input data comprised gait analysis data alongside a generic model. This model was subsequently adapted for each subject by scaling parameters such as height, weight, and maximum isometric muscle force. The concurrent optimization of muscle activation and kinematics routine was employed to estimate joint kinematics, joint kinetics, and muscle forces. Subsequent calculations were performed to determine joint contact forces and patellar cartilage pressure. Reproduced from (1). © 2024 Guggenberger et al.. The figure was published in an open-access article distributed under the terms of the Creative Commons CC BY license 4.0 (http://creativecommons.org/licenses/by/4.0/).

This study involved the computation of joint angles, external joint moments, muscle forces, joint contact forces, and patellofemoral contact pressures. Musculoskeletal simulations were conducted employing scaled models of each participant alongside their respective gait data (Figure 12). Primary kinematics, including pelvic motion, hip flexion, hip abduction, and internal/external rotation of the hip, as well as knee and ankle flexion, were determined by inverse kinematics, which minimized the weighted sum of squared differences between the position of experimental and model markers. External joint moments were calculated based on inverse dynamics. The COMAK routine (182,183) was utilized to simultaneously estimate muscle activations and secondary knee kinematics, by minimizing the weighted sum of muscle activations and contact energy. Based on the obtained muscle forces joint reaction loadings were calculated (176). Cartilage contact pressures were estimated utilizing an elastic

foundation model (162–164). The elastic modulus and Poisson's ratio for the cartilage were established at 5 MPa and 0.45, respectively (210,211). Furthermore, a uniform cartilage thickness of 3 mm on each joint surface of the tibiofemoral and patellofemoral joint was chosen (152,212).

2.2.3 Data analysis

To explore the effects of gait patterns on knee joint loading, and patellofemoral contact pressure the following data analysis was performed. Each gait cycle was time-normalized to 101 discrete points, ranging from 0 to 100 % of the gait cycle. Ground reaction forces, external moments, contact forces, and contact pressures were normalized to the body weight (body weight = body mass × gravitational acceleration) of each participant. A minimum of five gait cycles were processed and subsequently averaged for each participant. Discrete parameters were computed prior to the averaging of curves and were averaged separately. Statistical analyses of these discrete parameters were conducted using SPSS v27 (IBM, New York, USA) and MATLAB (The Mathworks Inc., Natick, MA, USA). To compare the waveforms between the patellofemoral instability group and the control group, Statistical Parametric Mapping (213), specifically the SPM1D package for MATLAB (available at http://www.spm1d.org), was employed.

The study also included a comparison of gait kinematic and knee joint loading waveforms across the sagittal, frontal, and transversal planes, as well as the muscle force waveforms of the rectus femoris, vastus medialis, and vastus lateralis between the patellofemoral instability and control groups. Given the pattern of patella dislocations, which typically occur during the initial phase of single support stance (characterized by knee flexion up to 30 degrees and quadriceps contraction), additional investigations were conducted into the maximum tibiofemoral and patellofemoral joint forces and patellofemoral cartilage pressure at this time point.

To evaluate discrete parameters, including demographic data, spatiotemporal gait parameters, and the peak knee joint contact forces and patellofemoral contact pressures at the onset of the single support stance phase, a structured analytical procedure was implemented. Initially, the Shapiro-Wilk test was utilized to assess the normality of distributions within each group (214). Depending on the outcome, data that followed a normal distribution were compared using independent t-tests, whereas non-normally distributed data were analyzed using the Mann-Whitney U tests (215,216). Additionally, Cohen’s d was calculated to estimate the effect size (217).

For the analysis of ground reaction force, joint kinematics, external moments, knee joint contact forces, and contact pressure waveforms between individuals with patellofemoral

instability and the control group, normality was verified using the normality test within the SPM1D package. For data adhering to normal distribution, the parametric version of the two-tailed t-test was applied, while for non-parametric data, the corresponding non-parametric test was employed. The significance level was set at an alpha of 0.05. To account for multiple comparisons, Bonferroni corrections were applied at different parameter levels (218). Specifically, for the comparison of patellofemoral cartilage pressure waveforms between both groups, resulting p-values were adjusted for three family-wise comparisons: peak pressure, mean pressure, and pressure area. Comparisons of the tibiofemoral and patellofemoral joint contact force waveforms were corrected separately for three family-wise comparisons: vertical, anterior-posterior, and medio-lateral forces. For the maximum values of joint contact forces and maximum values of patellofemoral cartilage pressure within the first 30 % of the stance phase, resulting p-values were adjusted in accordance with the corresponding waveforms for three family-wise comparisons: vertical, anterior-posterior, and medio-lateral tibiofemoral forces; and vertical, anterior-posterior, medio-lateral patellofemoral forces; along with peak pressure, mean pressure, and pressure area.

2.3 Methods study 2: Impact of femoral and tibial torsion on medio-lateral patellofemoral joint loading

To investigate the second research question, musculoskeletal simulations were conducted using a retrospective dataset, which comprised three-dimensional gait analysis data and rotational MR scans from individuals diagnosed with patellofemoral instability. The primary objective was to investigate the impact of femoral version and tibial torsion on the patellofemoral joint loading. The secondary objective was to evaluate the influence of femoral version, when neglecting tibial torsion, as done in previous cadaver (96) and musculoskeletal simulation studies (22,189). The primary outcome measure was the medio-lateral joint reaction force exerted on the patellofemoral joint.

2.3.1 Participants and retrospective data

The inclusion criteria for the second research question were defined as the availability of three-dimensional gait analysis data, rotational MR images, and a history of recurrent patellofemoral instability (at least three patella dislocations). Individuals presenting with additional leg injuries or neurological disorders were excluded from participation. Overall, 277 individuals were found in the clinical database of the Medical University of Graz receiving treatment for patellofemoral instability between the years 2010 and 2022. Of those, 66 were referred to gait analysis. Further, 26 were excluded due to missing rotational MR data (N = 18) other knee injuries

(N = 3), neurological conditions (N = 1), or suboptimal data quality (N = 4), resulting in a total of 40 individuals being included in the study.
Gait analysis data of the participants were available captured with the plug-in gait marker set (N = 32) (55,57), or the modified Cleveland marker set (N = 8) (56).
Retrospective available rotational MR scans were used to quantify femoral version (110,111) and tibial torsion (112).

2.3.2 Musculoskeletal simulations

For each participant, three distinct models were developed (Figure 13). The first model, termed the generic-torsion model, was a scaled modified version of the Rajagopal model (159). The modified Rajagopal model is a version of the Rajagopal model (143) incorporating the more complex multi-compartment knee joint from the Lerner model (151). This generic-torsion model was characterized by a femoral version of 21 degrees and tibial torsion of 24 degrees. The second model, the torsion-informed model, was based on the same generic framework but incorporated personalized femoral version and tibial torsion values derived from rotational MR data. The third model, referred to as the femoral-version model, was similarly based on the generic model but personalized only in terms of the femoral version. The Torsion Tool (155) was employed to customize the femoral version and tibial torsion in the second and third models. Each model was scaled to match the participant's anthropometry using data from three-dimensional motion capture (208). Maximum isometric muscle forces were adjusted for each participant based on squared body weight (scaling factor = participant's squared body weight / generic model's squared body weight) (165,166).
Due to the limited number of markers placed on the foot segment in both marker sets, the metatarsophalangeal and subtalar joints were locked in all musculoskeletal models. This is a common practice that has been used in previous studies (17,209). Notably, all models facilitated ankle plantar- and dorsiflexion.

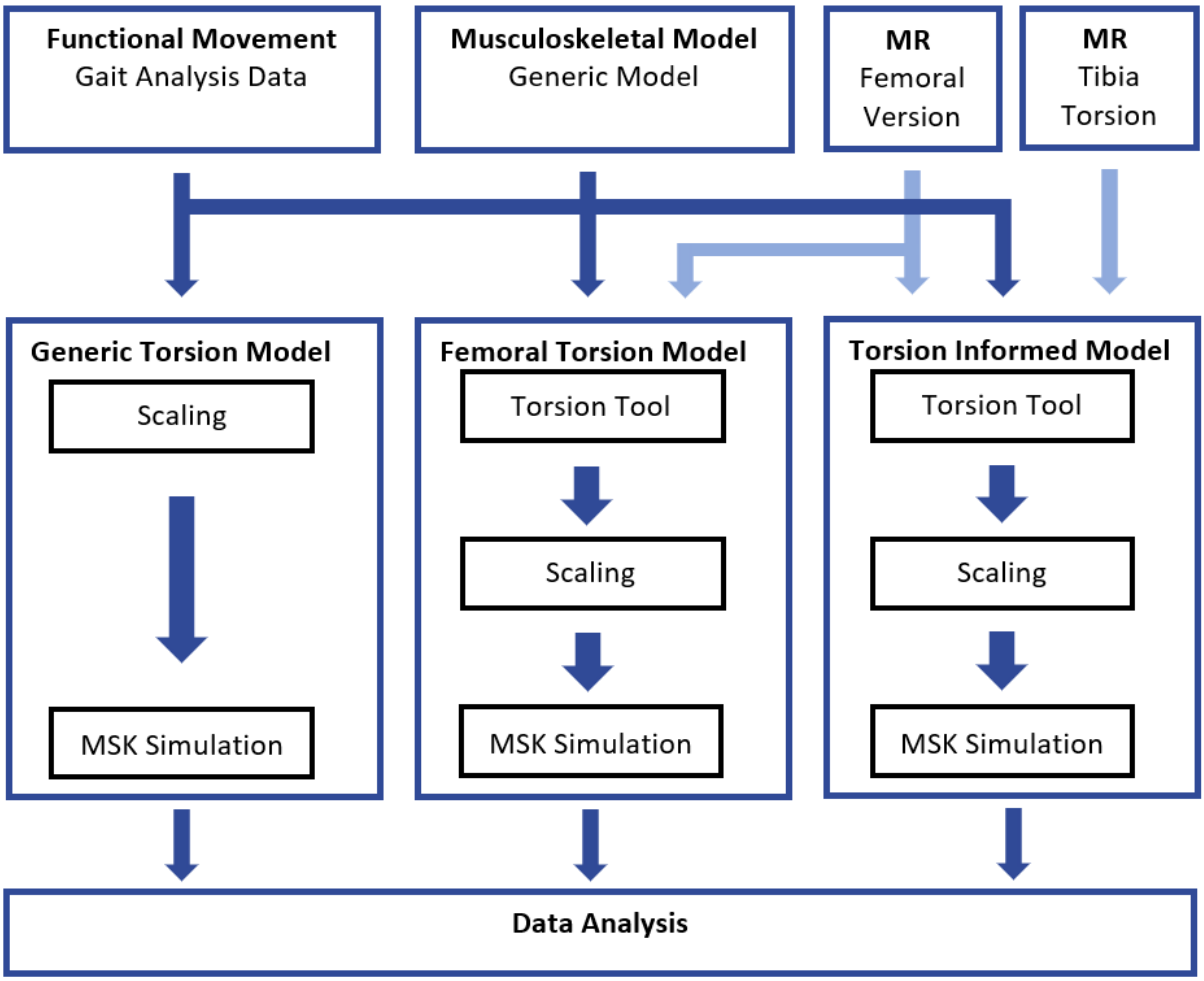

Figure 13: Schematic simulation workflow. The workflow integrates gait analysis data and the generic modified Rajagopal model as inputs for all three models. Additionally, MR data were utilized for personalizing the femoral-version and torsion-informed models. For each participant three models were processed: 1.) Generic-torsion model: Scaled to each participant's anthropometry and followed by musculoskeletal simulations. 2.) Femoral-version model: Personalized according to the femoral version derived from MR data, scaled, and subjected to musculoskeletal simulations. 3.) Torsion-informed model: Customized to include both femoral version and tibial torsion as per MR data, scaled, and then musculoskeletal simulations are conducted. Abbreviations: MSK = Musculoskeletal. This figure was created by the author of this thesis.

Musculoskeletal simulations were performed for each participant using the three models in OpenSim 4.4. (Figure 13) (16). Inverse kinematics and inverse dynamics were utilized to determine joint angles and moments, respectively. Static optimization was applied to estimate muscle activations and forces. Subsequently, joint reaction loads were computed from these results (176). Comparative analyses of knee joint loading, muscle forces, and hip muscle lever arms during walking were conducted between the generic-torsion model and the torsion-informed models for each participant.

2.3.3 Data analysis

To investigate the impact of femoral version and tibial torsion on the patellofemoral joint loading the following data analysis was performed. For each participant, a minimum of three gait cycles from the affected side were simulated and subsequently averaged. In cases of bilateral patellofemoral instability, one leg was selected at random for simulation. The results of the musculoskeletal simulations were time-normalized to span the entire gait cycle duration (0-100 %). Additionally, patellofemoral joint contact forces and muscle forces were normalized to the body weight (body weight = body mass × gravitational acceleration) of each participant. Given the tendency for patellar dislocations to occur during early stages of knee flexion and under quadriceps muscle contraction (49), the analysis was concentrated on the initial 20 % of the gait cycle, corresponding to the loading response and first single stance phase. The analysis focused on three specific patellofemoral loading parameters during this phase: (i) maximum medio-lateral patellofemoral force, (ii) root mean square (RMS) of medio-lateral patellofemoral force, and (iii) maximum resultant patellofemoral joint reaction force. Individuals with patellofemoral instability walk with variations in their gait pattern (26,64) and this can alter the loading of the patellofemoral joint (1). To mitigate potential confounding factors, such as variability in gait patterns, differences in joint reaction forces between the generic-torsion model and the corresponding personalized torsion model (either torsion-informed or femoral-version model) were calculated (Figure 14).

Correlation analyses were conducted to explore relationships between morphological parameters and simulation results (differences between models). These analyses were performed using MATLAB 2022a (Mathworks Inc., Natick, MA, USA) and SPSS 29 (IBM, New York, USA), employing Spearman correlations to ascertain the robustness of the analysis. The level of significance was set at an alpha of 0.05.

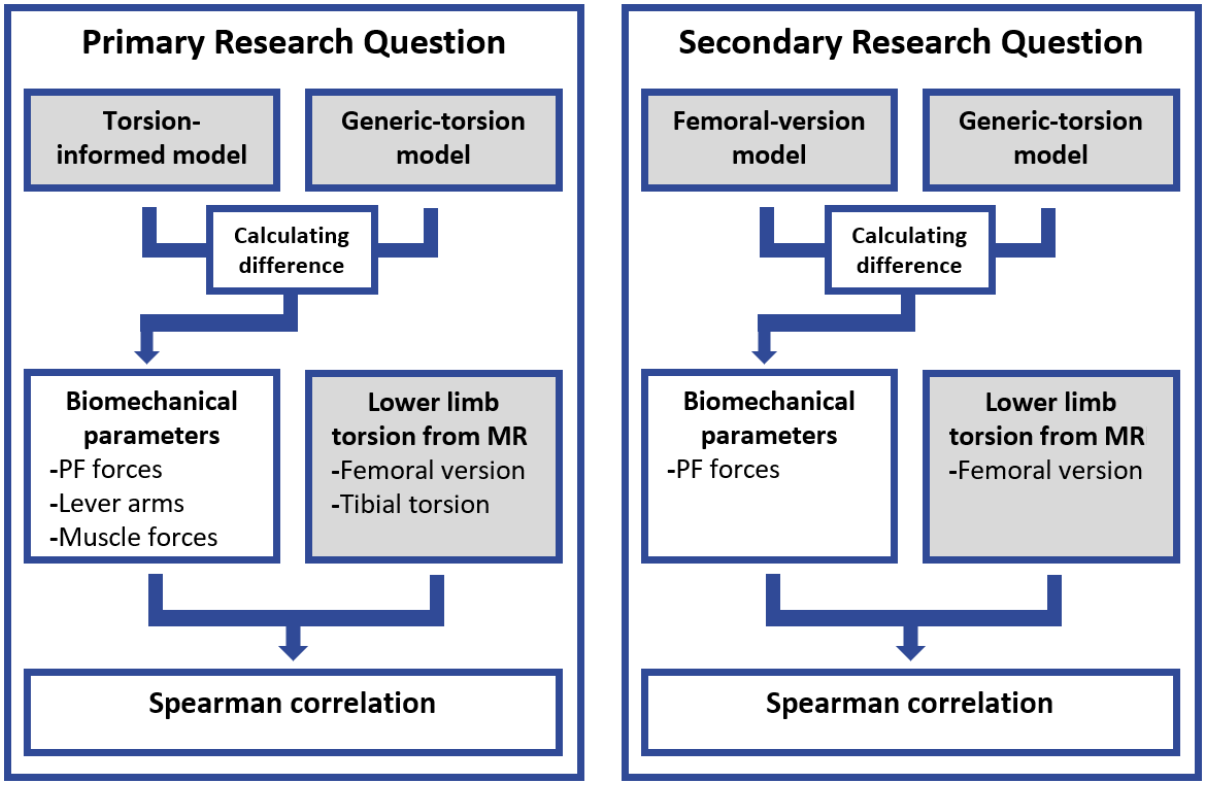

Figure 14: Schematic representation of data analysis. This figure outlines the analytical framework employed in the study. For the primary research question, differences in patellofemoral joint reaction forces, hip muscle lever arms, and muscle forces between the torsion-informed model and the generic-torsion model were quantified. Subsequently, Spearman correlations were performed to assess the relationships between these biomechanical parameters and anatomical variables, specifically femoral version and tibial torsion. For the secondary research question, differences in patellofemoral joint reaction forces between the femoral-version model and the generic-torsion model were computed. Following this, Spearman correlations were conducted to explore the association between the patellofemoral joint reaction forces and femoral version. Calculating differences between simulation results facilitates a targeted investigation of the influence of specific anatomical parameters on biomechanical outcomes. Abbreviations: PF = Patellofemoral. This figure was created by the author of this thesis.

The following correlation analyses were conducted to test the hypotheses. The primary objective focused on examining the impact of lower limb torsion (femoral version and tibial torsion) on patellofemoral joint loading. For this purpose, differences in patellofemoral force between the generic-torsion model and the torsion-informed model were correlated with the femoral version and tibial torsion values. Furthermore, tibial torsion and femoral version were correlated to differences in hip rotation, hip flexion, knee progression, and knee flexion angles observed between the generic-torsion models and the torsion-informed models. The secondary objective aimed to assess the implications of omitting tibial torsion from the analysis. Here, differences in patellofemoral force between the generic-torsion model and the femoral-version model were correlated with femoral version values. Subsequently, results from the primary and secondary objectives were compared to evaluate how the exclusion of tibial torsion influences the conclusions of the study.

To explore the potential relationship between femoral version, tibial torsion, and patellofemoral loading, a multiple linear regression analysis was conducted. This analysis assessed the

differences in maximum patellofemoral loading between the generic-torsion and torsion-informed models.

Additionally, to examine the forces exerted, the patellofemoral forces calculated in the torsion-informed model were correlated with tibial torsion and femoral version. Furthermore, another multiple linear regression analysis was performed to evaluate the maximum patellofemoral loading in the torsion-informed model, utilizing femoral version and tibial torsion as independent variables.

Previous simulation-based research has indicated that femoral version influences the lever arms and muscle forces of several hip muscles (22,157,189). Building on this, the current study also explored the effects of femoral version and tibial torsion on the lever arms of hip muscles. Correlations were performed between the differences in mean lever arms and RMS of muscle forces between the generic-torsion model and the torsion-informed model, and the femoral version and tibial torsion values. Previous to this analysis RMS muscle forces were normalized to participants' body weight. This comprehensive analysis aims to provide a deeper understanding of the biomechanical interactions influenced by anatomical variations in the lower limbs.

2.4 Methods study 3: Impact of femoral derotation osteotomy on the patellofemoral joint loading

To address the third research question musculoskeletal simulations were performed based on the retrospective data set. For each participant two distinct musculoskeletal models were created: (i) a personalized model informed by torsional data derived from medical imaging, and (ii) an identical model that additionally incorporated a simulated FDO. The primary outcome measure was the medio-lateral joint reaction force exerted on the patellofemoral joint.

2.4.1 Participants and retrospective data

The participants included into the second study, which investigated the impact of femoral version and tibial torsion on the patellofemoral joint loading (2.3.1 Participants and retrospective data) were screened for their femoral version angle. All participants with a femoral version greater than 30 degrees were included into this study. A femoral version angle of 30 degrees was selected, as it was identified as a potential threshold for considering FDO in patients exhibiting patellofemoral instability (135,219). Following these criteria, the study encompassed 16 participants diagnosed with patellofemoral instability.

Gait analysis data of the participants were available captured with the plug-in gait marker set (N = 15) (55,57), or the modified Cleveland marker set (N = 1) (56). Retrospective available rotational MR scans were used to quantify femoral version (110,111) and tibial torsion (112).

2.4.2 Musculoskeletal simulations

For each participant, two individualized models were developed using MR and three-dimensional motion capture data (Figure 15). The initial model, (pre-surgery model), was a scaled adaptation of the modified Rajagopal model (159), which is the Rajagopal model (143) with integrated multi-compartment knee joint structure from the Lerner model (151). Personalization of femoral version and tibial torsion for each participant and model was achieved by adjusting for the individual's lower limb torsion, employing the Torsion Tool for OpenSim (154,155). The subsequent model retained the same personalization but incorporated a simulated FDO on the side with patellofemoral instability, setting the femoral version to 12 degrees (post-surgery model). This adjustment to 12 degrees reflects the mean femoral version post-FDO in patients with patellofemoral instability, as established in a systematic review (135). Additionally, the maximum isometric muscle forces for each model were scaled based on the square of the body weight (scaling factor = participant's squared body weight / generic model's squared body weight) (165,166).

Due to the limited number of markers placed on the foot segment in both marker sets, the metatarsophalangeal and subtalar joints were locked in all musculoskeletal models. This is a common practice that has been used in previous studies (17,209). Notably, all models facilitated ankle plantar- and dorsiflexion.

Musculoskeletal simulations were executed using OpenSim (16) for each participant utilizing gait analysis data and the two models (pre-surgery and post-surgery) as delineated in Figure 15. Inverse kinematics and inverse dynamics were used to calculate joint angles and moments, respectively. To estimate muscle forces, static optimization was applied, which minimized the sum of squared muscle activations (180). Subsequently, joint reaction analysis was employed to determine joint contact forces (176).

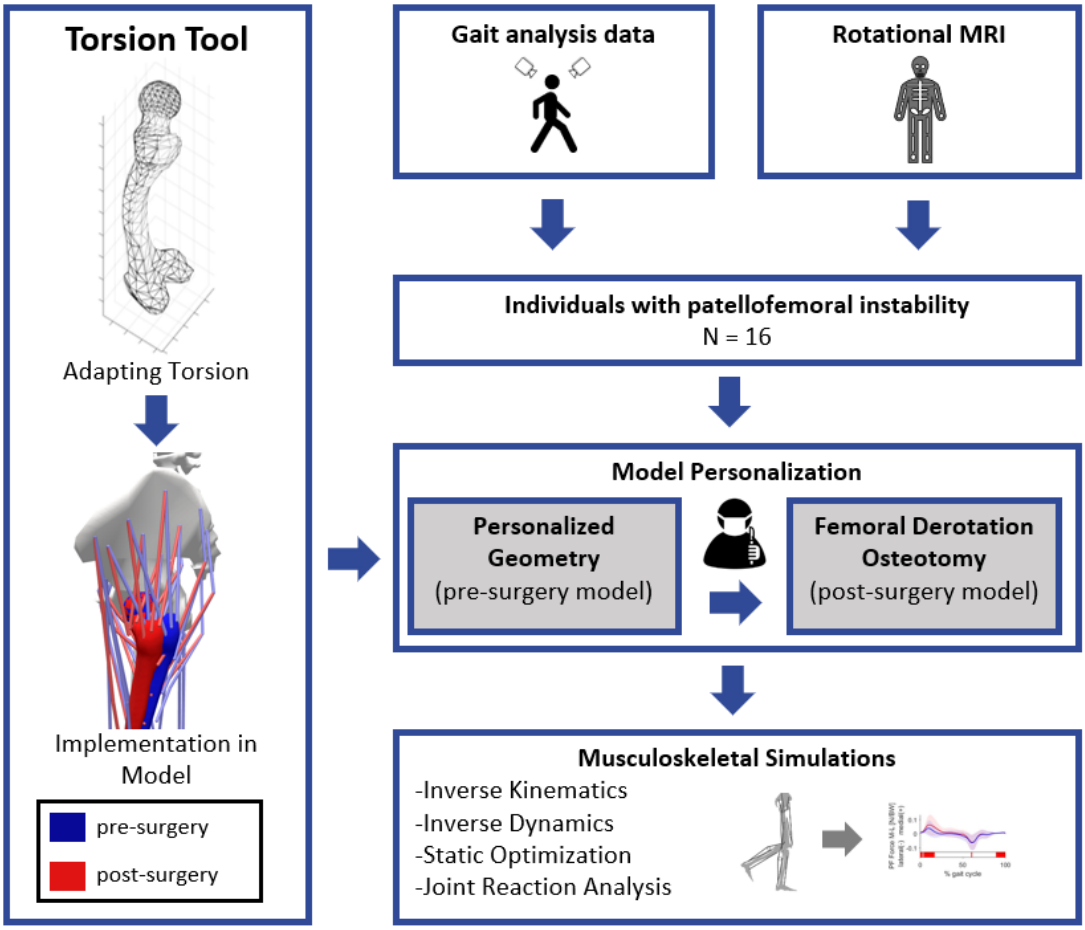

Figure 15: Schematic representation of model generation and simulation workflow. For each participant, two distinct models were created. Personalization of each model was achieved by adjusting for femoral version and tibial torsion, utilizing the Torsion Tool depicted on the left side of the figure. At the bottom in the Torsion Tool box, the elements colored in blue symbolize the femur and associated musculature (represented as strings) prior to surgery, whereas the structures in red denote the femur and muscles post-surgery. Notably, in the post-surgery model, the femoral version on the affected side was adjusted to 12 degrees. Each model was then scaled to match the individual anthropometry of the participants. Following these adjustments, musculoskeletal simulations were conducted using OpenSim. This figure was created by the author of this thesis.

2.4.3 Data analysis

To investigate the effect of FDO on patellofemoral joint loading in individuals with patellofemoral instability the following data analysis was performed. For each participant and corresponding model, a minimum of three gait cycles were simulated. The waveforms derived from these simulations were time-normalized to the duration of a gait cycle, ranging from 0 to 100 %, and subsequently averaged across all trials. Joint moments, muscle forces, muscle moments, and joint loads were normalized relative to body weight (body weight = body mass × gravitational acceleration). To assess differences between the pre- and post-surgery model waveforms, statistical parametric mapping was employed using the SPM1D package within MATLAB (available at http://www.spm1d.org). The Shapiro-Wilk test was utilized to verify the normality of data distributions (214). In instances of non-normal distribution, non-parametric

equivalents of the statistical tests were applied. Correlational analyses were conducted using Pearson correlation coefficients (220). The significance level was set at an alpha of 0.05. For joint force waveforms, analyzed in three anatomical directions (vertical, anterior-posterior, and medio-lateral), the significance threshold was adjusted using a Bonferroni correction, dividing the alpha level by three (218).

The analysis focused on evaluating alterations attributed to FDO in (i) patellofemoral joint forces, (ii) hip muscle moments, and (iii) quadriceps force. Additionally, (iv) successful and unsuccessful FDO cases were comparatively assessed. A successful FDO outcome was defined by a reduction in the lateralizing force at the patellofemoral joint. For cases deemed unsuccessful, further examination was conducted to discern differences in joint kinematics, joint kinetics, and muscle forces in comparison to successful cases. All unsuccessful cases were excluded from the correlation analyses.

In the analysis of patellofemoral joint forces, both waveforms and peak forces were evaluated. Waveforms were examined in the vertical, anterior-posterior, and medio-lateral directions, comparing pre- and post-surgery models. Peak forces were specifically analyzed during the initial single stance phase, which occurs between 5-20 % of the gait cycle. This phase was chosen based on evidence suggesting that patella dislocations frequently occur during scenarios of low knee flexion (0 to 30 degrees), single leg loading, and active quadriceps (49), conditions that are closely replicated during the first single stance phase. The peak medio-lateral patellofemoral joint force was statistically compared between the pre- and post-surgery states using either a dependent t-test or a Wilcoxon test (215,221). Additionally, to explore whether a larger initial femoral version could potentially medialize patellofemoral forces more effectively, a correlation was conducted between the initial femoral version and the change in peak medio-lateral patellofemoral joint contact forces from pre- to post-surgery.

Previous research presented modifications in muscle moment arms associated with internal femoral version, particularly affecting the gluteal muscles (157,189). Consequently, this investigation involved a comparative analysis of gluteal muscle moments, specifically examining flexion and adduction moments between pre- and post-surgery models.

Additionally, the quadriceps forces influence the patellofemoral loading (4,157,222). To assess the impact of FDO on quadriceps muscle force, a correlation was conducted between the change in RMS forces of the rectus femoris, vastus lateralis, and vastus medialis muscles from pre- to post-surgery, and the alteration in peak medio-lateral patellofemoral joint force.

Joint angle waveforms and joint moment waveforms were compared between successful and unsuccessful FDO outcomes to determine if variations in gait pattern influenced the success of the FDO. However, due to the limited sample size of unsuccessful cases (N = 2), no statistical comparisons were conducted between the successful and unsuccessful groups.

3 Results

3.1 Results study 1: Impact of gait patterns on patellofemoral joint loadings

The results presented in this chapter are based on the study Guggenberger et al. (1).The patellofemoral instability group and the control group exhibited no statistically significant differences in demographic and anthropometric measures such as age, sex, height, body weight, and body mass index, as detailed in Table 1. For the patellofemoral instability group, radiographic assessments were conducted on 20 participants, revealing an average Caton-Deschamps index of 1.20 ± 0.14, a tibial tuberosity to trochlear groove distance of 15.6 ± 3.1 mm, a femoral version of 24.5 ± 9.7 degrees, and a tibial torsion of 34.6 ± 8.0 degrees. The classification of trochlear dysplasia among these participants followed the Dejour classification, distributed as type A (N = 7), B (N = 5), C (N = 6), and D (N = 2).

Table 1: Demographic information. The demographic parameters are displayed in the format of mean values accompanied by standard deviations (mean (standard deviation)). Parameters that exhibited statistically significant differences between the groups are emphasized in bold. Given that all parameters were normally distributed, they were analyzed using independent t-tests. Abbreviations: PFI = patellofemoral instability Reproduced from (1). © 2024 Guggenberger et al.. The table was published in an open-access article distributed under the terms of the Creative Commons CC BY license 4.0 (http://creativecommons.org/licenses/by/4.0/).

	PFI Group	**Control Group**	**p-Value**	**Cohen's d**
Age [years]	15.6 (1.8)	15.2 (1.2)	0.370	0.28
Sex [male/female]	3/18	3/14		
Height [m]	1.6 (0.1)	1.7 (0.1)	0.529	0.21
Body Weight [kg]	61.1 (11.9)	60.7 (11.2)	0.905	0.04
Body-Mass-Index	21.4 (3.9)	21.7 (3.3)	0.867	0.06
Cadence [1/min]	112.1 (9.9)	111.1 (5.8)	0.734	0.11
Stride length [m]	127.2 (8.8)	128.7 (11.1)	0.651	0.15
Step width [cm]	8.3 (1.8)	8.9 (1.4)	0.208	0.42
Gait speed normalized to leg length [1/s]	0.15 (0.01)	0.15 (0.02)	0.800	0.08
Stance phase [%]	**62.5 (1.4)**	**60.7 (1.4)**	**<0.001**	**1.29**
Swing phase [%]	**37.5 (1.4)**	**39.3 (1.4)**	**<0.001**	**1.29**
Loading Response [%]	**11.7 (1.5)**	**9.9 (1.3)**	**<0.001**	**1.28**
Single stance phase [%]	**37.8 (1.6)**	**40.2 (1.5)**	**<0.001**	**1.55**
Pre swing phase [%]	**13.0 (1.5)**	**10.6 (1.5)**	**<0.001**	**1.56**

Gait parameters such as cadence, stride length, step width, and gait speed, normalized to leg length, showed no significant differences between the groups. However, temporal aspects of the gait cycle differed. The patellofemoral instability group exhibited a longer stance phase, and a shorter swing phase compared to the control group. Furthermore, the double supported stance phases, loading response, and pre-swing phase durations were significantly longer, while the single stance phase was shorter in the patellofemoral instability group relative to the control group.

3.1.1 Ground reaction forces

Mediolateral ground reaction forces were significantly reduced in individuals diagnosed with patellofemoral instability compared to healthy controls, while no significant differences were observed in vertical and anterior-posterior ground reaction forces between the groups (Figure 16).

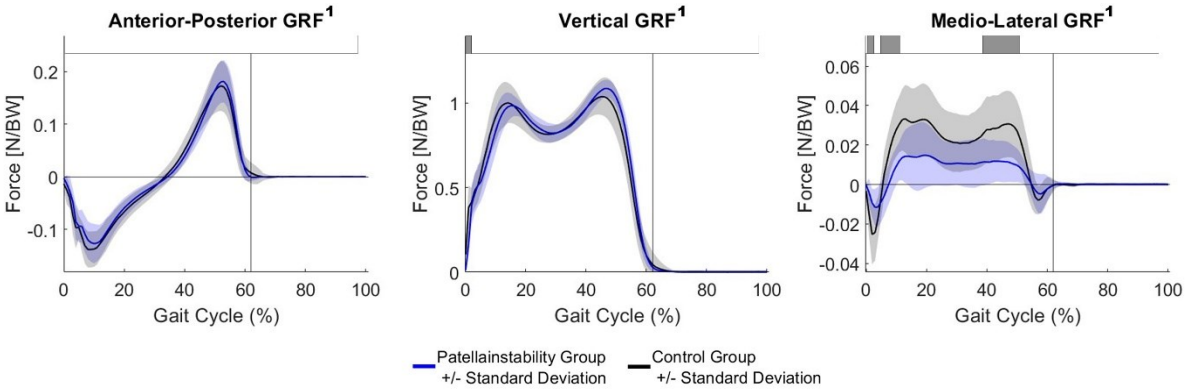

Figure 16: Ground reaction forces. The mean ground reaction forces are represented by the blue line for the patellofemoral instability group and the black line for the control group, with the accompanying one standard deviation for each group. Horizontal grey bars positioned at the top of the graph denote areas where significant differences between the two groups have been identified through statistical parametric mapping. A superscript '1' adjacent to the figure title indicates the non-parametric distribution of waveform data, necessitating the use of a non-parametric version of statistical parametric mapping. This figure was created by the author of this thesis. Abbreviations: BW = body weight, GRF = ground reaction force. Reproduced from (1). © 2024 Guggenberger et al.. The figure was published in an open-access article distributed under the terms of the Creative Commons CC BY license 4.0 (http://creativecommons.org/licenses/by/4.0/).

3.1.2 Joint kinematics

The maximum marker errors associated with the inverse kinematic calculations remained below the recommended best practice thresholds of OpenSim for all study participants (174). During the gait cycle, the patellofemoral instability group demonstrated reduced knee flexion angles during both the loading response and swing phase. Additionally, this group exhibited decreased pelvis and hip abduction at the end of the stance phase, coupled with increased hip internal rotation and knee external rotation (Figure 17).

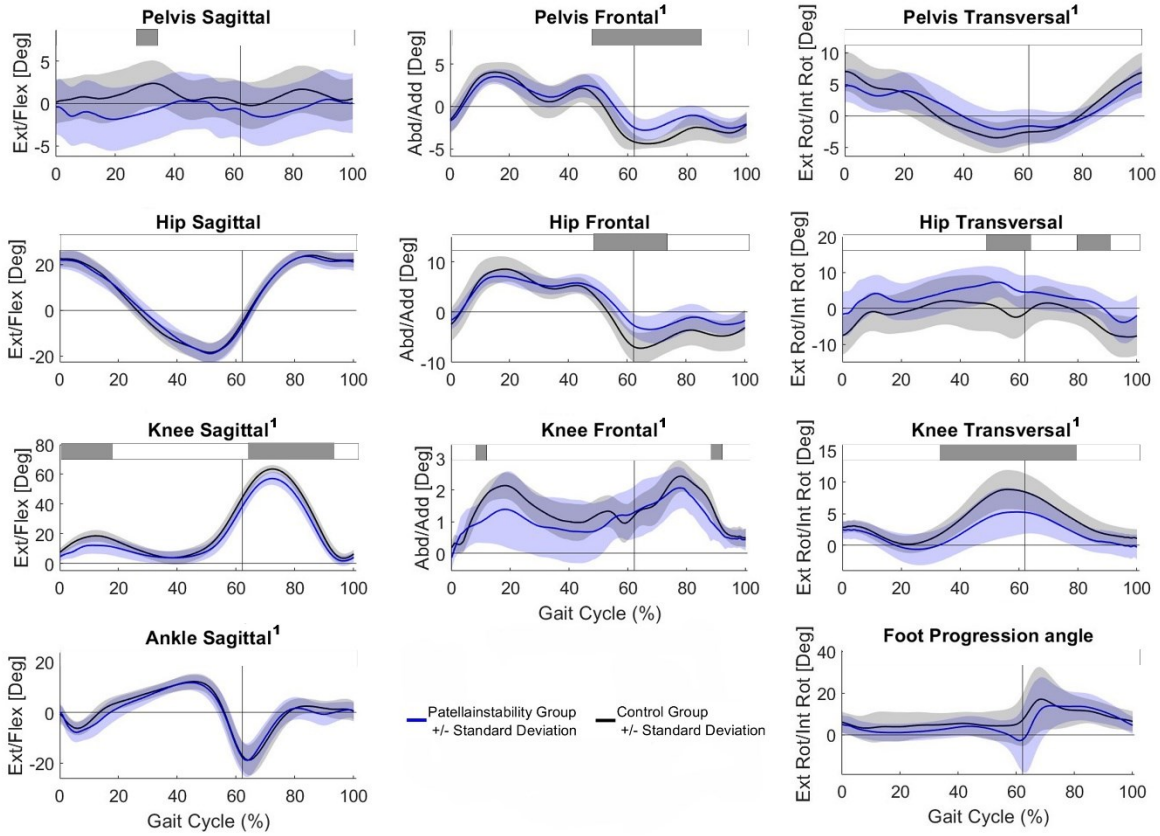

Figure 17: Joint kinematics. The mean joint angles are represented by a blue line for the patellofemoral instability group and a black line for the control group, each accompanied by one standard deviation (SD). Horizontal grey bars at the top of the figure indicate regions where significant differences have been identified between the two groups using statistical parametric mapping. A superscript '1' next to the figure title indicates a non-parametric waveform distribution, necessitating the employment of a non-parametric version of statistical parametric mapping. Reproduced from (1). © 2024 Guggenberger et al.. The figure was published in an open-access article distributed under the terms of the Creative Commons CC BY license 4.0 (http://creativecommons.org/licenses/by/4.0/).

3.1.3 Joint kinetics

The patellofemoral instability group exhibited significantly lower knee flexion moments during the loading response compared to the control group. In the frontal plane, there were reductions in hip abduction and internal rotation moments, as well as knee abduction moments, relative to the control group. Variability in frontal plane moments, as indicated by a larger standard deviation, was also noted during the stance phase in the patellofemoral instability group (Figure 18). Furthermore, joint power was decreased in the patellofemoral instability group during the loading response, midstance, and late swing phase.

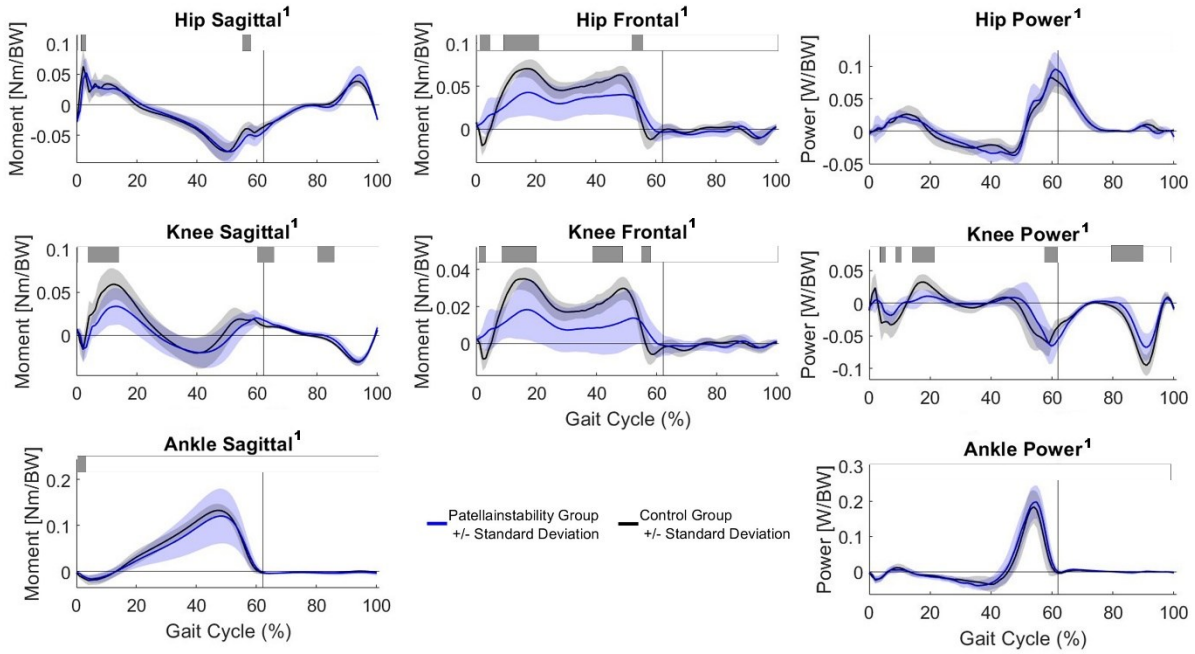

Figure 18: Joint kinetics. The mean moments and power are represented by a blue line for the patellofemoral instability group and a black line for the control group, each accompanied by one standard deviation (SD). Horizontal grey bars at the top of the figure indicate regions where significant differences have been identified between the two groups using statistical parametric mapping. A superscript '1' next to the figure title indicates a non-parametric waveform distribution, necessitating the employment of a non-parametric version of statistical parametric mapping. Reproduced from (1).

3.1.4 Muscle Forces

Significantly lower forces were observed in the rectus femoris, vastus medialis, and vastus lateralis muscles during the loading response in the patellofemoral instability group (Figure 19). Conversely, an increase in vastus medialis muscle force was noted during the early swing phase.

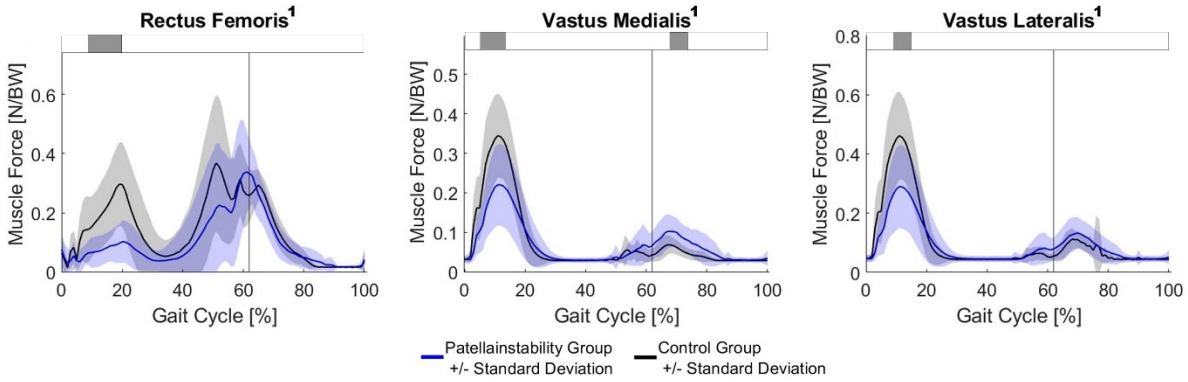

Figure 19: Muscle forces. The mean muscle forces are represented by a blue line for the patellofemoral instability group and a black line for the control group, each accompanied by one standard deviation (SD). Horizontal grey bars at the top of the figure indicate regions where significant differences have been identified between the two groups using statistical parametric mapping. A superscript '1' next to the figure title indicates a non-parametric waveform distribution, necessitating the employment of a non-parametric version of statistical parametric mapping. This figure was created by the author of this thesis. Abbreviations: BW = body weight. Reproduced from (1). © 2024 Guggenberger et al.. The figure was published in an open-access article distributed under the terms of the Creative Commons CC BY license 4.0 (http://creativecommons.org/licenses/by/4.0/).

3.1.5 Joint contact forces and patella cartilage pressure

In the loading response phase, the patellofemoral instability group exhibited lower tibiofemoral and patellofemoral joint contact forces (Figure 20). Additionally, higher patellofemoral joint contact forces were observed at the onset of the swing phase in this group. Although the maximum and mean patellofemoral cartilage pressures, as well as the contact area during the loading response phase, tended to be lower in the patellofemoral instability group compared to the control group, these differences were not statistically significant (Figure 20).

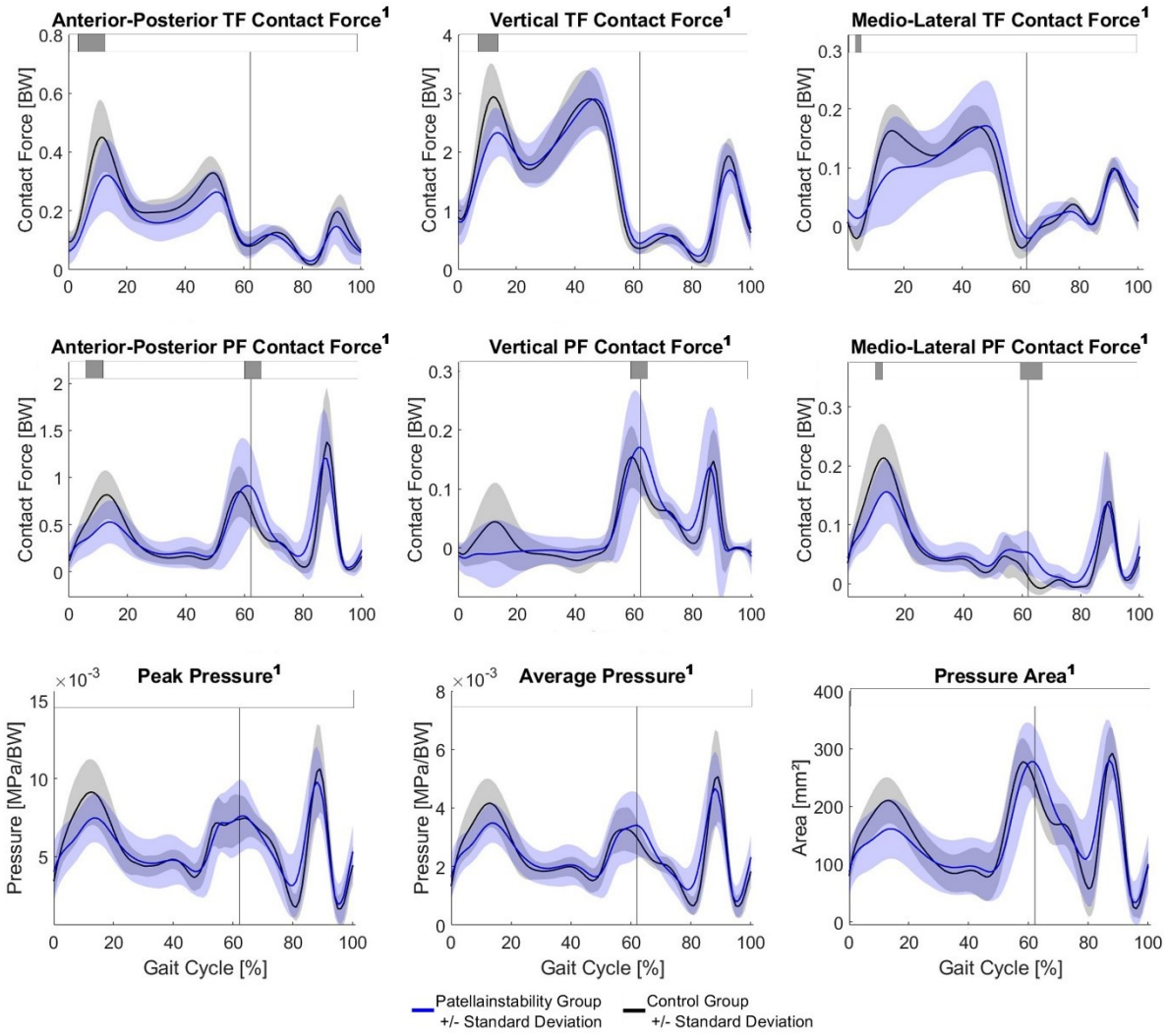

Figure 20: Patellofemoral joint contact forces, cartilage pressure and contact area. The mean forces, pressure and areas are represented by a blue line for the patellofemoral instability group and a black line for the control group, each accompanied by one standard deviation (SD). Horizontal grey bars at the top of the figure indicate regions where significant differences have been identified between the two groups using statistical parametric mapping. A superscript '1' next to the figure title indicates a non-parametric waveform distribution, necessitating the employment of a non-parametric version of statistical parametric mapping. Reproduced from (1). © 2024 Guggenberger et al.. The figure was published in an open-access article distributed under the terms of the Creative Commons CC BY license 4.0 (http://creativecommons.org/licenses/by/4.0/).

3.1.6 Maximum contact forces and maximum patellofemoral contact pressure

During the initial 30 % of the stance phase, which includes the loading response and midstance phases, the patellofemoral instability group showed lower maximum forces and pressures, as well as a reduced maximum contact area, in comparison to the control group (Table 2).

Table 2: Maximum forces and pressure within the first 30 % of the gait cycle. The data are presented in terms of mean values accompanied by standard deviations (mean (SD)). Parameters demonstrating significant differences between the groups are highlighted in bold. Parameters marked with a superscript '1' were not normally distributed and were thus analyzed using the Mann-Whitney U test. Abbreviations: A-P = anterior-posterior, F = force, M-L = medio-lateral, PFI = patellofemoral instability. Reproduced from (1).

	PFI Group	**Control Group**	**p-Value**	**Cohen's d**
Vertical Tibiofemoral F [N/kg]	**2.49 (0.43)**	**3.01 (0.55)**	**0.009**	**1.06**
A-P Tibiofemoral F [N/kg]	**0.33 (0.13)**	**0.46 (0.13)**	**0.012**	**1.01**
M-L Tibiofemoral F[1] [N/kg]	0.13 (0.07)	0.17 (0.05)	0.054	0.66
Vertical Patellofemoral F[1] [N/kg]	0.01 (0.04)	0.05 (0.06)	0.063	0.83
A-P patellofemoral F [N/kg]	**0.55 (0.23)**	**0.84 (0.26)**	**0.003**	**1.19**
M-L patellofemoral F[1] [N/kg]	**0.16 (0.05)**	**0.22 (0.06)**	**0.012**	**1.02**
Peak pressure [MPa/kg]	**0.08 (0.01)**	**0.097 (0.02)**	**0.030**	**0.91**
Mean pressure [MPa/kg]	**0.0036 (0.0006)**	**0.0043 (0.0008)**	**0.027**	**0.89**
Pressure area [mm²]	**164.66 (51.17)**	**212.13 (39.71)**	**0.009**	**1.02**

3.2 Results study 2: Impact of femoral and tibial torsion on medio-lateral patellofemoral joint loading

The study sample comprised 40 participants, of which 37 were female and 3 were male. The mean age of the participants was 15.8 ± 1.6 years (Table 3). The average femoral version observed among the participants was 25.0 ± 10.8 degrees, and the mean tibial torsion was 35.6 ± 7.8 degrees (Figure 21). The marker errors associated with the inverse kinematics fell below the best practice recommendations provided by OpenSim (174).

Table 3: Demographic data. The parameters are presented as mean values followed by standard deviations (mean (SD)). Parameters that are marked with an asterisk were available for only 33 participants. Abbreviations: TT-TG = distance between the tibial tuberosity and the trochlear groove, CDI = Caton-Deschamps index.

Demographic Data	
Age [years]	15.8 (1.6)
Sex [male/female]	3/37
Height [m]	1.68 (0.07)
Body Weight [kg]	59.8 (10.6)
Body-Mass-Index	21.3 (3.6)
Tibial torsion [°]	35.6 (7.8)
Femoral version [°]	25.0 (10.8)
TT-TG[41]* [mm]	16.5 (4.9)
CDI[42]*	1.18 (0.15)
Dejour[43]* [A/B/C/D]	5/13/10/5
Walking speed [m/s]	1.19 (0.14)
Walking speed normalized to height [1/s]	0.71 (0.08)

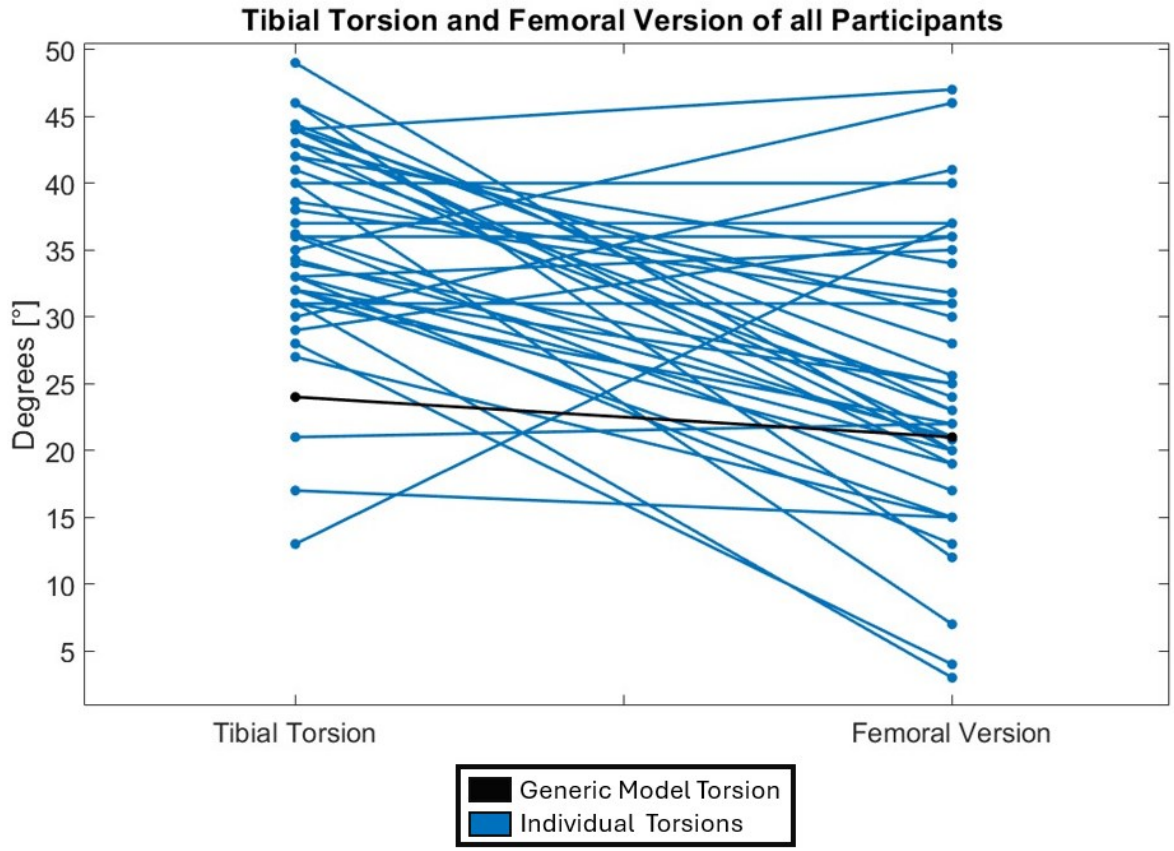

Figure 21: Femoral version and tibial torsion measurements for each participant. Each participant is represented by a pair of connected dots, where the left dot indicates the tibial torsion and the right dot denotes the femoral version specific to that individual. This figure was created by the author of this thesis.

3.2.1 Impact of lower limb torsion on patellofemoral joint loading

The analysis revealed a mean difference of 4.0° ± 10.8° in femoral version and 11.6° ± 7.8° in tibial torsion between the generic-torsion and torsion-informed models. Correspondingly, the maximum medio-lateral and overall patellofemoral forces exhibited mean absolute differences of 0.09 ± 0.07 BW and 0.15 ± 0.10 BW, respectively.

The analysis revealed that femoral version did not exhibit a significant correlation with differences in medio-lateral patellofemoral force between the generic-torsion and torsion-informed models (rho = 0.01, p = 0.967 for maximum forces; rho = 0.13, p = 0.425 for RMS forces). Additionally, femoral version showed no significant correlation with differences in resultant patellofemoral forces (rho = -0.27, p = 0.087) (Figure 22a).

Conversely, tibial torsion demonstrated a significant positive correlation with differences in maximum medio-lateral patellofemoral force between the generic-torsion and torsion-informed models (rho = 0.39, p = 0.014), suggesting that higher tibial torsion is associated with increased maximum lateralizing force. However, there was no significant correlation observed for differences in RMS medio-lateral patellofemoral force (rho = 0.15, p = 0.328). A significant

negative correlation was found between tibial torsion and differences in resultant patellofemoral loading between the models (rho = -0.42, p = 0.007) (Figure 22b).

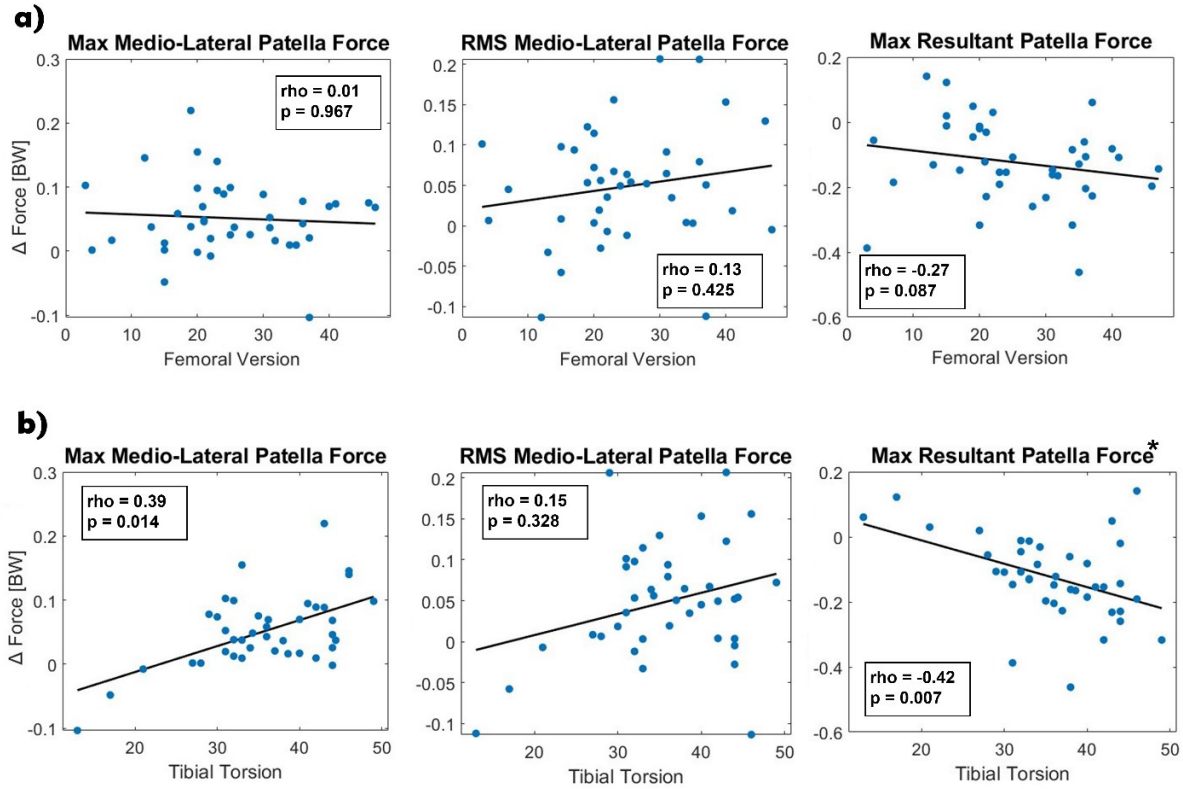

Figure 22: Scatterplots lower limb torsion and patellofemoral forces. The scatterplots presented illustrate the relationships between femoral version (a) and tibial torsion (b) with variations in patellofemoral forces when comparing the generic-torsion model to the torsion-informed model. In each plot, the black line represents a least squares fitted line, indicating the trend of the data. An asterisk marks instances where a statistically significant Spearman correlation was identified. Abbreviations: BW = body weight, Max = maximum, RMS = Root Mean Square. This figure was created by the author of this thesis.

Tibial torsion demonstrated a significant correlation with variations in gait patterns between the generic-torsion and torsion-informed models. Specifically, tibial torsion was associated with changes toward a more internally rotated knee progression angle (rho = 0.81, $p < 0.001$), increased hip internal rotation (rho = 0.93, $p < 0.001$), reduced hip flexion (rho = -0.44, $p = 0.005$), and decreased knee flexion angle (rho = -0.77, $p < 0.001$). Conversely, femoral version did not exhibit any significant correlations with kinematic changes between the two models.

A multiple linear regression analysis identified a significant relationship between the difference in maximum medio-lateral patellofemoral force and both tibial torsion and femoral version, with an r^2 of 0.21 ($F = 5.97$, $p = 0.006$). While tibial torsion showed a significant association with the difference in maximum medio-lateral patellofemoral force, femoral version did not demonstrate a significant relationship (Table 4).

Table 4: Regression coefficients and significance. Regression coefficients for a regression model between the difference in maximum medio-lateral patellofemoral force and both tibial torsion and femoral version. Significant variables are highlighted with an asterisk.

Variable	Coefficient	Standard Error	t-value	p-value
Constant	-0.112	0.062	-1.81	0.078
Tibial torsion*	0.005	0.002	3.34	0.002
Femoral version	0.001	0.001	0.68	0.498

Furthermore, femoral version exhibited no significant correlation with medio-lateral patellofemoral force (rho = 0.13, p = 0.469; rho = 0.08, p = 0.637 for maximum and RMS forces, respectively), nor was it associated with variations in resultant patellofemoral forces (rho = -0.21, p = 0.173) (Figure 23a). Conversely, tibial torsion demonstrated a significant positive correlation with both maximum (rho = 0.37, p = 0.019) and RMS (rho = 0.44, p = 0.004) medio-lateral patellofemoral forces, indicating that higher tibial torsion is associated with increased maximum lateralizing force (Figure 23b). Additionally, tibial torsion was inversely correlated with resultant patellofemoral loading (rho = -0.37, p = 0.016).

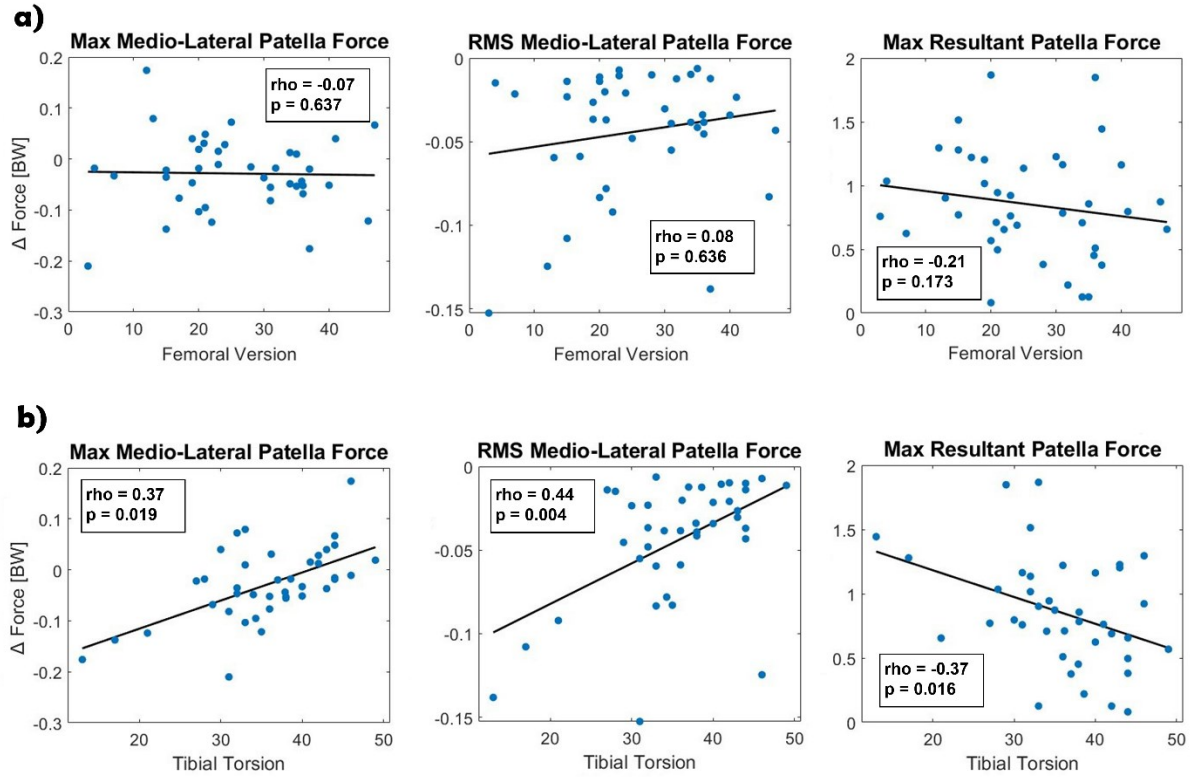

Figure 23: Scatterplots and Spearman correlation coefficients. Scatterplots showing the relationship between femoral version (a) and tibial torsions (b) and differences in patellofemoral forces between generic-torsion model and torsion-informed model. The black line represents a least square fitted line. A superscript asterisk represents a significant Spearman correlation. BW = body weight, Max = maximum, RMS = Root Mean Square. This figure was created by the author of this thesis.

A multiple linear regression analysis identified a significant relationship between the difference in peak medio-lateral patellofemoral force and both tibial torsion and femoral version, yielding an r^2 of 0.30 ($F = 9.26$, $p < 0.001$). The analysis further revealed that while tibial torsion significantly influenced the difference in maximum medio-lateral force, femoral version did not exhibit a significant relationship (Table 5).

Table 5: Regression coefficients and significance. Significant variables are highlighted with an asterisk.

Variable	Coefficient	Standard Error	t-value	p-value
Constant	-0.216	0.050	-4.32	< 0.001
Tibial torsion*	0.005	0.001	4.30	< 0.001
Femoral version	0.000	0.001	0.21	0.839

3.2.2 Impact of neglecting tibial torsion on correlation results

For the secondary objective of this study, the impact of neglecting tibial torsion on the findings was assessed. A mean difference of 4.0° ± 10.8° in femoral version between the generic-torsion and femoral-version models was found. The maximum medio-lateral patellofemoral force and the resultant patellofemoral force exhibited mean absolute differences of 0.02 ± 0.02 BW and 0.07 ± 0.06 BW, respectively.

When tibial torsion was not considered, significant correlations were observed between femoral version and differences in medio-lateral patellofemoral force (rho = 0.65, $p < 0.001$ for maximum forces; rho = 0.59, $p < 0.001$ for RMS forces), as well as with differences in resultant patellofemoral force between the generic-torsion and the femoral-version models (rho = -0.58, $p < 0.001$). Notably, a higher femoral version was associated with a lower medializing or higher lateralizing force (Figure 24). These results contrast with those from the primary investigation, suggesting a significant interaction effect of tibial torsion on the relationship between femoral version and patellofemoral forces.

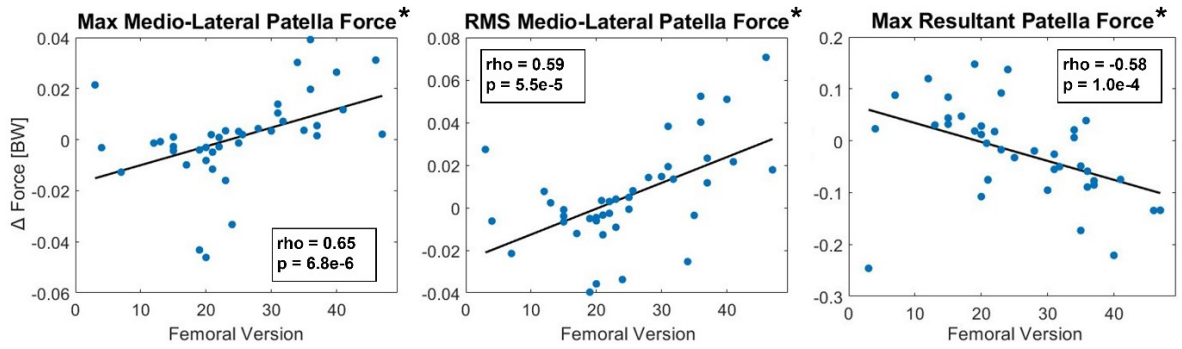

Figure 24: Scatterplots femoral version. The scatterplots depicted here illustrate the relationship between femoral version and the differential patellofemoral forces observed between the generic-torsion model and the femoral-version model. In each plot, the black line represents a least squares fitted line, indicating the trend of the data. An asterisk marks instances where a statistically significant Spearman correlation was identified. Abbreviations: BW = body weight, Max = maximum, RMS = Root Mean Square. This figure was created by the author of this thesis.

3.2.3 Hip muscle lever arms

Femoral version demonstrated a correlation with differences in mean gluteal muscle lever arms between the generic-torsion and torsion-informed models. Similarly, tibial torsion was correlated with differences in gluteal muscle lever arms between these models (Table 6). Although hip muscle lever arms are not directly influenced by tibial torsion in the model's neutral pose, further investigation into potential contributing factors was conducted. A correlation was identified between tibial torsion and differences in hip rotation between the torsion-informed and generic-torsion models (rho = 0.97, $p < 0.001$), whereas no significant correlation was found between femoral version and differences in hip rotation (rho = 0.1, $p = 0.55$). It was noted that a more externally rotated tibia was associated with a more internally rotated hip. After controlling for hip rotation, the correlation between gluteal muscle lever arms and tibial torsion ceased to be statistically significant, while the correlation coefficient between femoral version and gluteal muscle lever arms increased (Table 6).

Table 6: Spearman correlation coefficients. Quantifying the relationships between femoral version, tibial torsion, and the differences in hip muscle lever arms observed between the Generic-Torsion Model and the Torsion-Informed Model. The correlations have been adjusted for variations in hip rotation. Statistical significance is denoted as follows: * indicates $p < 0.05$; ** indicates $p < 0.001$. Abbreviations: FV = femoral version, TT = tibial torsion

	FV	FV adjusted	TT	TT adjusted
Gluteus minimus	-0.78**	-0.98**	0.51**	0.07
Gluteus medius	-0.78**	-0.97**	0.51**	0.09
Gluteus maximus	-0.79**	-0.95**	0.47*	0.09
Psoas	0.73**	0.85**	-0.39*	-0.004
Rectus femoris	0.11	0.20	-0.48*	0.23

3.2.4 Muscle forces

Femoral version and tibial torsion were found to correlate with differences in the RMS of normalized muscle forces between the torsion-informed and generic-torsion models (Table 7 and Appendix 1). Specifically, femoral version exhibited correlations with differences in the muscle forces of the gluteus medius, gluteus minimus, rectus femoris, and vastus lateralis between the models. Meanwhile, tibial torsion was associated with variations in the muscle forces of the gluteus maximus, biceps femoris, and rectus femoris between the models.

Table 7: Spearman correlation coefficients. Assessing the relationships between femoral version, tibial torsion, and changes in RMS muscle forces between the generic-torsion model and the torsion-informed model. Statistical significance is indicated as follows: * denotes $p < 0.05$; ** denotes $p < 0.001$.

	Femoral Version	**Tibial Torsion**
Biceps femoris long head	-0.38*	0.67**
Biceps femoris short head	0.27	0.60**
Gastrocnemius	-0.08	0.27
Gluteus maximus	-0.21	-0.42*
Gluteus medius	-0.57**	0.46*
Gluteus minimus	0.73**	-0.19
Rectus femoris	0.33*	-0.41*
Vastus lateralis	-0.59**	-0.17
Vastus medialis	-0.07	-0.19
Tibialis anterior	0.15	0.49*

3.3 Results study 3: Impact of femoral derotation osteotomy on the patellofemoral joint loading

The participants exhibited a mean femoral version of 36.1 ± 4.9 degrees and tibial torsion of 35.6 ± 7.2 degrees (Table 8, Figure 25 and Figure 26). None of the participants presented a genu varum or valgum deformity. The inverse kinematics marker tracking errors remained below the recommended OpenSim best practice thresholds (174).

Table 8: Demographic data. The parameters within this table are provided in the format of mean values accompanied by standard deviations (mean (SD)). Abbreviations: TT-TG = distance between tibial tuberosity and trochlea groove; CDI = Caton-Deschamps index.

Demographic Data	
Age [years]	15.8 (1.9)
Sex [male/female]	1/15
Height [m]	1.68 (0.08)
Body Weight [kg]	60.2 (9.6)
Body-Mass-Index	21.4 (3.2)
Tibial torsion [°]	35.6 (7.2)
Femoral version [°]	36.1 (4.9)
TT-TG [mm]	15.3 (4.3)
CDI	1.24 (0.15)
Dejour [A/B/C/D]	1/9/2/4

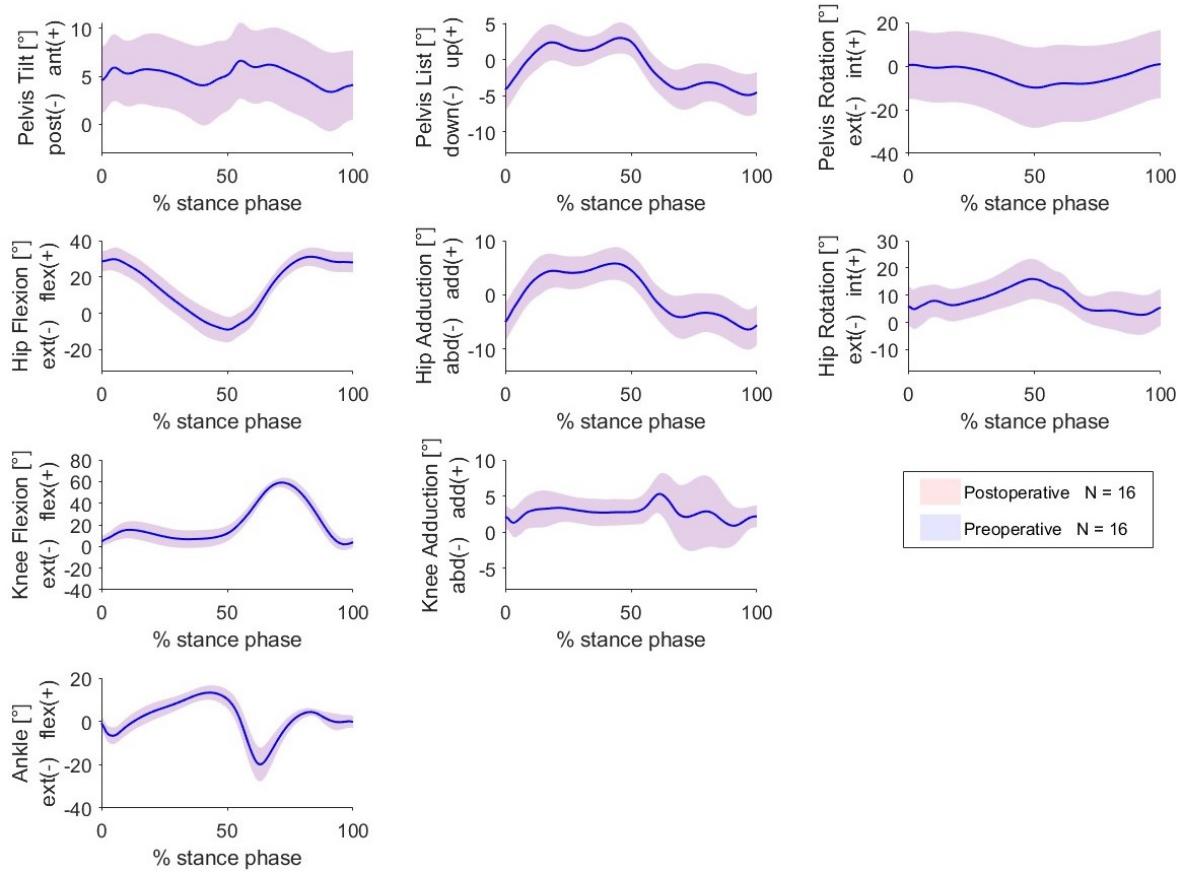

Figure 25: Joint kinematics. The mean joint angles are represented by a blue line for the pre-surgery models and by a red line for the post-surgery model, each accompanied by one standard deviation. As joint angles did not differ in the simulations between both models, the data of the post-surgery models are completely overlapped. This figure was created by the author of this thesis.

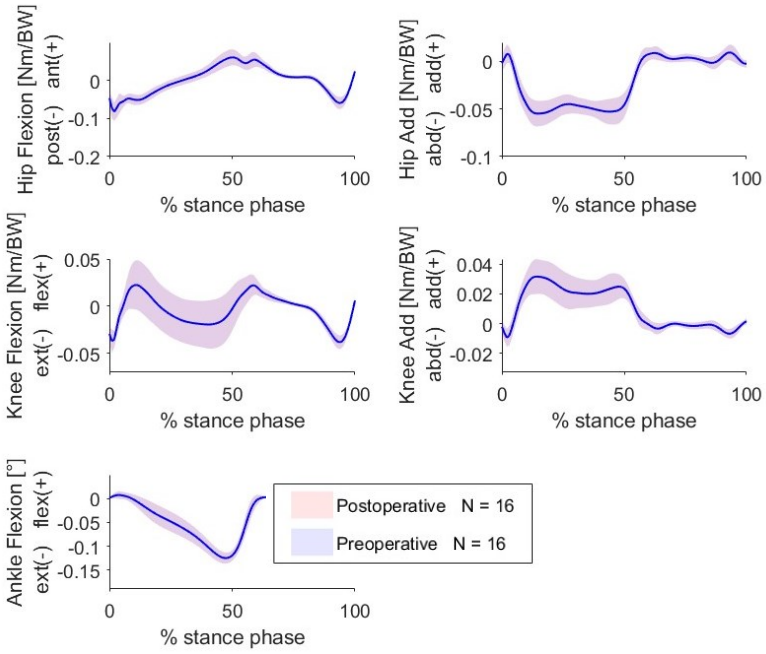

Figure 26: External joint moments. The mean external joint moments are represented by a blue line for the pre-surgery models and by a red line for the post-surgery model, each accompanied by one standard deviation. As external joint moments did not differ in the simulations between both models, the data of the post-surgery model are completely overlapped. Abbreviations: Nm/BW = Newton meter/body weight. This figure was created by the author of this thesis.

3.3.1 Pre- and post-surgical joint contact forces

The simulated FDO significantly influenced the contact forces at both the tibiofemoral and patellofemoral joints (Figure 27a and Figure 28). Specifically, the patellofemoral force exhibited a medial shift during the loading response and mid-stance phases of gait. Among the participants, fourteen individuals demonstrated a more medial patellofemoral force following the simulated FDO, categorizing these instances as successful interventions. Conversely, in two participants (12.5 %), the patellofemoral forces remained unchanged post-FDO, indicating unsuccessful derotations, as shown in Figure 27b.

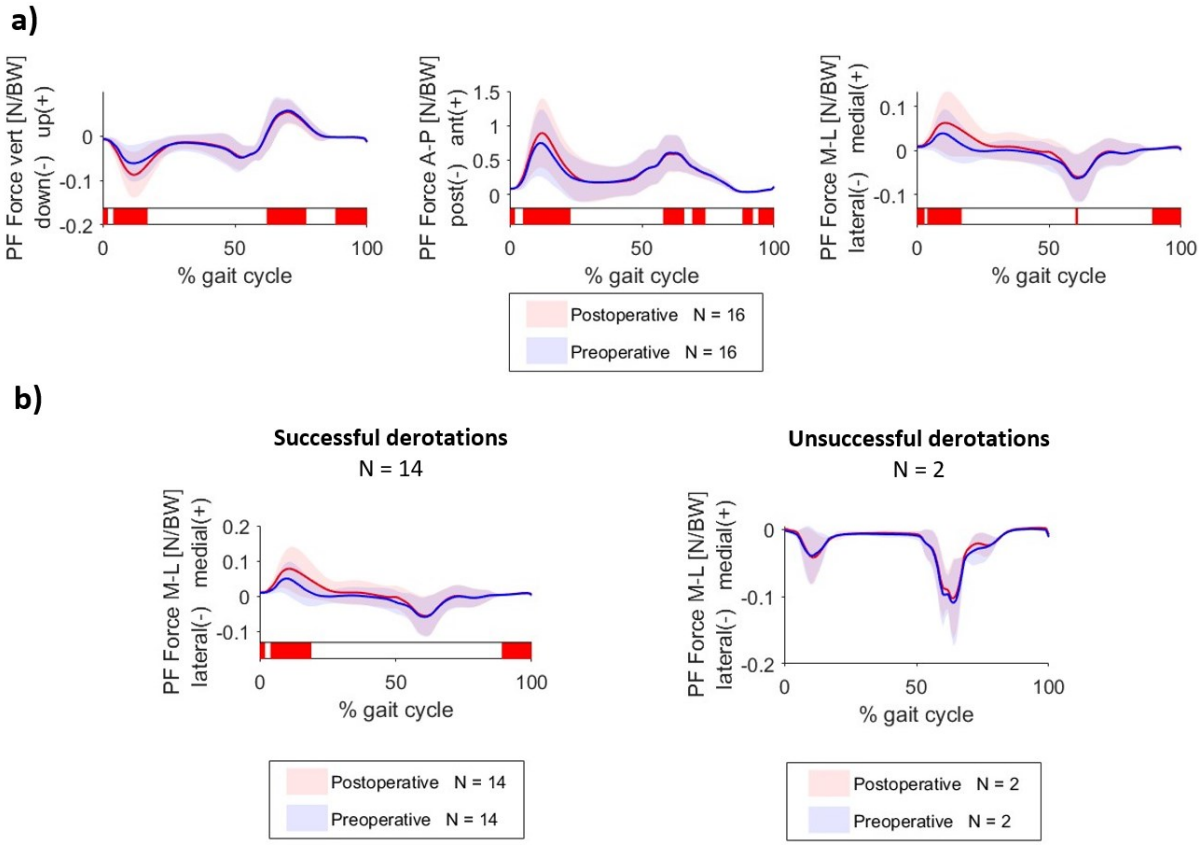

Figure 27: Patellofemoral joint contact forces. a) Patellofemoral joint contact forces in three anatomical planes before (blue waveforms) and after (red waveforms) the simulated FDO. b) Examines the medio-lateral patellofemoral joint contact forces, subdivided into results from individuals with successful outcomes (left subplot) and those with unsuccessful outcomes (right subplot) post-FDO. A colored horizontal bar beneath each subfigure highlights significant differences, as determined by statistical parametric mapping analysis. Abbreviations: A-P = anterior-posterior, M-L = medio-lateral, N/BW = Newton/body weight, PF = patellofemoral, vert = vertical. This figure was created by the author of this thesis.

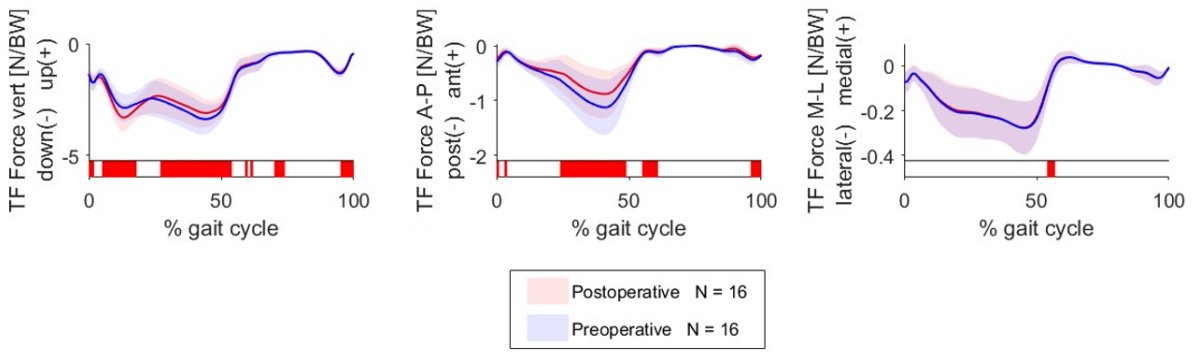

Figure 28: Tibiofemoral joint contact forces. Tibiofemoral joint contact forces in three anatomical planes before (blue waveforms) and after (red waveforms) the simulated FDO. A colored horizontal bar beneath each subfigure highlights significant differences, as determined by statistical parametric mapping analysis. Abbreviations: A-P = anterior-posterior, M-L = medio-lateral, N/BW = Newton/body weight, PF = patellofemoral, vert = vertical. This figure was created by the author of this thesis.

3.3.2 Peak medio-lateral patellofemoral joint force in single stance

The peak medio-lateral patellofemoral joint forces during single stance exhibited a medial shift following FDO. The mean force prior to surgery was 0.04 times body weight, which increased to 0.07 body weight post-surgery (N = 16, $p < 0.001$) (Figure 29). Furthermore, the alteration in peak medio-lateral patellofemoral forces due to the FDO demonstrated a strong correlation with the initial femoral version angle in individuals who experienced successful FDO outcomes ($r = 0.86$, $p < 0.001$).

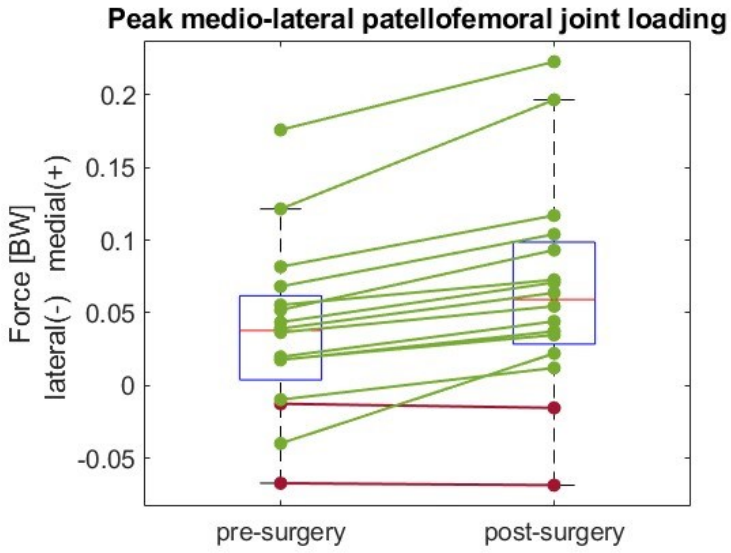

Figure 29: Peak medio-lateral patellofemoral joint force. Each dot corresponds to the peak force recorded for one individual pre- and post-surgery. The values for each individual are connected by a line. Lines colored green denote cases where the surgery was deemed successful, whereas red lines indicate unsuccessful outcomes. This figure was created by the author of this thesis.

3.3.3 Muscle moments and muscle forces

The simulated FDO resulted in a decrease in the hip extension muscle moment of the gluteus medius. Conversely, an increase was observed in the flexion moment of the gluteus minimus as well as in the abduction moments of both the gluteus medius and maximus (Figure 30).

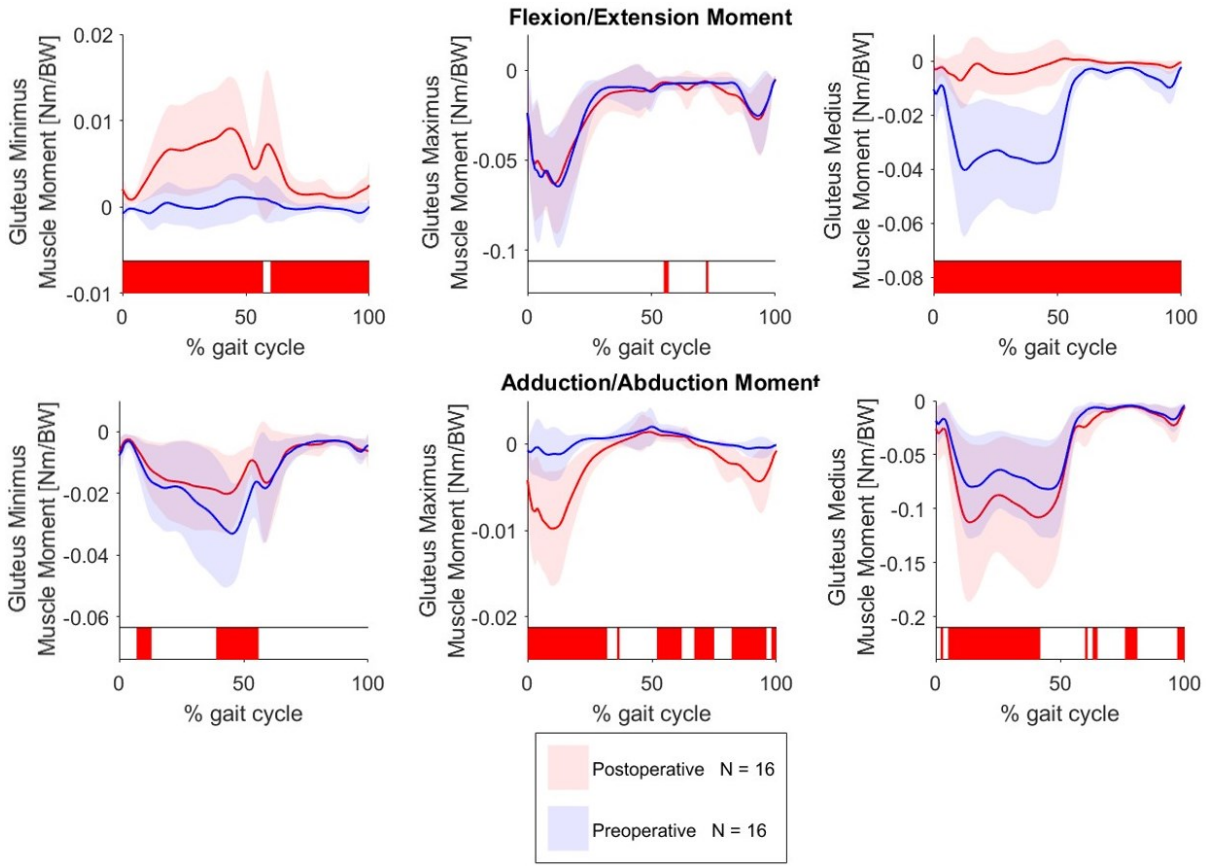

Figure 30: Gluteal muscle moments. The moments of gluteus minimus, medius, and maximus are depicted for each muscle in the sagittal plane (top row) and the frontal plane (bottom row). Beneath each subfigure, a colored horizontal bar is displayed, which indicates the presence of significant differences as determined through statistical parametric mapping analysis. Abbreviations: Nm/BW = Newton meter/body weight. This figure was created by the author of this thesis.

The pre- to post-surgery change in RMS rectus femoris muscle force exhibited a strong inverse correlation with the change in peak medio-lateral patellofemoral forces ($r = -0.86$, $p < 0.001$) among the successful cases (Figure 31). Additionally, changes in RMS vastus lateralis muscle force ($r = 0.67$, $p = 0.009$) and RMS vastus medialis muscle force ($r = 0.54$, $p = 0.044$) from pre- to post-surgery were positively correlated with alterations in medio-lateral patellofemoral joint contact force in the successful cases. Nevertheless, the scatterplots demonstrated a spread in the data points between RMS force of the vastus medialis and the medio-lateral patellofemoral force.

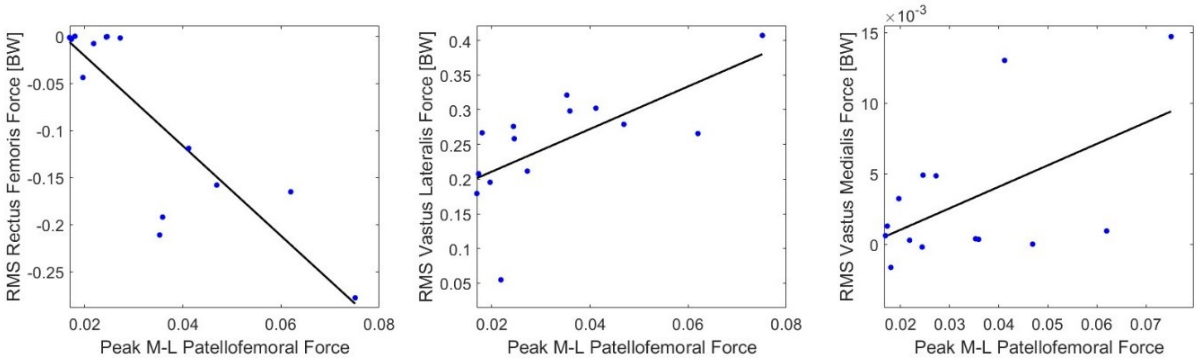

Figure 31: Scatterplots muscle forces and peak patellofemoral forces of the successful cases. The scatterplots illustrate the relationship between the differences in root mean square muscle forces and the differences in medio-lateral patellofemoral forces pre- and post-surgery. In each plot, the black line represents a least squares fitted line, indicating the trend of the data. Abbreviations: M-L = medio-lateral, RMS = root mean square. This figure was created by the author of this thesis.

3.3.4 Successful and unsuccessful femoral derotation osteotomy

The two individuals exhibiting unsuccessful FDO demonstrated femoral versions of 34° and 47°, and tibial torsions of 42° and 44°, respectively. Both subjects were diagnosed with trochlear dysplasia, classified according as Dejour type C. All other radiographic parameters remained within one standard deviation of the mean values observed in the study cohort.

Individuals who had unsuccessful FDO presented reduced knee flexion during the stance phase and increased hip internal rotation throughout the entire gait cycle compared to those with successful FDO outcomes (Figure 32a). Additionally, these individuals demonstrated a decreased external knee flexion moment during the stance phase (Figure 32b). The rectus femoris muscle forces during the stance phase were lower in individuals with an unsuccessful compared to successful FDO, and these forces showed minimal change following the simulated FDO (Figure 32c).

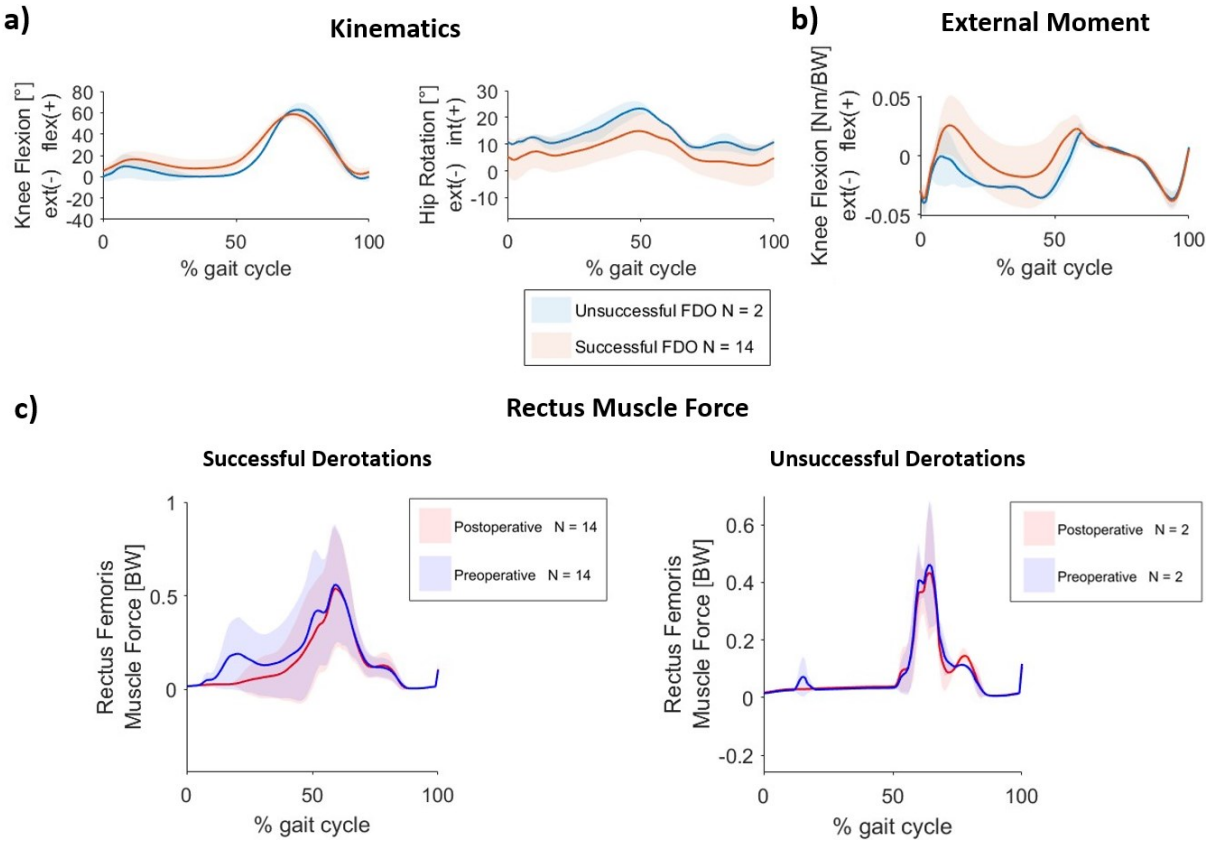

Figure 32: Differences between successful and unsuccessful cases. This figure delineates the differences in kinematics, kinetics, and muscle forces between successful and unsuccessful outcomes following FDO. a) Displays the knee flexion and hip rotation angles, comparing successful to unsuccessful cases. b) Displays the external knee flexion moments for both successful and unsuccessful cases. c) Displays the force exerted by the Rectus Femoris muscle in successful versus unsuccessful cases. Abbreviations: FDO = femoral derotation osteotomy, Nm/BW = Newton meter/body weight. This figure was created by the author of this thesis.

4 Discussion and conclusions

4.1 Discussion study 1: Impact of gait patterns on patellofemoral joint loadings

The discussion in this chapter is based on the study Guggenberger et al. (1).The first research question of this thesis aimed to examine the influence of altered gait pattern in adolescents with patellofemoral instability on knee joint loading. Individuals with patellofemoral instability exhibited distinct gait patterns compared to a typically developing control group. Specifically, altered gait kinematics and kinetics were observed in the patellofemoral instability group, leading to a reduction in quadriceps muscle force during the loading response. This decrease in quadriceps activation contributed to reduced tibiofemoral and patellofemoral joint contact forces. Consistent with the hypothesis, the patient-specific gait pattern resulted in decreased medio-lateral patellofemoral contact forces during the initial 30 % of the gait cycle. Notably, despite the results presented lower maximum patellofemoral cartilage pressure during this phase in the patellofemoral instability group, no significant differences were found between the groups in the corresponding waveform.

The patellofemoral instability group demonstrated a prolonged stance phase, extended double supported stance phase, and shortened single stance phase relative to the control group. The increased duration of double support may enhance stability, allowing for gait adjustments and corrections (223). This observation supports the hypothesis that individuals with patellofemoral instability modify their gait due to perceived instability, utilizing the double supported phases to sustain support for the affected leg as long as possible. Another rationale, particularly for the elongation of the loading response phase, could be the extended time required for load shifting between legs. In the loading response, eccentric knee flexion serves as a mechanism for shock absorption (224). A prolonged loading response duration could facilitate a reduction in the reliance on knee joint flexion for damping, thereby lowering knee joint angles. This theory is corroborated by the significantly reduced knee power observed during the loading response phase in the patellofemoral instability participants compared to the control group.

The patellofemoral instability group exhibited less knee flexion during the loading response compared to the control group. Previous research has indicated a correlation between reduced knee flexion and decreased dorsiflexion, known as the plantarflexion/knee-extension coupling (59). Plantarflexion/knee-extension coupling is believed to enhance knee joint stability despite lower quadriceps muscle activity by retracting the tibia via soleus muscle activity (225). Contrary to previous studies, no significant differences in ankle kinematics between the patellofemoral instability group and the control group were found (59).

The patellofemoral instability group displayed internal hip rotation and external rotation of the tibia, a pattern frequently observed in individuals with patellofemoral instability (26). This is commonly observed in individuals with increased femoral version and tibial torsion and is in line with the bony morphology of the participants of this study. External tibial rotation is a predisposing factor for patella dislocation (49). Additionally, internal rotation of the femur affects the Q-angle, thereby lateralizing the direction of rectus femoris muscle force (226), suggesting that deviations in hip and knee rotation might be inherent to the primary pathology rather than compensatory adaptations in gait (64). Future research should explore the effects of gait retraining focusing on transversal plane adjustments on the stability of the patellofemoral joint (154,227).

During the loading response phase, the patellofemoral instability group exhibited reduced external knee flexion moments compared to the control group. The angle of knee flexion influences the lever arm between the knee joint and the ground reaction force (228). Consequently, a less flexed knee may contribute to the diminished knee flexion moment observed. Reduced knee moments alleviate the requirement for substantial knee extensor muscle forces, thereby facilitating an unloading of the knee joint.

In the frontal plane, the patellofemoral instability group demonstrated decreased hip and knee joint moments. This reduction may be attributed to compensatory trunk kinematics, which modify the direction of the ground reaction force, thus diminishing the moments in the frontal plane (229). Although not directly addressed in this thesis, future research should explore the influence of trunk movement on the gait patterns of individuals with patellofemoral instability. The noted disparities in joint kinematics and medio-lateral ground reaction forces could account for the observed reduction in knee and hip abduction moments.

Musculoskeletal simulations indicated that the gluteus maximus compensates for a deficiency in gluteus medius strength to generate the hip abduction moment (230). In addition to the hip abduction moment, the gluteus maximus also produces a hip extension moment. This action is counterbalanced by the rectus femoris, resulting in increased co-contraction and consequently elevated joint loads at both the hip and knee joints (157). Individuals with patellofemoral instability who exhibit weakened gluteus medius strength (231) may adopt an altered gait pattern that reduces the hip abduction moment. Therefore, the observed reduction in hip abduction moments could serve as a compensatory mechanism for individuals with patellofemoral instability to unload the knee joint. Contrasting these findings, another study reported increased knee abduction moments in individuals with patellofemoral instability (232). Furthermore, the results presented a reduction in tibiofemoral and patellofemoral joint contact forces during the loading response phase among participants with patellofemoral instability compared to the control group. The patellofemoral instability group exhibited modified gait kinematics and kinetics, characterized by a decreased knee flexion angle and moment, as

well as a reduced hip abduction moment. These changes resulted in diminished quadriceps muscle forces. The adoption of a less flexed knee joint to minimize quadriceps muscle force, termed quadriceps avoidance pattern (59), is a phenomenon also observed in other pathologies such as patellofemoral pain syndrome (233). This pattern effectively reduces the tension exerted by the quadriceps on the patella, thereby decreasing the compressive force on the knee joint (234).

Alterations in joint kinematics and kinetics in the subjects with patellofemoral instability led to a reduction in lateral patellofemoral contact force. Lateralizing forces, particularly when combined with disadvantageous anatomical features such as a shallow trochlea, elevate the risk of patella dislocation (235). Additionally, increased femoral version and hip internal rotation can amplify lateralizing forces due to the altered lines of action of the rectus femoris and vastus lateralis muscles (226). This mechanism is particularly pertinent in individuals with patellofemoral instability, as elevated femoral version is commonly observed in this population (236) and was also noted within the cohort of this thesis.

Another potential factor contributing to the adoption of the quadriceps avoidance gait pattern may be pain. A study conducted six months post-dislocation revealed load-dependent pain in individuals with patellofemoral instability, with 39 % of patients experiencing pain during running activities, while minimal pain was reported during sedentary activities (70). Given that the mechanical loads during walking are intermediate between running and sedentary states, minimal pain is anticipated in the patellofemoral instability group. A prospective study that observed a gait pattern in individuals with patellofemoral instability similar to the investigated patellofemoral instability group, reported no pain in their cohort, suggesting no direct correlation between pain and walking strategy (59). Future investigations should incorporate a comprehensive pain assessment to investigate the relationship between gait patterns and pain in individuals with patellofemoral instability.

Regarding patellofemoral cartilage pressure, waveform analysis revealed no significant differences in pressures between the patellofemoral instability and control groups. The patellofemoral instability group exhibited reduced knee flexion during the loading response, consequently decreasing the contact area between the patella and the trochlea groove (237). Since the calculation of contact pressure is contingent upon both the applied force and the contact area, the diminished contact area could elucidate the absence of significant differences in cartilage pressure in the waveforms, despite the reduced joint contact force. Conversely, during the initial 30 % of the gait cycle, maximum pressure values were significantly lower in the patellofemoral instability group, indicating reduced patellar cartilage loading in these individuals.

4.2 Discussion study 2: Impact of femoral and tibial torsion on medio-lateral patellofemoral joint loading

The primary aim of the second study of this thesis was to investigate the impact of lower limb torsion on patellofemoral joint loading in individuals diagnosed with patellofemoral instability. Musculoskeletal simulations were performed on an extensive cohort of 40 participants, all of whom had experienced recurrent patellofemoral dislocations. It was found that tibial torsion was significantly correlated with variations in maximum medio-lateral patellofemoral force between the generic-torsion and torsion-informed models. Conversely, femoral version did not show a significant correlation with changes in medio-lateral patellofemoral forces between the generic-torsion and torsion-informed models. Notably, when the musculoskeletal models were personalized only to the femoral version, thus excluding individual variations in tibial torsion, a moderate to high correlation was observed between femoral version and differences in medio-lateral patellofemoral force between the generic-torsion and femoral-version models.

A mean absolute difference of 0.09 BW was observed in maximum medio-lateral patellofemoral force between the generic-torsion and torsion-informed models. Given the average participant weight of 59.8 kg, this translates to a change in the medio-lateral force of approximately 54 N toward a more lateralizing direction as a result of lower limb torsion. When compared to the maximum strain force of the medial patellofemoral ligament, which is approximately 208 N (238), this represents a significant alteration that could potentially impact the stability of the patellofemoral joint by increasing the lateralizing traction on the patella.

The results revealed that tibial torsion was correlated with differences in maximum medio-lateral patellofemoral force between the generic-torsion and torsion-informed models, as well as with the maximum medio-lateral patellofemoral force in the torsion-informed models. An increased tibial torsion was associated with a greater lateralizing force, a finding that aligns with results from cadaver studies which have shown increased pressure on the lateral patellar facet (44,239). Two aspects are particularly relevant when evaluating the influence of tibial torsion on the stability of the patellofemoral joint. First, tibial torsion may induce kinematic changes as a compensatory mechanism (240). This assertion is corroborated by the observed correlations between tibial torsion and variations in knee flexion, knee progression, hip flexion, and hip rotation between the generic-torsion and torsion-informed models. Second, although not modified and consequently not examined in this study, the position and orientation of the tibial tubercle are critical in determining patellar alignment in relation to tibial anatomy (241). Given that proximal tibial torsion can lead to a displacement of the tibial tuberosity, prior research has suggested that proximal tibial derotation osteotomies might be beneficial in stabilizing the patellofemoral joint (134,242). Drawing on the insights from previous studies

and the findings from the current investigation, it is evident that excessive tibial torsion should be considered a significant factor affecting the stability of the patellofemoral joint.

No significant correlation was found between femoral version and changes in medio-lateral patellofemoral forces between the generic-torsion and the torsion-informed model. Furthermore, the analysis revealed no significant correlation between femoral version and the absolute medio-lateral patellofemoral forces in the torsion-informed models. This result diverges from earlier findings in both musculoskeletal simulation studies (22,189) and cadaver research (44,96), which have predominantly highlighted an increase in lateral patellofemoral loading with greater femoral version. Considering that non-traumatic patella dislocations commonly occur to the lateral side (6), these results are of relevance. For the secondary objective, the effects of isolated personalization of femoral version on joint loads were explored, similar to previous studies. This analysis revealed moderate to strong correlations between femoral version and differences in medio-lateral patellofemoral force between the generic-torsion and the femoral-version models, suggesting that excessive femoral version may destabilize the patella by increasing its lateral displacement. However, these results have to be interpreted with caution, as tibial torsion was neglected in these simulations. Thereby these simulations were not fully representing the actual biomechanical situation. When personalized tibial torsion was considered alongside femoral version, the influence of femoral version on patellofemoral joint loading was altered, indicating that findings from studies focusing solely on femoral version while neglecting tibial torsion should be approached with caution.

Tibial torsion exhibited a strong correlation with differences in hip rotation and knee progression angle between the generic-torsion and torsion-informed models, potentially elucidating its impact on patellofemoral joint loads. Hip rotation influences the knee progression and thus the global orientation of the knee joint, and when the ground reaction force remains constant, variations in knee progression angle may lead to a redistribution of forces along the anatomical axes of the knee joint. An increase in internal hip rotation and knee progression angle might, therefore, result in a more lateralized ground reaction force impacting the knee. A study investigating the effects of kinematics and bony morphology on hip joint loading demonstrated that kinematics have a more pronounced impact on hip joint loading than morphology (141). Given the strong correlation between hip rotation, knee progression angle and tibial torsion, this may explain the more pronounced correlations between patellofemoral joint loading and tibial torsion compared to those between patellofemoral joint loading and femoral version in models with subject-specific lower limb torsion.

The modification of muscle lever arms and the resultant forces may elucidate the influence of lower limb torsion on patellofemoral joint loads. In the torsion-informed models, the variations

in hip muscles' lever arms were found to correlate with both femoral version and tibial torsion. This correlation between femoral version and hip muscle lever arms aligns with findings from previous musculoskeletal simulation studies (157,243). Upon controlling for differences in hip rotation, it was noted that the correlations between tibial torsion and differences in gluteal muscle lever arms decreased, whereas those between femoral version and differences in gluteal muscle lever arms between the generic-torsion and the torsion-informed models increased. Thus, tibial torsion indirectly affected hip muscle lever arms by altering hip rotation.
This study presented contrasting results regarding the correlations between differences in medio-lateral patellofemoral force and femoral version when incorporating personalized lower limb torsion as opposed to omitting tibial torsion. Models that included subject-specific lower limb torsion offered a higher degree of personalization, thereby providing a more accurate representation of the participants' anatomical features. Femoral version may potentially destabilize the patellofemoral joint. However, it is essential to consider this effect in context with other contributory factors, such as the individual's walking pattern and tibial torsion. These elements could counterbalance the destabilizing influence of femoral version on the patellofemoral joint and thus should be integrated into planning the therapeutic strategy.
In addition to soft tissue procedures, femoral derotation osteotomies are employed in the treatment of recurrent patellofemoral instability (135). Currently, the predominant method for decision-making in this context relies on the use of femoral version thresholds or the application of individual surgeon preferences. For example, some studies suggested that a femoral version exceeding 30 degrees may serve as a useful criterion for undertaking a FDO (244,245). However, in light of the findings of the present thesis, a decision-making criterion based solely on the femoral version value seems insufficient, as other factors such as tibial torsion and individual movement patterns also significantly influence the medio-lateral stability of the patellofemoral joint. Overlooking these factors could potentially lead to suboptimal outcomes following a FDO.
The necessity to implement functional assessments, such as three-dimensional gait analysis, is underscored by the findings of the regression analysis. The regression analysis showed that lower limb torsion alone accounted for only 21% of the variance in the changes observed in maximum medio-lateral patellofemoral force. This suggests that the majority of the changes observed in medio-lateral forces were due to gait pattern or other factors. Using functional assessments is particularly important in cases of malalignment syndrome characterized by excessive femoral version and tibial torsion. In such scenarios, both femoral version and tibial torsion should be considered in the development of a comprehensive treatment plan (137). In conjunction with the clinically established application of three-dimensional gait analysis, the evaluation of complex movement patterns, which could more likely predispose individuals to patellar dislocation, could potentially further increase the relevance of functional assessments

in planning treatment strategies. Future research should aim to establish a set of both morphological and functional criteria to determine the appropriateness of addressing patellofemoral instability with derotation osteotomies.

4.3 Discussion study 3: Impact of femoral derotation osteotomy on the patellofemoral joint loading

The third research question of this thesis aimed to examine the impact of FDO on medio-lateral patellofemoral forces in individuals experiencing patellofemoral instability. The findings indicate that simulated FDO generally results in the medialization of patellofemoral forces. However, it is noteworthy that in two participants (12.5 % of the cohort) FDO did not lead to a medial shift in patellofemoral forces. This lack of change is likely attributable to differing gait patterns observed in these participants compared to those who experienced successful outcomes from FDO.

A significant medial shift in patellofemoral joint force was observed during the single stance phase following the simulated FDO. Given the mean participant weight of 60.2 kg and the mean change in peak medio-lateral patellofemoral joint force of 0.03 body weight, the resultant additional peak medializing force was 17 N (range: 9 N to 46 N). When comparing this value to the mean maximum tensile strength of the medial patellofemoral ligament, which is approximately 208 N (238), the effect of the FDO constitutes less than 10 % (range: 4 % to 22 %) of this force value. Furthermore, the changes in medializing force exhibited a strong correlation with the initial femoral version angle, suggesting that the influence of FDO on patellofemoral forces is more pronounced in individuals with a greater correction of femoral version. Thus, from a biomechanical perspective, additional FDO can provide benefits by increasing the medializing force on the patellofemoral joint in cases of excessive femoral version. When integrated with other therapeutic interventions, such as medial patellofemoral ligament reconstruction or tibial tuberosity transfer, FDO may improve treatment outcomes for recurrent patellofemoral instability (135).

The present personalized simulations enhanced the understanding of the biomechanical alterations induced by FDO on muscle forces. Specifically, a decrease in rectus femoris force correlated with a shift towards a more medial peak patellofemoral joint force post-FDO. Supporting literature indicates that excessive femoral version may lead to increased co-contraction of hip flexor and extensor muscles, thereby augmenting rectus femoris force (157). Consequently, the reduction of femoral version through FDO could result in a decreased rectus femoris muscle force, as found in this thesis. This finding is corroborated by the observed reduction in the gluteus medius hip extension muscle moment post-FDO. Given that the rectus

femoris is a biarticular muscle, it exerts a direct influence on the patellofemoral joint contact forces (29). In contrast to the rectus femoris, increases in force observed in the vastus medialis and vastus lateralis were correlated with changes in peak medio-lateral patellofemoral joint force. This relationship may originate from the reduction in rectus femoris force while the external knee flexion moment remained constant, necessitating a compensatory increase in the forces of the vasti muscles. Therefore, the post-FDO alterations in medio-lateral patellofemoral loading could be attributed to a decrease in rectus femoris force accompanied by a compensatory increase in vastus medialis force.

In two participants (12.5 % of the cohort), FDO did not lead to an increased medializing force on the patellofemoral joint. An analysis comparing gait patterns between successful and unsuccessful cases revealed that the unsuccessful cases were characterized by reduced knee flexion during the stance phase and an increased internal rotation of the hip. This internal rotation of the hip may contribute to an increased dynamic Q-angle, potentially enhancing the lateralizing force exerted on the patella (246,247). Furthermore, the reduced knee flexion observed in the unsuccessful cases led to a diminished external knee flexion moment, which consequently decreased the force exerted by the rectus femoris muscle during the stance phase (59,234). One of the primary effects of FDO is hypothesized to be the reduction of rectus femoris muscle force. If the initial force exerted by the rectus femoris is already low, as observed in these two participants, only minimal alterations in rectus femoris forces are achievable through FDO. This minimal change could explain why the patellofemoral joint contact force remained unchanged in these two cases.

The observed unsuccessful cases underscore the critical role of walking patterns in determining the effectiveness of FDO. The importance of gait patterns is further corroborated by another study, which revealed that the influence of femoral version on knee joint loading is modulated by an individual's joint kinematics (248). In the present results, the impact of FDO was exclusively assessed during gait. Considering the significance of movement patterns, it is plausible that the effects of FDO could be more pronounced if individuals engaged in activities that involve higher knee flexion moments. This suggests that broader evaluations encompassing a variety of physical activities may provide a more comprehensive understanding of the biomechanical outcomes of FDO.

In this study it was assumed that FDO does not modify the participants' gait patterns. This assumption allowed to isolate and examine the direct impact of FDO on joint loads, eliminating potential confounding factors. However, recent research indicated that individuals with idiopathic torsional deformities exhibited reduced hip flexion, knee flexion, and hip internal rotation angles following FDO (249). Such alterations in gait patterns could potentially influence changes in medio-lateral patellofemoral joint loads. Consequently, future studies should explore how FDO affects gait patterns and, in turn, how these changes impact joint

loads in individuals with patellofemoral instability. This would be essential for a more comprehensive understanding of the biomechanical consequences of FDO.

The results of the present work corroborate the prevailing understanding that FDO can beneficially affect the stability of the patellofemoral joint in individuals with recurrent patellofemoral instability (135), by increased medializing forces at the patellofemoral joint. However, the modest alterations observed in medio-lateral patellofemoral forces suggest that utilizing FDO as a standalone treatment for patellofemoral instability may not be optimal. Moreover, the effectiveness of FDO is significantly influenced by individual-specific movement patterns. Consequently, it is imperative to consider not only the femoral version but also functional movements, such as those assessed through gait analysis, in the planning and evaluation of FDO interventions. This comprehensive approach is vital for optimizing therapeutic outcomes.

4.4 General discussion

This thesis represents the first investigation utilizing musculoskeletal modelling, to address the effects of individual gait pattern and lower limb torsion on the patellofemoral loading in a cohort of patellofemoral instability patients. Joint loads are critical biomechanical parameters, which facilitate a better understanding of pathologies, their prevention and treatment (250,251). Measuring joint loads is currently a substantial challenge. In vivo and in vitro, joint loads can only be quantified through the use of instrumented implants or by examining cadaver specimens (74,76,178). While instrumented implants are highly invasive and costly, simulating physiological muscle activation in cadaver studies is challenging. Additionally, these methods predominantly provide data for an older population, complicating the acquisition of insights into biomechanical alterations in pathologies that primarily affect children and adolescents (29). Musculoskeletal simulations offer a methodology that estimates muscle activation and forces derived from movement patterns, enabling researchers to examine the musculoskeletal system without complex and invasive experiments on living organisms (16). These simulations enable to investigate the interplay between joint movements, muscle forces, and joint loads (16,138). Consequently, simulations facilitate the exploration of compensatory mechanisms across various pathologies (16,138). For example, musculoskeletal simulations have revealed that the increased internal rotation observed in the gait of children with cerebral palsy is not due to the shortening of the adductors. Instead, it results from increased femoral anteversion and altered mechanics of the hip joint (252). For patellofemoral instability, it was possible to show that a shallow trochlea increases the loading on the medial patellofemoral ligament and thus increases the relevance of this structure to prevent dislocation (19).

Within the first study of this thesis, musculoskeletal simulations were employed to investigate the impact of gait patterns on knee joint loading in individuals with patellofemoral instability (1). Alterations in gait may arise from multiple causes, such as neuromotor impairments, muscle weakness, restricted range of motion, or other deformities like lower limb torsion (52). Additional factors, including fear, pain, or a sensation of instability, can also influence gait patterns (253). In the first study of this thesis, notable differences in gait were observed between the group with patellofemoral instability and the control group of typically developing children and adolescents (1). It was found that these modifications contributed to a decrease in the load exerted on the knee joint (1). Specifically, a reduction in lateralizing patellofemoral forces might be indicative of an adaptation in the gait pattern aimed at stabilizing the patellofemoral joint. A reduction of lateralizing force could be significant for individuals with patellofemoral instability, as patellar dislocations occur predominantly laterally. Summarizing the first study highlighted that the gait pattern in individuals with patellofemoral instability significantly alters patellofemoral joint loading and thus functional movement should be accounted in studies and treatment planning aiming on patellofemoral instability (1).

Among different morphological parameters, femoral version and tibial torsion are considered as risk factors for patellofemoral instability (96,97). Thus, the effect of femoral version and tibial torsion on patellofemoral loading was investigated in this thesis. Interestingly, femoral version did not correlate to changes in medio-lateral patellofemoral loading in the second study of this thesis. In contrast, when neglecting individual tibial torsion, femoral version correlated to changes in patellofemoral loading. Furthermore, tibial torsion, correlated to changes in patellofemoral loading, which could be explained by alterations in knee progression angle. These results suggest that focusing on a single morphological parameter and neglecting the load exerted by functional movements may be too simplistic to fully understand its biomechanical impact, particularly since movement patterns significantly influence joint loading (1,141). Hence, it appears crucial to consider all relevant morphological parameters and functional movement patterns to gain a more realistic insight into the biomechanical alterations of patellofemoral joint loading. This is especially relevant as there seems to be no general correlation between morphology and gait patterns in individuals with patellofemoral instability (61,64). Therefore, morphological parameters should be examined for each individual, taking into account the person-specific movement patterns. Summarizing the second study of the thesis, it is essential not to merely focus on single static morphological parameter but also to consider its biomechanical interactions with other factors, particularly movement patterns, to understand the multifaceted nature of biomechanical dynamics in patellofemoral instability.

For optimal treatment outcomes, a deeper understanding of the surgical consequences, specifically, what changes occur and how various structures are affected, is imperative.

Musculoskeletal simulations can play a relevant role in elucidating these aspects. Parameters derived from such simulations have the potential to aid in clinical decision-making and intervention planning. Research highlighted for instance the significance of trochlea shape in the effectiveness of tibial tuberosity osteotomies in treating patellofemoral instability. In individuals with a shallow trochlea, either lateralization or medialization of the tibial tubercle may decrease stability, making medialization of the tibial tubercle less effective for patella stabilization (25). As investigated in the third study of this thesis, simulated FDO generally enhanced patellofemoral stability by increasing the medial component of the patellofemoral force. Nevertheless, FDO did not yield positive outcomes in 12.5 % of the participants, likely attributed to their specific gait patterns. Moreover, even in successful cases, the alterations in patellofemoral force were modest (mean peak force change of 17 N) between the pre- and post-FDO models. Summarizing, the third study highlighted that the interaction between movement patterns and bony morphology is crucial when devising treatment strategies for patellofemoral instability.

4.5 Strengths and weaknesses of the thesis

Musculoskeletal modelling-based studies often rely on small sample sizes due to the lack of experimental data and the time needed to personalize the models and conduct the musculoskeletal simulations. A strength of this work is therefore the large sample size, compared to other musculoskeletal modelling-based studies focusing on patellofemoral instability or patellofemoral joint loading (N=38-40 versus N<17 in previous studies (19,20,22–25,189,205)). The large sample size enabled to conduct more robust statistical analysis and even analyze a subsample of the second study (in the third study).

The utilization of musculoskeletal modelling to quantify biomechanical parameters in clinical populations offers several advantages compared to traditional experimental and cadaver studies. One benefit is that it enables to non-invasively estimate internal forces for a specific patient, taking into account a patient's walking pattern and musculoskeletal geometry (254). Additionally, musculoskeletal modelling facilitates the exploration of what-if scenarios. Within the context of the present thesis, it was possible to assess the isolated effect of femoral version, and the combined effect with tibial torsion on the patellofemoral loading. Further, it was possible to investigate the isolated effect of FDO on patellofemoral loading and how it is altered by individual gait patterns (1).

Another advantage of musculoskeletal modelling is its capability to concurrently investigate individual morphology and functional movement patterns (16,22,138). This aspect is particularly pertinent for pathologies or diseases that significantly affect the musculoskeletal system and thus might alter the gait pattern. Unlike cadaver studies, which typically employ

predefined loadings to reconstruct muscle activity, musculoskeletal simulations strive to estimate realistic activation patterns (29). Musculoskeletal modelling does not only facilitate the investigation of compensational gait strategies, as demonstrated in the first study of this thesis, but also enables the exploration of the interactions between morphological parameters and gait patterns. By applying modifications to the models, musculoskeletal modelling facilitates the execution of what-if simulations (138). Accordingly, within the scope of the second objective of this thesis, it was possible to demonstrate an interaction among medio-lateral patellofemoral joint loading, femoral version, tibial torsion, and hip rotation. Furthermore, the third study showed, that the movement pattern can alter treatment outcomes and lead to unsatisfactory results in surgical strategies like FDO.

One consideration when interpreting the findings of this study is the use of different generic models for the first study compared to the second and third study. Specifically, a generic version of the Lenhart model (152) was used in the first study, while the subsequent studies utilized the modified Rajagopal model (1,159). This decision was predicated on the ease of processing the modified Rajagopal model and the unnecessary additional complexity of the Lenhart model for the investigations pertaining to the aims of the second and third study. Consequently, it is important to acknowledge that there may be slight variations in the estimated muscle forces and joint reaction loads across the models used in this thesis (255,256). Beside variance in the used models, discrepancies could also arise from the different calculation methods employed for estimating muscle forces (173,257). Muscle forces in the first study were calculated using the COMAK routine (1,202,202), whereas static optimization was utilized for the second and third study (170,174). While static optimization is based solely on minimizing squared muscle activation, the COMAK routine minimizes squared muscle activation while concurrently solving secondary knee kinematics (e.g. translational movements in the knee joint). The COMAK routine as well as static optimization presented reliable results, when investigating gait patterns (19,23,180). However, these different optimization approaches could lead to slightly different muscle forces and joint loads. Notably, the overarching results and conclusions from each study were based on a consistent modelling workflow. Using different modelling approaches might change the absolute values of estimated muscle forces and joint loads.

Musculoskeletal models offer several possibilities for personalization, yet addressing all potential modifications can be challenging. Within the framework of this thesis, each model was scaled to match the individual anthropometry, including size and weight, of each participant. Additionally, the maximum isometric muscle force for each muscle was scaled for each participant. However, muscle paths and other muscle-specific parameters were not individually recorded and adjusted. The measurement and adjustment of these individual muscle parameters are both time-consuming and complex (153,258), hence they are seldom

addressed in studies based on musculoskeletal modeling (17,23,248). Nevertheless, this limitation could result in variations in muscle forces and joint reaction loadings in individuals with patellofemoral instability.

Slightly different scaling methods for the maximum isometric muscle forces were used in the first study (scaled to body height) (1) compared to the second and third study (scaled to body weight). Both of these methods were already used before and scale the maximum isometric force of all muscles with the same scaling factor (165–167). Based on the submaximal muscle forces exerted while walking, only minor to no deviations in simulation results originated by the different scaling methods are expected.

The Torsion Tool (154,155) was employed to customize femoral version and tibial torsion, as well as to facilitate FDO. While the models effectively incorporated individualized femoral version and tibial torsion, other axial morphologies of the lower limb, such as the femoral neck-shaft angle (157) and frontal knee alignment (259), were neglected. Even though the cohort did not differ in frontal plane alignment of the knee joint, compared to a norm collective, these individual geometries could potentially impact the simulation results (157,259). The individual lower limb torsion and the simulation of FDO was modified consistently along the femoral and tibial shaft (155), which might diverge from the real location of the bony torsion and in vivo application of FDO. Despite the Torsion tool's adaption of femoral version and tibial torsion, it delineated to the value measured in rotational MR imaging. This may lead to minor discrepancies between simulated and actual muscle lines and therefore estimated muscle forces and joint loads.

In the present thesis, knee morphology was not individually personalized for each participant, leading to potential inaccuracies in joint reaction loadings and particularly in patella cartilage pressure (19). This limitation must be considered when interpreting the results. In the first study of this thesis, investigating the gait pattern of individuals with patellofemoral instability, this simplification allowed to solely investigate the impact of the gait pattern on the joint loading, even though the results might slightly differ from the real loading of the patellofemoral joint (1). For the second and third study, comparisons were made between two models that differed only in femoral version and tibial torsion. Consequently, the influence of morphological parameters other than femoral version and tibial torsion was likely controlled in these analyses.

In all models, the metatarsal and subtalar joints were locked, a common practice in musculoskeletal simulations when only two markers are present on the foot segment (18,209,260). The clinical marker sets used in the retrospective data set had only two markers placed on the foot segment. While this allows the tracking of foot progression angle and ankle flexion, in- and eversion are not measurable. However, given the role of the subtalar joint in affecting the rotational alignment of the lower limb, as indicated by study (261), this locking

might have impacted the joint kinematics (169) and, subsequently, the loads on the patellofemoral joint.

This thesis is based on the analysis of a retrospective dataset concerning individuals with patellofemoral instability. Therefore, the scope of analysis was confined to the available clinical data. Consequently, certain pertinent information regarding the study population was absent, most notably patient-related outcome measures. This omission meant that comprehensive data concerning pain experienced in daily life was not accessible. Having information on pain could have provided valuable context for interpreting the results. It is conceivable that a number of participants experienced pain, prompting them to adjust their gait patterns to reduce load on the knee joint (11). However, a prospective study that only included patients without pain found a comparable gait pattern to the cohort investigated in this thesis (1,59).

The gait analysis data incorporated in this thesis were collected over a period spanning from 2010 to 2022. During this interval, a significant methodological update occurred in 2018 when the marker set used for gait analysis was changed from the Plugin-gait marker model to the Cleveland marker model, in the gait laboratory. The primary distinction between these two models lies in the configuration of the thigh and shank markers (55,56). The Plugin-gait model employs a single marker on each thigh and shank, whereas the modified Cleveland marker set utilizes a cluster of three markers on each thigh and shank segment. This modification necessitated a slightly different inverse kinematics setup due to the varying number of markers (one versus three) that required weighting. However, the scaling and all other setups remained consistent. According to a prior study that examined different marker sets, the impact of these changes on simulation results is generally minor (169).

4.6 Future perspectives

The presented thesis utilized musculoskeletal modelling to investigate patellofemoral joint loading in individuals with patellofemoral instability and provided insights into the biomechanical alterations associated with this condition. Based on the retrospective nature of this work and the simplifications made, several avenues for future research have been identified to enhance the understanding and treatment of patellofemoral instability.

The integration of patient-related outcome measures into prospective clinical studies is crucial for evaluating the subjective aspects of patient recovery and satisfaction. By conducting long-term follow-ups that assess both the biomechanical and subjective outcomes of treatments, it is possible to gain a more comprehensive understanding of the effectiveness of different surgical interventions. This dual-focus approach would not only support the biomechanical data provided by simulations but also align treatment approaches more closely with patient satisfaction and quality of life improvements.

To further enhance the precision of musculoskeletal simulations, future research should prioritize the development of models that incorporate highly detailed, patient-specific geometries of the patellofemoral joint. This approach would involve utilizing advanced imaging techniques to capture the subject-specific anatomical features of each patient's knee structure. The integration of these personalized details into simulation models would likely improve the accuracy of predictions regarding more realistic conditions for joint reaction force and cartilage pressure estimation. Further, it would enable a better insight into how different surgical adjustments might impact individual biomechanical function, potentially leading to more personalized and effective treatment plans. A recently published study presented an open-source workflow speeding up the integration of personalized knee morphology in musculoskeletal models (262). Using this workflow could enable the simulation of larger cohorts with highly personalized knee models.

Another step would be to develop models that can predict post-surgical movement pattern adaptation and therefore also estimate long-term functional outcomes. Such models would be invaluable in designing personalized rehabilitation programs that are optimized for the most favorable result, based on predicted post-surgical biomechanics. One possibility would be the use of the OpenSim tool MOCO, which allows the prediction of gait patterns based on a musculoskeletal model and a mathematical cost function describing the goal of the movement (144,263,264). Post-surgery gait data could then be used to validate these predictions. In the available retrospective data set no post-surgical gait data were available and thus it was not possible to investigate the change of gait pattern due to surgical intervention. Future research focusing on the gait changes due to surgical intervention would be of relevance, as a recent study presented changes in gait pattern after FDO (249).

In the context of this thesis, FDO has been investigated as a surgical strategy for the treatment of patellofemoral instability. Future research could focus on the comparative analysis of different surgical strategies for the treatment of patellofemoral instability. Using what-if-simulations would allow to test the efficacy of different or combined surgical strategies on the same individual (23,25,265). These comparisons would not only help in refining surgical techniques but also aid in establishing standardized protocols that maximize efficacy while minimizing invasive surgeries. A long-term goal could be the development of an in-silico simulation tool, which allows to test different surgeries on the model of a patient, to find the individual optimal treatment. Such a tool has already been developed for surgeries in individuals with cerebral palsy (266) and could potentially also be developed for patellofemoral instability. Challenges for such a development for patellofemoral instability could be determining how detailed the models need to be to obtain reliable results. Whilst bony interventions may be easier to implement, soft tissue interventions such as medial patellofemoral ligament reconstruction may be more challenging due to the nature of the

models. In addition, further work would be required to implement such a tool into clinical practice, as it would need to be validated and accepted by clinical staff.

The continuation of research in this area has the potential to advance the treatment of patellofemoral instability. By focusing on prospective patient-centered studies, personalized simulations, and the comparative analyses of surgical interventions, future research can significantly contribute to the optimization of patient outcomes in patellofemoral instability treatment.

4.7 Conclusion

Musculoskeletal simulations were used to explore the effects of individual gait pattern, femoral version, tibial torsion and FDO on the loading of the patellofemoral joint in individuals with patellofemoral instability. Compared to a cohort of healthy controls, participants with patellofemoral instability demonstrated reduced knee flexion during the stance phase of walking, which required lower quadriceps muscle forces. This decrease in quadriceps muscle forces led to a reduction in both tibiofemoral and patellofemoral joint contact forces. Notably, the diminished lateralizing force exerted on the patella may potentially lower the risk of patellar dislocation and provides a plausible explanation for the altered gait patterns observed in individuals with patellofemoral instability. These findings underscore the significance of considering the patient-specific gait patterns during the analysis of knee loads in individuals with patellofemoral instability.

Investigating the effects of femoral version on the patellofemoral loading showed contradictory results when including or neglecting individual tibial torsion. An increase in femoral version potentially compromises the stability of the patellofemoral joint, whereas the influence of this factor appears to be mitigated when tibial torsion was personalized in the models. Consequently, research findings that exclusively focuses on femoral version should be interpreted with caution. From a clinical perspective, the findings suggest that the decision for a FDO solely based on the morphological assessment of the femur could lead to unexpected and adverse outcomes. Therefore, it is imperative that clinical decisions be tailored to the individual, incorporating a comprehensive evaluation that includes an assessment of femoral version, tibial torsion, and functional movement patterns. Moreover, the results of this thesis underscore the necessity of considering excessive tibial torsion as a contributory factor to the stability of the patellofemoral joint.

Simulated FDO resulted in a medial shift of patellofemoral forces in individuals with patellofemoral instability. Notably, in two participants, FDO had no effect on the medio-lateral distribution of patellofemoral forces, potentially due to a gait pattern that imposed minimal demands on the rectus femoris muscle. Combining FDO with medial patellofemoral ligament

reconstruction may constitute an effective strategy for addressing patellofemoral instability in subjects presenting with excessive femoral version. Furthermore, the findings of this thesis clearly highlight the importance of incorporating functional movement assessments in planning FDO to maximize therapeutic efficacy.

5 References

1. Guggenberger B, Horsak B, Habersack A, Kruse A, Smith CR, Kainz H, et al. Patient-specific gait pattern in individuals with patellofemoral instability reduces knee joint loads. Sci Rep. 2024 Nov 18;14(1):28520.

2. Galla M, Lobenhoffer P. Frakturen der Patella. Der Chirurg. 2005 Oct;76(10):987–99.

3. Grelsamer RP, Weinstein CH. Applied Biomechanics of the Patella. Clinical Orthopaedics and Related Research. 2001 Aug;389:9–14.

4. Fox A, Wanivenhaus F, Rodeo S. The Basic Science of the Patella: Structure, Composition, and Function. Journal of Knee Surgery. 2012 Jun 16;25(02):127–42.

5. Post WR, Fithian DC. Patellofemoral Instability: A Consensus Statement From the AOSSM/PFF Patellofemoral Instability Workshop. Orthopaedic Journal of Sports Medicine. 2018 Jan 1;6(1):232596711775035.

6. Hasler CC, Studer D. Patella instability in children and adolescents. EFORT Open Reviews. 2016 May;1(5):160–6.

7. Vetrano M, Oliva F, Bisicchia S, Bossa M, De Carli A, Di Lorenzo L, et al. I.S.Mu.L.T. first-time patellar dislocation guidelines. Muscle Ligaments and Tendons J. 2019 Jan;07(01):1.

8. Sanders TL, Pareek A, Hewett TE, Stuart MJ, Dahm DL, Krych AJ. Incidence of First-Time Lateral Patellar Dislocation: A 21-Year Population-Based Study. Sports Health: A Multidisciplinary Approach. 2018 Mar 10;10(2):146–51.

9. Hurley CRK, Rush MJK. Patellar instability in children and adolescents. Current Orthopaedic Practice. 2015 Sep;26(5):458–65.

10. Fithian DC, Paxton EW, Stone ML, Silva P, Davis DK, Elias DA, et al. Epidemiology and Natural History of Acute Patellar Dislocation. The American Journal of Sports Medicine. 2004 Jul 30;32(5):1114–21.

11. Frosch S, Balcarek P, Walde T, Schüttrumpf J, Wachowski M, Ferleman KG, et al. Die Therapie der Patellaluxation: eine systematische Literaturanalyse. Zeitschrift für Orthopädie und Unfallchirurgie. 2011 May 3;149(06):630–45.

12. Bolsterlee B, Veeger DHEJ, Chadwick EK. Clinical applications of musculoskeletal modelling for the shoulder and upper limb. Medical & Biological Engineering & Computing. 2013 Sep 20;51(9):953–63.

13. Kainz H, Hoang H, Pitto L, Wesseling M, Van Rossom S, Van Campenhout A, et al. Selective dorsal rhizotomy improves muscle forces during walking in children with spastic cerebral palsy. Clinical Biomechanics. 2019 May;65:26–33.

14. Meireles S, De Groote F, Reeves ND, Verschueren S, Maganaris C, Luyten F, et al. Knee contact forces are not altered in early knee osteoarthritis. Gait & Posture. 2016 Mar;45:115–20.

15. Damsgaard M, Rasmussen J, Christensen ST, Surma E, de Zee M. Analysis of musculoskeletal systems in the AnyBody Modeling System. Simulation Modelling Practice and Theory. 2006 Nov;14(8):1100–11.

16. Delp SL, Anderson FC, Arnold AS, Loan P, Habib A, John CT, et al. OpenSim: Open-Source Software to Create and Analyze Dynamic Simulations of Movement. IEEE Transactions on Biomedical Engineering. 2007 Nov;54(11):1940–50.

17. Kainz H, Killen BA, Van Campenhout A, Desloovere K, Garcia Aznar JM, Shefelbine S, et al. ESB Clinical Biomechanics Award 2020: Pelvis and hip movement strategies discriminate typical and pathological femoral growth – Insights gained from a multi-scale mechanobiological modelling framework. Clinical Biomechanics. 2021 Jul;87:105405.

18. Van Rossom S, Kainz H, Wesseling M, Papageorgiou E, De Groote F, Van Campenhout A, et al. Single-event multilevel surgery, but not botulinum toxin injections normalize joint loading in cerebral palsy patients. Clinical Biomechanics. 2020 Jun;76:105025.

19. Clouthier AL, Smith CR, Vignos MF, Thelen DG, Deluzio KJ, Rainbow MJ. The effect of articular geometry features identified using statistical shape modelling on knee biomechanics. Medical Engineering & Physics. 2019 Apr;66:47–55.

20. Wheatley MGA, Clouthier AL, Thelen DG, Rainbow MJ. Patella Apex Influences Patellar Ligament Forces and Ratio. Journal of Biomechanical Engineering [Internet]. 2021 Aug 1;143(8). Available from: https://asmedigitalcollection.asme.org/biomechanical/article/143/8/081014/1109464/Patella-Apex-Influences-Patellar-Ligament-Forces

21. Besier TF, Gold GE, Delp SL, Fredericson M, Beaupré GS. The influence of femoral internal and external rotation on cartilage stresses within the patellofemoral joint. Journal of Orthopaedic Research. 2008 Dec;26(12):1627–35.

22. Wheatley BB, Chaclas NA, Seeley MA. Patellofemoral joint load and knee abduction/adduction moment are sensitive to variations in femoral version and individual muscle forces. Journal Orthopaedic Research. 2023 Mar;41(3):570–82.

23. Clouthier AL, Borschneck D, Smith CR, Vignos MF, Thelen DG, Deluzio KJ, et al. Influence of Articular Geometry and Tibial Tubercle Location on Patellofemoral Kinematics and Contact Mechanics. Journal of Applied Biomechanics. 2022 Feb 1;38(1):58–66.

24. Yin L, Liao TC, Yang L, Powers CM. Does Patella Tendon Tenodesis Improve Tibial Tubercle Distalization in Treating Patella Alta? A Computational Study. Clinical Orthopaedics & Related Research. 2016 Nov;474(11):2451–61.

25. Clouthier AL, Borschneck D, Thelen DG, Deluzio KJ, Rainbow MJ. Relationship Between Lateral Patellar Stability and Tibial Tubercle Location for Varying Patellofemoral Geometries. Journal of Biomechanical Engineering [Internet]. 2019 Dec 1;141(12). Available from: https://asmedigitalcollection.asme.org/biomechanical/article/doi/10.1115/1.4045231/1065796/Relationship-Between-Lateral-Patellar-Stability

26. Habersack A, Kraus T, Kruse A, Regvar K, Maier M, Svehlik M. Gait Pathology in Subjects with Patellofemoral Instability: A Systematic Review. IJERPH. 2022 Aug 23;19(17):10491.

27. Platzer W, Spitzer G, Platzer W. Bewegungsapparat. 11., überarbeitete Auflage. Stuttgart: Thieme; 2013. 467 p. (Taschenatlas Anatomie).

28. Hirschmann MT, Müller W. Complex function of the knee joint: the current understanding of the knee. Knee Surg Sports Traumatol Arthrosc. 2015 Oct;23(10):2780–8.

29. Wheatley MGA, Rainbow MJ, Clouthier AL. Patellofemoral Mechanics: a Review of Pathomechanics and Research Approaches. Curr Rev Musculoskelet Med. 2020 Jun;13(3):326–37.

30. Schünke M, Schulte E, Schumacher U, Voll M, Wesker K. Prometheus. Allgemeine Anatomie und Bewegungssystem. 6. edition. Stuttgart New York: Georg Thieme Verlag; 2022. 631 p.

31. Aagaard H, Verdonk R. Function of the normal meniscus and consequences of meniscal resection. Scandinavian Med Sci Sports. 1999 Jun;9(3):134–40.

32. Fox AJS, Wanivenhaus F, Burge AJ, Warren RF, Rodeo SA. The human meniscus: A review of anatomy, function, injury, and advances in treatment. Clinical Anatomy. 2015 Mar;28(2):269–87.

33. Müller W, Morscher E, Muspach R. Das Knie: Form, Funktion und ligamentäre Wiederherstellungschirurgie. Berlin Heidelberg New York: Springer; 1982. 352 p.

34. Jagodzinski M, Friederich NF, Müller W. Das Knie: Form, Funktion und ligamentäre Wiederherstellungschirurgie. 2. edition. Berlin Heidelberg: Springer; 2016. 210 p.

35. Runer A, Wierer G, Keshmiri A, Schoettle P, Liebensteiner M, Frings J. Anatomie und Biomechanik des Patellofemoralgelenks. Arthroskopie. 2023 Dec;36(6):373–81.

36. Dejour H, Walch G, Neyret P, Adeleine P. Dysplasia of the femoral trochlea. Revue de chirurgie orthopedique et reparatrice de l'appareil moteur. 1990;76(1):45–54.

37. Warren LF, Marshall JL. The supporting structures and layers on the medial side of the knee: an anatomical analysis. J Bone Joint Surg Am. 1979 Jan;61(1):56–62.

38. Amis AA. Current Concepts on Anatomy and Biomechanics of Patellar Stability. Sports Medicine and Arthroscopy Review. 2007 Jun;15(2):48–56.

39. Kohn D, Abermann E, editors. Expertise Knie. Stuttgart New York: Georg Thieme Verlag; 2016. 501 p. (Expertise Orthopädie und Unfallchirurgie).

40. Luyckx T, Didden K, Vandenneucker H, Labey L, Innocenti B, Bellemans J. Is there a biomechanical explanation for anterior knee pain in patients with patella alta?: influence of patellar height on patellofemoral contact force, contact area and contact pressure. The Journal of Bone and Joint Surgery British volume. 2009 Mar;91-B(3):344–50.

41. Fulkerson, J P, Shea, K P. Disorders of patellofemoral alignment. The Journal of Bone & Joint Surgery. 1990 Oct;72(9):1424-9.

42. Schindler OS, Scott NW. Basic kinematics and biomechanics of the patello-femoral joint Part 1 : The native patella. Acta Orthopaedica Belgica. 2011;77(4):421–31.

43. Colvin AC, West RV. Patellar Instability: The Journal of Bone and Joint Surgery-American Volume. 2008 Dec;90(12):2751–62.

44. Lee TQ, Morris G, Csintalan RP. The Influence of Tibial and Femoral Rotation on Patellofemoral Contact Area and Pressure. J Orthop Sports Phys Ther. 2003 Nov;33(11):686–93.

45. Lee TQ, Anzel SH, Bennett KA, Pang D, Kim WC. The influence of fixed rotational deformities of the femur on the patellofemoral contact pressures in human cadaver knees. Clin Orthop Relat Res. 1994 May;(302):69–74.

46. Khasawneh RR, Allouh MZ, Abu-El-Rub E. Measurement of the quadriceps (Q) angle with respect to various body parameters in young Arab population. Li Y, editor. PLoS ONE. 2019 Jun 13;14(6):e0218387.

47. Smith TO, Davies L, O'Driscoll ML, Donell ST. An evaluation of the clinical tests and outcome measures used to assess patellar instability. The Knee. 2008 Aug;15(4):255–62.

48. Kujala UM, Kvist M, Österman K, Friberg O, Aalto T. Factors Predisposing Army Conscripts to Knee Exertion Injuries Incurred in a Physical Training Program. Clinical Orthopaedics and Related Research. 1986 Sep;(210):203-12.

49. Dewan V, Webb MSL, Prakash D, Malik A, Gella S, Kipps C. When does the patella dislocate? A systematic review of biomechanical & kinematic studies. Journal of Orthopaedics. 2020 Jul;20:70–7.

50. Nikku R, Nietosvaara Y, Aalto K, Kallio PE. The mechanism of primary patellar dislocation: trauma history of 126 patients. Acta Orthop. 2009 Aug;80(4):432–4.

51. Stefancin JJ, Parker RD. First-time Traumatic Patellar Dislocation: A Systematic Review. Clinical Orthopaedics and Related Research. 2007 Feb;455:93–101.

52. Perry J. Gait analysis: normal and pathological function. Thorofare, NJ: SLACK; 1992. 524 p.

53. Götz-Neumann K. Gehen verstehen: Ganganalyse in der Physiotherapie. 4. edition. Stuttgart New York: Georg Thieme Verlag; 2016. 211 p.

54. Baker R. Measuring walking: a handbook of clinical gait analysis. London: Mac Keith Press; 2013. 229 p.

55. Kadaba MP, Ramakrishnan HK, Wootten ME. Measurement of lower extremity kinematics during level walking. Journal of Orthopaedic Research. 1990 May;8(3):383–92.

56. Svoboda B, Kranzl A. A study of the reproducibility of the marker application of the Cleveland Clinic Marker Set including the Plug-In Gait Upper Body Model in clinical gait analysis. Gait & Posture. 2012 Jun;36:S62–3.

57. Davis RB, Õunpuu S, Tyburski D, Gage JR. A gait analysis data collection and reduction technique. Human Movement Science. 1991 Oct;10(5):575–87.

58. Vicon. Vicon Nexus Reference Guide [Internet]. 2016. Available from: https://docs.vicon.com/display/Nexus25/PDF+downloads+for+Vicon+Nexus?preview=/50888706/50889381/Vicon%20Nexus%20Reference%20Guide.pdf

59. Camathias C, Ammann E, Meier RL, Rutz E, Vavken P, Studer K. Recurrent patellar dislocations in adolescents result in decreased knee flexion during the entire gait cycle. Knee Surg Sports Traumatol Arthrosc. 2020 Jul;28(7):2053–66.

60. Sowiński T, Syczewska M, Kwiatkowski K, Kalinowska M. [Characteristic of the patients' gait with recurrent lateral patella dislocation]. Pol Merkur Lekarski. 2010 Jul;29(169):27–9.

61. Schranz C, Belohlavek T, Sperl M, Kraus T, Svehlik M. Does femoral anteversion and internally rotated gait correlate in subjects with patellofemoral instability? Clinical Biomechanics. 2021 Apr;84:105333.

62. Lucas KCH, Jacobs C, Lattermann C, Noehren B. Gait deviations and muscle strength deficits in subjects with patellar instability. The Knee. 2020 Aug;27(4):1285–90.

63. Clark DA, Simpson DL, Eldridge J, Colborne GR. Patellar instability and quadriceps avoidance affect walking knee moments. The Knee. 2016 Jan;23(1):78–84.

64. Schranz C, Sperl M, Kraus T, Guggenberger B, Kruse A, Habersack A, et al. Different gait pattern in adolescence with patellofemoral instability. Clinical Biomechanics. 2023 Aug;108:106067.

65. Senavongse W, Amis AA. The effects of articular, retinacular, or muscular deficiencies on patellofemoral joint stability: A BIOMECHANICAL STUDY *IN VITRO*. The Journal of Bone and Joint Surgery British volume. 2005 Apr;87-B(4):577–82.

66. Goh JC, Lee PY, Bose K. A cadaver study of the function of the oblique part of vastus medialis. J Bone Joint Surg Br. 1995 Mar;77(2):225–31.

67. Farahmand F, Tahmasbi MN, Amis AA. Lateral force–displacement behaviour of the human patella and its variation with knee flexion – a biomechanical study in vitro. Journal of Biomechanics. 1998 Dec;31(12):1147–52.

68. Sakai N, Luo ZP, Rand JA, An KN. The influence of weakness in the vastus medialis oblique muscle on the patellofemoral joint: an in vitro biomechanical study. Clinical Biomechanics. 2000 Jun;15(5):335–9.

69. Stokes, M., Young, A. Investigations of quadriceps inhibition: implications for clinical practice. Physiotherapy. 1984;70(11).

70. Atkin DM, Fithian DC, Marangi KS, Stone ML, Dobson BE, Mendelsohn C. Characteristics of Patients with Primary Acute Lateral Patellar Dislocation and Their Recovery within the First 6 Months of Injury. Am J Sports Med. 2000 Jul;28(4):472–9.

71. Stanitski CL. Articular Hypermobility and Chondral Injury in Patients With Acute Patellar Dislocation. Am J Sports Med. 1995 Mar;23(2):146–50.

72. Rünow A. The dislocating patella. Etiology and prognosis in relation to generalized joint laxity and anatomy of the patellar articulation. Acta Orthop Scand Suppl. 1983;201:1–53.

73. Buckens CFM, Saris DBF. Reconstruction of the Medial Patellofemoral Ligament for Treatment of Patellofemoral Instability: A Systematic Review. Am J Sports Med. 2010 Jan;38(1):181–8.

74. Desio SM, Burks RT, Bachus KN. Soft Tissue Restraints to Lateral Patellar Translation in the Human Knee. Am J Sports Med. 1998 Jan;26(1):59–65.

75. Avikainen VJ, Nikku RK, Seppänen-Lehmonen TK. Adductor magnus tenodesis for patellar dislocation. Technique and preliminary results. Clin Orthop Relat Res. 1993 Dec;(297):12–6.

76. Conlan T, Garth WP, Lemons JE. Evaluation of the medial soft-tissue restraints of the extensor mechanism of the knee.: The Journal of Bone & Joint Surgery. 1993 May;75(5):682–93.

77. Hautamaa PV, Fithian DC, Kaufman KR, Daniel DM, Pohlmeyer AM. Medial Soft Tissue Restraints in Lateral Patellar Instability and Repair: Clinical Orthopaedics and Related Research. 1998 Apr;349:174–82.

78. Arendt EA, Fithian DC, Cohen E. Current concepts of lateral patella dislocation. Clinics in Sports Medicine. 2002 Jul;21(3):499–519.

79. Larson RL, Cabaud HE, Slocum DB, James SL, Keenan T, Hutchinson T. The patellar compression syndrome: surgical treatment by lateral retinacular release. Clin Orthop Relat Res. 1978;(134):158–67.

80. Christoforakis J, Bull AMJ, Strachan RK, Shymkiw R, Senavongse W, Amis AA. Effects of lateral retinacular release on the lateral stability of the patella. Knee Surg Sports Traumatol Arthrosc. 2006 Mar;14(3):273–7.

81. Powers CM, Lilley JC, Lee TQ. The effects of axial and multi-plane loading of the extensor mechanism on the patellofemoral joint. Clinical Biomechanics. 1998 Dec;13(8):616–24.

82. Merican AM, Kondo E, Amis AA. The effect on patellofemoral joint stability of selective cutting of lateral retinacular and capsular structures. Journal of Biomechanics. 2009 Feb;42(3):291–6.

83. Dejour H, Walch G, Nove-Josserand L, Guier Ch. Factors of patellar instability: An anatomic radiographic study. Knee Surgery, Sports Traumatology, Arthroscopy. 1994 Mar;2(1):19–26.

84. Dejour D, Le Coultre B. Osteotomies in Patello-Femoral Instabilities. Sports Medicine and Arthroscopy Review. 2007 Mar;15(1):39–46.

85. Hing CB, Shepstone L, Marshall T, Donell ST. A Laterally Positioned Concave Trochlear Groove Prevents Patellar Dislocation. Clinical Orthopaedics & Related Research. 2006 Jun;447:187–94.

86. Panni AS, Cerciello S, Maffulli N, Di Cesare M, Servien E, Neyret P. Patellar shape can be a predisposing factor in patellar instability. Knee Surg Sports Traumatol Arthrosc. 2011 Apr;19(4):663–70.

87. Jimenez AE, Levy BJ, Grimm NL, Andelman SM, Cheng C, Hedgecock JP, et al. Relationship Between Patellar Morphology and Known Anatomic Risk Factors for Patellofemoral Instability. Orthopaedic Journal of Sports Medicine. 2021 Mar 1;9(3):232596712098869.

88. Servien E, Ait Si Selmi T, Neyret P. [Study of the patellar apex in objective patellar dislocation]. Rev Chir Orthop Reparatrice Appar Mot. 2003 Nov;89(7):605–12.

89. Barnett AJ, Gardner ROE, Lankester BJA, Wakeley CJ, Eldridge JDJ. Magnetic resonance imaging of the patella: A COMPARISON OF THE MORPHOLOGY OF THE PATELLA IN NORMAL AND DYSPLASTIC KNEES. The Journal of Bone and Joint Surgery British volume. 2007 Jun;89-B(6):761–5.

90. Mizuno Y, Kumagai M, Mattessich SM, Elias JJ, Ramrattan N, Cosgarea AJ, et al. Q-angle influences tibiofemoral and patellofemoral kinematics. Journal Orthopaedic Research. 2001 Sep;19(5):834–40.

91. Simmons, E., Cameron, J. Patella Alta and Recurrent Dislocation of the Patella. Clinical Orthopaedics and Related Research. 1992 Jan;(274):265-9.

92. Miller TT, Staron RB, Feldman F. Patellar height on sagittal MR imaging of the knee. American Journal of Roentgenology. 1996 Aug;167(2):339–41.

93. Fithian D, Paxton E, Cohen A. Indications in the Treatment of Patellar Instability. J Knee Surg. 2010 Jan 27;17(01):47–56.

94. Ward SR, Powers CM. The influence of patella alta on patellofemoral joint stress during normal and fast walking. Clinical Biomechanics. 2004 Dec;19(10):1040–7.

95. McWalter EJ, Cibere J, MacIntyre NJ, Nicolaou S, Schulzer M, Wilson DR. Relationship Between Varus-Valgus Alignment and Patellar Kinematics in Individuals with Knee Osteoarthritis: The Journal of Bone and Joint Surgery-American Volume. 2007 Dec;89(12):2723–31.

96. Kaiser P, Schmoelz W, Schoettle P, Zwierzina M, Heinrichs C, Attal R. Increased internal femoral torsion can be regarded as a risk factor for patellar instability — A biomechanical study. Clinical Biomechanics. 2017 Aug;47:103–9.

97. Hefzy MS, Jackson WT, Saddemi SR, Hsieh YF. Effects of tibial rotations on patellar tracking and patello-femoral contact areas. Journal of Biomedical Engineering. 1992 Jul;14(4):329–43.

98. Kim HK, Shiraj S, Anton C, Horn PS. The patellofemoral joint: do age and gender affect skeletal maturation of the osseous morphology in children? Pediatr Radiol. 2014 Feb;44(2):141–8.

99. Kim HK, Shiraj S, Kang CH, Anton C, Kim DH, Horn PS. Patellofemoral Instability in Children: Correlation Between Risk Factors, Injury Patterns, and Severity of Cartilage Damage. American Journal of Roentgenology. 2016 Jun;206(6):1321–8.

100. Toms AP, Cahir J, Swift L, Donell ST. Imaging the femoral sulcus with ultrasound, CT, and MRI: reliability and generalizability in patients with patellar instability. Skeletal Radiol. 2009 Apr;38(4):329–38.

101. Stepanovich M, Bomar JD, Pennock AT. Are the Current Classifications and Radiographic Measurements for Trochlear Dysplasia Appropriate in the Skeletally Immature Patient? Orthopaedic Journal of Sports Medicine. 2016 Oct 1;4(10):232596711666949.

102. Wiberg G. Roentgenographs and Anatomic Studies on the Femoropatellar Joint: With Special Reference to Chondromalacia Patellae. Acta Orthopaedica Scandinavica. 1941 Jan;12(1–4):319–410.

103. Jibri Z, Jamieson P, Rakhra KS, Sampaio ML, Dervin G. Patellar maltracking: an update on the diagnosis and treatment strategies. Insights Imaging. 2019 Dec;10(1):65.

104. Charles MD, Haloman S, Chen L, Ward SR, Fithian D, Afra R. Magnetic Resonance Imaging–Based Topographical Differences Between Control and Recurrent Patellofemoral Instability Patients. Am J Sports Med. 2013 Feb;41(2):374–84.

105. Laurin CA, Lévesque HP, Dussault R, Labelle H, Peides JP. The abnormal lateral patellofemoral angle: a diagnostic roentgenographic sign of recurrent patellar subluxation. J Bone Joint Surg Am. 1978 Jan;60(1):55–60.

106. Urch SE, Tritle BA, Donald Shelbourne K, Gray T. Axial Linear Patellar Displacement: A New Measurement of Patellofemoral Congruence. Am J Sports Med. 2009 May;37(5):970–3.

107. Paul RW, Brutico JM, Wright ML, Erickson BJ, Tjoumakaris FP, Freedman KB, et al. Strong Agreement Between Magnetic Resonance Imaging and Radiographs for Caton–Deschamps Index in Patients With Patellofemoral Instability. Arthroscopy, Sports Medicine, and Rehabilitation. 2021 Dec;3(6):e1621–8.

108. Caton J. [Method of measuring the height of the patella]. Acta Orthop Belg. 1989;55(3):385–6.

109. Caton J, Deschamps G, Chambat P, Lerat JL, Dejour H. [Patella infera. Apropos of 128 cases]. Rev Chir Orthop Reparatrice Appar Mot. 1982;68(5):317–25.

110. Schneider B, Laubenberger J, Jemlich S, Groene K, Weber HM, Langer M. Measurement of femoral antetorsion and tibial torsion by magnetic resonance imaging. BJR. 1997 Jun;70(834):575–9.

111. Guenther KP, Tomczak R, Kessler S, Pfeiffer T, Puhl W. Measurement of femoral anteversion by magnetic resonance imaging — evaluation of a new technique in children and adolescents. European Journal of Radiology. 1995 Nov;21(1):47–52.

112. Rosskopf AB, Buck FM, Pfirrmann CWA, Ramseier LE. Femoral and tibial torsion measurements in children and adolescents: comparison of MRI and 3D models based on low-dose biplanar radiographs. Skeletal Radiol. 2017 Apr;46(4):469–76.

113. Scorcelletti M, Reeves ND, Rittweger J, Ireland A. Femoral anteversion: significance and measurement. Journal of Anatomy. 2020 Nov;237(5):811–26.

114. Snow M. Tibial Torsion and Patellofemoral Pain and Instability in the Adult Population: Current Concept Review. Curr Rev Musculoskelet Med. 2021 Jan 8;14(1):67–75.

115. Regalado G, Lintula H, Kokki H, Kröger H, Väätäinen U, Eskelinen M. Six-year outcome after non-surgical versus surgical treatment of acute primary patellar dislocation in adolescents: a prospective randomized trial. Knee Surg Sports Traumatol Arthrosc. 2016 Jan;24(1):6–11.

116. Sillanpää PJ, Mattila VM, Mäenpää H, Kiuru M, Visuri T, Pihlajamäki H. Treatment with and without Initial Stabilizing Surgery for Primary Traumatic Patellar Dislocation: A Prospective Randomized Study. The Journal of Bone and Joint Surgery-American Volume. 2009 Feb;91(2):263–73.

117. Nikku R, Nietosvaara Y, Aalto K, Kallio PE. Operative treatment of primary patellar dislocation does not improve medium-term outcome: A 7-year follow-up report and risk analysis of 127 randomized patients. Acta Orthopaedica. 2005 Jan;76(5):699–704.

118. Mehta VM, Inoue M, Nomura E, Fithian DC. An Algorithm Guiding the Evaluation and Treatment of Acute Primary Patellar Dislocations. Sports Medicine and Arthroscopy Review. 2007 Jun;15(2):78–81.

119. Beasley LS, Vidal AF. Traumatic patellar dislocation in children and adolescents: treatment update and literature review: Current Opinion in Pediatrics. 2004 Feb;16(1):29–36.

120. Mäenpää H, Huhtala H, Lento MUK. Recurrence after patellar dislocation Redislocation in 37/75 patients followed for 6-24 years. Acta Orthopaedica Scandinavica. 1997 Jan;68(5):424–6.

121. Rivera JE. Open versus Closed Kinetic Chain Rehabilitation of the Lower Extremity: A Functional and Biomechanical Analysis. Journal of Sport Rehabilitation. 1994 May;3(2):154–67.

122. Stensdotter AK, Hodges PW, Mellor R, Sundelin G, H??Ger-Ross C. Quadriceps Activation in Closed and in Open Kinetic Chain Exercise: Medicine & Science in Sports & Exercise. 2003 Dec;35(12):2043–7.

123. Rehn B, Lidström J, Skoglund J, Lindström B. Effects on leg muscular performance from whole-body vibration exercise: a systematic review. Scandinavian Med Sci Sports. 2007 Feb;17(1):2–11.

124. Hinton RY, Sharma KM. Acute and recurrent patellar instability in the young athlete. Orthopedic Clinics of North America. 2003 Jul;34(3):385–96.

125. Nonweiler DE, DeLee JC. The Diagnosis and Treatment of Medial Subluxation of the Patella After Lateral Retinacular Release. Am J Sports Med. 1994 Sep;22(5):680–6.

126. Kolowich PA, Paulos LE, Rosenberg TD, Farnsworth S. Lateral release of the patella: Indications and contraindications. Am J Sports Med. 1990 Jul;18(4):359–65.

127. Stephen JM, Lumpaopong P, Dodds AL, Williams A, Amis AA. The Effect of Tibial Tuberosity Medialization and Lateralization on Patellofemoral Joint Kinematics, Contact Mechanics, and Stability. Am J Sports Med. 2015 Jan;43(1):186–94.

128. Elias JJ, Smith BW, Daney BT. Biomechanical Analysis of Tibial Tuberosity Medialization and Medial Patellofemoral Ligament Reconstruction. Sports Medicine and Arthroscopy Review. 2017 Jun;25(2):58–63.

129. Kraus T, Lidder S, Švehlík M, Rippel K, Schneider F, Eberl R, et al. Patella re-alignment in children with a modified Grammont technique: Outcome in 65 knees after mean 8 years. Acta Orthopaedica. 2012 Oct;83(5):504–10.

130. Magnussen RA, De Simone V, Lustig S, Neyret P, Flanigan DC. Treatment of patella alta in patients with episodic patellar dislocation: a systematic review. Knee Surg Sports Traumatol Arthrosc. 2014 Oct;22(10):2545–50.

131. Mayer C, Magnussen RA, Servien E, Demey G, Jacobi M, Neyret P, et al. Patellar Tendon Tenodesis in Association With Tibial Tubercle Distalization for the Treatment of Episodic Patellar Dislocation With Patella Alta. Am J Sports Med. 2012 Feb;40(2):346–51.

132. Barber FA, McGarry JE. Elmslie–Trillat Procedure for the Treatment of Recurrent Patellar Instability. Arthroscopy: The Journal of Arthroscopic & Related Surgery. 2008 Jan;24(1):77–81.

133. Weiker GT, Black KP. The anterior femoral osteotomy for patellofemoral instability. Am J Knee Surg. 1997;10(4):221–7.

134. Cameron JC, Saha S. External Tibial Torsion: An Underrecognized Cause of Recurrent Patellar Dislocation. Clinical Orthopaedics and Related Research. 1996 Jul;328:177–84.

135. Zhang Z, Cao Y, Song G, Li Y, Zheng T, Zhang H. Derotational Femoral Osteotomy for Treating Recurrent Patellar Dislocation in the Presence of Increased Femoral Anteversion: A Systematic Review. Orthopaedic Journal of Sports Medicine. 2021 Nov 1;9(11):232596712110571.

136. Nelitz M. Femoral Derotational Osteotomies. Curr Rev Musculoskelet Med. 2018 Jun;11(2):272–9.

137. Bruce WD, Stevens PM. Surgical Correction of Miserable Malalignment Syndrome: Journal of Pediatric Orthopaedics. 2004;392–6.

138. Seth A, Hicks JL, Uchida TK, Habib A, Dembia CL, Dunne JJ, et al. OpenSim: Simulating musculoskeletal dynamics and neuromuscular control to study human and animal movement. Schneidman D, editor. PLOS Computational Biology. 2018 Jul 26;14(7):e1006223.

139. Killen BA, Falisse A, De Groote F, Jonkers I. In Silico-Enhanced Treatment and Rehabilitation Planning for Patients with Musculoskeletal Disorders: Can Musculoskeletal Modelling and Dynamic Simulations Really Impact Current Clinical Practice? Applied Sciences. 2020 Oct 16;10(20):7255.

140. Bulat M, Korkmaz Can N, Arslan YZ, Herzog W. Musculoskeletal Simulation Tools for Understanding Mechanisms of Lower-Limb Sports Injuries: Current Sports Medicine Reports. 2019 Jun;18(6):210–6.

141. Koller W, Baca A, Kainz H. The gait pattern and not the femoral morphology is the main contributor to asymmetric hip joint loading. Fernandes R, editor. PLoS ONE. 2023 Sep 26;18(9):e0291789.

142. Arnold EM, Ward SR, Lieber RL, Delp SL. A Model of the Lower Limb for Analysis of Human Movement. Annals of Biomedical Engineering. 2010 Feb 3;38(2):269–79.

143. Rajagopal A, Dembia CL, DeMers MS, Delp DD, Hicks JL, Delp SL. Full-Body Musculoskeletal Model for Muscle-Driven Simulation of Human Gait. IEEE Trans Biomed Eng. 2016 Oct;63(10):2068–79.

144. Dembia CL, Bianco NA, Falisse A, Hicks JL, Delp SL. OpenSim Moco: Musculoskeletal optimal control. Campbell KS, editor. PLoS Comput Biol. 2020 Dec 28;16(12):e1008493.

145. Falisse A, Bar-On L, Desloovere K, Jonkers I, De Groote F. A spasticity model based on feedback from muscle force explains muscle activity during passive stretches and gait in children with cerebral palsy. Di Giminiani R, editor. PLoS ONE. 2018 Dec 7;13(12):e0208811.

146. Ezati M, Ghannadi B, McPhee J. A review of simulation methods for human movement dynamics with emphasis on gait. Multibody Syst Dyn. 2019 Nov;47(3):265–92.

147. Delp SL, Loan JP, Hoy MG, Zajac FE, Topp EL, Rosen JM. An interactive graphics-based model of the lower extremity to study orthopaedic surgical procedures. IEEE Trans Biomed Eng. 1990 Aug;37(8):757–67.

148. Uhlrich SD, Uchida TK, Lee MR, Delp SL. Ten steps to becoming a musculoskeletal simulation expert: A half-century of progress and outlook for the future. Journal of Biomechanics. 2023 Jun;154:111623.

149. Hicks J. OpenSim's Capabilities [Internet]. 2013. Available from: https://opensimconfluence.atlassian.net/wiki/spaces/OpenSim/pages/53087561/OpenSim+s+Capabilities

150. OpenSim [Internet]. [cited 2024 Nov 20]. Available from: https://simtk.org/projects/opensim#:~:text=OpenSim%20is%20a%20freely%20available%2C%20user%20extensible%20software,the%20work%20being%20performed%20using%20OpenSim%20at%20opensim.stanford.edu.

151. Lerner ZF, DeMers MS, Delp SL, Browning RC. How tibiofemoral alignment and contact locations affect predictions of medial and lateral tibiofemoral contact forces. Journal of Biomechanics. 2015 Feb;48(4):644–50.

152. Lenhart RL, Kaiser J, Smith CR, Thelen DG. Prediction and Validation of Load-Dependent Behavior of the Tibiofemoral and Patellofemoral Joints During Movement. Annals of Biomedical Engineering. 2015 Nov 28;43(11):2675–85.

153. Kainz H, Wesseling M, Jonkers I. Generic scaled versus subject-specific models for the calculation of musculoskeletal loading in cerebral palsy gait: Effect of personalized musculoskeletal geometry outweighs the effect of personalized neural control. Clinical Biomechanics. 2021 Jul;87:105402.

154. Kainz H, Koller W, Wallnöfer E, Bader TR, Mindler GT, Kranzl A. A framework based on subject-specific musculoskeletal models and Monte Carlo simulations to personalize muscle coordination retraining. Sci Rep. 2024 Feb 12;14(1):3567.

155. Veerkamp K, Kainz H, Killen BA, Jónasdóttir H, van der Krogt MM. Torsion Tool: An automated tool for personalising femoral and tibial geometries in OpenSim musculoskeletal models. Journal of Biomechanics. 2021 Aug;125:110589.

156. Modenese L, Barzan M, Carty CP. Dependency of lower limb joint reaction forces on femoral version. Gait & Posture. 2021 Jul;88:318–21.

157. Kainz H, Mindler GT, Kranzl A. Influence of femoral anteversion angle and neck-shaft angle on muscle forces and joint loading during walking. O'Sullivan R, editor. PLoS ONE. 2023 Oct 12;18(10):e0291458.

158. Zajac FE. Muscle and tendon: properties, models, scaling, and application to biomechanics and motor control. Crit Rev Biomed Eng. 1989;17(4):359–411.

159. Kaneda JM, Seagers KA, Uhlrich SD, Kolesar JA, Thomas KA, Delp SL. Can static optimization detect changes in peak medial knee contact forces induced by gait modifications? Journal of Biomechanics. 2023 May;152:111569.

160. Geier A, Tischer T, Bader R. Simulation of varying femoral attachment sites of medial patellofemoral ligament using a musculoskeletal multi-body model. Current Directions in Biomedical Engineering. 2015 Sep 1;1(1):547–51.

161. Herrmann S, Lenz R, Geier A, Lehner S, Souffrant R, Woernle C, et al. Muskuloskelettale Modellierung des patellofemoralen Gelenks. Der Orthopäde. 2012 Apr 5;41(4):252–9.

162. Bei Y, Fregly BJ. Multibody dynamic simulation of knee contact mechanics. Medical Engineering & Physics. 2004 Nov;26(9):777–89.

163. Guess TM, Liu H, Bhashyam S, Thiagarajan G. A multibody knee model with discrete cartilage prediction of tibio-femoral contact mechanics. Computer Methods in Biomechanics and Biomedical Engineering. 2013 Mar;16(3):256–70.

164. Thelen DG, Won Choi K, Schmitz AM. Co-Simulation of Neuromuscular Dynamics and Knee Mechanics During Human Walking. Journal of Biomechanical Engineering [Internet]. 2014 Feb 1;136(2). Available from: https://asmedigitalcollection.asme.org/biomechanical/article/doi/10.1115/1.4026358/442947/CoSimulation-of-Neuromuscular-Dynamics-and-Knee

165. Kainz H, Goudriaan M, Falisse A, Huenaerts C, Desloovere K, De Groote F, et al. The influence of maximum isometric muscle force scaling on estimated muscle forces from musculoskeletal models of children with cerebral palsy. Gait & Posture. 2018 Sep;65:213–20.

166. Van Der Krogt MM, Bar-On L, Kindt T, Desloovere K, Harlaar J. Neuro-musculoskeletal simulation of instrumented contracture and spasticity assessment in children with cerebral palsy. J NeuroEngineering Rehabil. 2016 Dec;13(1):64.

167. Steele KM, Van Der Krogt MM, Schwartz MH, Delp SL. How much muscle strength is required to walk in a crouch gait? Journal of Biomechanics. 2012 Oct;45(15):2564–9.

168. Koller W, Baca A, Kainz H. Impact of scaling errors of the thigh and shank segments on musculoskeletal simulation results. Gait & Posture. 2021 Jun;87:65–74.

169. Kainz H, Modenese L, Lloyd DG, Maine S, Walsh HPJ, Carty CP. Joint kinematic calculation based on clinical direct kinematic versus inverse kinematic gait models. Journal of Biomechanics. 2016 Jun;49(9):1658–69.

170. Jennifer Hicks. How Static Optimization Works [Internet]. OpenSim Documentation. 2018. Available from: https://opensimconfluence.atlassian.net/wiki/spaces/OpenSim/pages/53089619/How+Static+Optimization+Works

171. Sylvester AD, Lautzenheiser SG, Kramer PA. A review of musculoskeletal modelling of human locomotion. Interface Focus. 2021 Oct 6;11(5):20200060.

172. De Groote F, Falisse A. Perspective on musculoskeletal modelling and predictive simulations of human movement to assess the neuromechanics of gait. Proc R Soc B. 2021 Mar 10;288(1946):20202432.

173. Wallnöfer EK, Kaufmann P, Koller W, Kainz H. Influences of EMG-informed musculoskeletal simulation approaches on estimations of lower limb muscle and joint contact forces. Gait & Posture. 2023 Mar;100:7–8.

174. Hicks JL, Uchida TK, Seth A, Rajagopal A, Delp SL. Is My Model Good Enough? Best Practices for Verification and Validation of Musculoskeletal Models and Simulations of Movement. Journal of Biomechanical Engineering. 2015 Feb 1;137(2):020905.

175. Romanato M, Volpe D, Guiotto A, Spolaor F, Sartori M, Sawacha Z. Electromyography-informed modeling for estimating muscle activation and force alterations in Parkinson's disease. Computer Methods in Biomechanics and Biomedical Engineering. 2022 Jan 2;25(1):14–26.

176. Steele KM, DeMers MS, Schwartz MH, Delp SL. Compressive tibiofemoral force during crouch gait. Gait & Posture. 2012 Apr;35(4):556–60.

177. Sasaki K, Neptune RR. Individual muscle contributions to the axial knee joint contact force during normal walking. Journal of Biomechanics. 2010 Oct;43(14):2780–4.

178. Bergmann G. Charité Universitätsmedizin. 2008. Orthoload. Available from: https://orthoload.com/

179. Lin YC, Walter JP, Banks SA, Pandy MG, Fregly BJ. Simultaneous prediction of muscle and contact forces in the knee during gait. Journal of Biomechanics. 2010 Mar;43(5):945–52.

180. Anderson FC, Pandy MG. Static and dynamic optimization solutions for gait are practically equivalent. Journal of Biomechanics. 2001 Feb;34(2):153–61.

181. Veerkamp K, Schallig W, Harlaar J, Pizzolato C, Carty CP, Lloyd DG, et al. The effects of electromyography-assisted modelling in estimating musculotendon forces during gait in children with cerebral palsy. Journal of Biomechanics. 2019 Jul;92:45–53.

182. Smith CR, Lenhart R, Kaiser J, Vignos M, Thelen D. Influence of Ligament Properties on Tibiofemoral Mechanics in Walking. J Knee Surg. 2015 Sep 26;29(02):099–106.

183. Smith CR. Simulating the effects of Anterior Cruciate Ligament Injury and Treatment on Cartilage Loading during Walking. University of Wisconsin-Madison; 2017.

184. Smith CR, Vignos MF, Lenhart RL, Kaiser J, Thelen DG. The Influence of Component Alignment and Ligament Properties on Tibiofemoral Contact Forces in Total Knee Replacement. Journal of Biomechanical Engineering [Internet]. 2016 Feb 1;138(2). Available from: https://asmedigitalcollection.asme.org/biomechanical/article/doi/10.1115/1.4032464/371493/The-Influence-of-Component-Alignment-and-Ligament

185. Smith CR, Won Choi K, Negrut D, Thelen DG. Efficient computation of cartilage contact pressures within dynamic simulations of movement. Computer Methods in Biomechanics and Biomedical Engineering: Imaging & Visualization. 2016 Sep 3;6(5):491–8.

186. Elias JJ, Kilambi S, Goerke DR, Cosgarea AJ. Improving vastus medialis obliquus function reduces pressure applied to lateral patellofemoral cartilage. Journal Orthopaedic Research. 2009 May;27(5):578–83.

187. Van Haver A, De Roo K, De Beule M, Labey L, De Baets P, Dejour D, et al. The Effect of Trochlear Dysplasia on Patellofemoral Biomechanics: A Cadaveric Study With Simulated Trochlear Deformities. Am J Sports Med. 2015 Jun;43(6):1354–61.

188. Kuroda R, Kambic H, Valdevit A, Andrish JT. Articular Cartilage Contact Pressure after Tibial Tuberosity Transfer: A Cadaveric Study. Am J Sports Med. 2001 Jul;29(4):403–9.

189. Passmore E, Graham HK, Pandy MG, Sangeux M. Hip- and patellofemoral-joint loading during gait are increased in children with idiopathic torsional deformities. Gait & Posture. 2018 Jun;63:228–35.

190. Lorenz A, Müller O, Kohler P, Wünschel M, Wülker N, Leichtle UG. The influence of asymmetric quadriceps loading on patellar tracking — An in vitro study. The Knee. 2012 Dec;19(6):818–22.

191. Stephen J, Alva A, Lumpaopong P, Williams A, Amis AA. A cadaveric model to evaluate the effect of unloading the medial quadriceps on patellar tracking and patellofemoral joint pressure and stability. J EXP ORTOP. 2018 Dec;5(1):34.

192. Singerman R, Davy DT, Goldberg VM. Effects of patella alta and patella infera on patellofemoral contact forces. Journal of Biomechanics. 1994 Aug;27(8):1059–65.

193. Ostermeier S, Stukenborg-Colsman C, Hurschler C, Wirth CJ. In Vitro Investigation of the Effect of Medial Patellofemoral Ligament Reconstruction and Medial Tibial Tuberosity Transfer on Lateral Patellar Stability. Arthroscopy: The Journal of Arthroscopic & Related Surgery. 2006 Mar;22(3):308–19.

194. Worlicek M, Moser B, Maderbacher G, Zentner R, Zeman F, Grifka J, et al. The influence of varus and valgus deviation on patellar kinematics in healthy knees: An exploratory cadaver study. The Knee. 2017 Aug;24(4):711–7.

195. Kainz H, Mindler GT, Kranzl A. How do the femoral anteversion angle and neck-shaft angle influence muscle forces and joint loading during walking? [Internet]. In Review; 2022 Nov [cited 2023 Apr 20]. Available from: https://www.researchsquare.com/article/rs-2293229/v1

196. Stief F, Holder J, Böhm H, Meurer A. Dynamische Analyse der Gelenkbelastung bei Beinachsendeformitäten in der Frontalebene: Stellenwert der instrumentellen Ganganalyse. Orthopäde. 2021 Jul;50(7):528–37.

197. Koller W, Gonçalves B, Baca A, Kainz H. Intra- and inter-subject variability of femoral growth plate stresses in typically developing children and children with cerebral palsy. Front Bioeng Biotechnol. 2023 Feb 24;11:1140527.

198. Carvalho I, Pinto SM, Chagas DDV, Praxedes Dos Santos JL, De Sousa Oliveira T, Batista LA. Robotic Gait Training for Individuals With Cerebral Palsy: A Systematic Review and Meta-Analysis. Archives of Physical Medicine and Rehabilitation. 2017 Nov;98(11):2332–44.

199. Ross CF. Finite element analysis in vertebrate biomechanics. Anat Rec. 2005 Apr;283A(2):253–8.

200. Maas SA, Ellis BJ, Ateshian GA, Weiss JA. FEBio: Finite Elements for Biomechanics. Journal of Biomechanical Engineering. 2012 Jan 1;134(1):011005.

201. Herrera A. Applications of finite element simulation in orthopedic and trauma surgery. WJO. 2012;3(4):25.

202. Smith CR, Brandon SCE, Thelen DG. Can altered neuromuscular coordination restore soft tissue loading patterns in anterior cruciate ligament and menisci deficient knees during walking? Journal of Biomechanics. 2019 Jan;82:124–33.

203. Ramaniraka NA, Terrier A, Theumann N, Siegrist O. Effects of the posterior cruciate ligament reconstruction on the biomechanics of the knee joint: a finite element analysis. Clinical Biomechanics. 2005 May;20(4):434–42.

204. Ren S, Shi H, Liu Z, Zhang J, Li H, Huang H, et al. Finite Element Analysis and Experimental Validation of the Anterior Cruciate Ligament and Implications for the Injury Mechanism. Bioengineering. 2022 Oct 21;9(10):590.

205. Jafari A, Farahmand F, Meghdari A. The effects of trochlear groove geometry on patellofemoral joint stability-a computer model study. Proceedings of the Institution of Mechanical Engineers, Part H: Journal of Engineering in Medicine. 2008 Jan 1;222(1):75–88.

206. Kainz H, Carty CP, Modenese L, Boyd RN, Lloyd DG. Estimation of the hip joint centre in human motion analysis: A systematic review. Clinical Biomechanics. 2015 May;30(4):319–29.

207. Harrington ME, Zavatsky AB, Lawson SEM, Yuan Z, Theologis TN. Prediction of the hip joint centre in adults, children, and patients with cerebral palsy based on magnetic resonance imaging. Journal of Biomechanics. 2007 Jan;40(3):595–602.

208. Kainz H, Hoang HX, Stockton C, Boyd RR, Lloyd DG, Carty CP. Accuracy and Reliability of Marker-Based Approaches to Scale the Pelvis, Thigh, and Shank Segments in Musculoskeletal Models. Journal of Applied Biomechanics. 2017 Oct 1;33(5):354–60.

209. Wesseling M, Kainz H, Hoekstra T, Van Rossom S, Desloovere K, De Groote F, et al. Botulinum toxin injections minimally affect modelled muscle forces during gait in children with cerebral palsy. Gait & Posture. 2020 Oct;82:54–60.

210. Blankevoort L, Huiskes R. Ligament-Bone Interaction in a Three-Dimensional Model of the Knee. Journal of Biomechanical Engineering. 1991 Aug 1;113(3):263–9.

211. Caruntu DI, Hefzy MS. 3-D Anatomically Based Dynamic Modeling of the Human Knee to Include Tibio-Femoral and Patello-Femoral Joints. Journal of Biomechanical Engineering. 2004 Feb 1;126(1):44–53.

212. Segal NA, Anderson DD, Iyer KS, Baker J, Torner JC, Lynch JA, et al. Baseline articular contact stress levels predict incident symptomatic knee osteoarthritis development in the MOST cohort. Journal of Orthopaedic Research. 2009 Jun 16;27(12):1562–8.

213. Pataky TC. One-dimensional statistical parametric mapping in Python. Computer Methods in Biomechanics and Biomedical Engineering. 2012 Mar;15(3):295–301.

214. Shapiro SS, Wilk MB. An analysis of variance test for normality (complete samples). Biometrika. 1965 Dec 1;52(3–4):591–611.

215. Kim TK. T test as a parametric statistic. Korean J Anesthesiol. 2015;68(6):540.

216. Mann HB, Whitney DR. On a Test of Whether one of Two Random Variables is Stochastically Larger than the Other. The Annals of Mathematical Statistics. 1947;18,50–60.

217. Cohen J. Statistic power analysis in the behavioral sciences. New York, NY: Academic Press. 1969.

218. Armstrong RA. When to use the Bonferroni correction. Ophthalmic Physiol Opt. 2014 Sep;34(5):502–8.

219. Zhang Z, Zhang H, Song G, Zheng T, Ni Q, Feng H. Increased femoral anteversion is associated with inferior clinical outcomes after MPFL reconstruction and combined tibial tubercle osteotomy for the treatment of recurrent patellar instability. Knee Surg Sports Traumatol Arthrosc. 2020 Jul;28(7):2261–9.

220. Sedgwick P. Pearson's correlation coefficient. BMJ. 2012 Jul 4;345(jul04 1):e4483–e4483.

221. Rosner B, Glynn RJ, Lee MT. The Wilcoxon Signed Rank Test for Paired Comparisons of Clustered Data. Biometrics. 2006 Mar;62(1):185–92.

222. Flury A, Jud L, Hoch A, Camenzind RS, Fucentese SF. Linear influence of distal femur osteotomy on the Q-angle: one degree of varization alters the Q-angle by one degree. Knee Surg Sports Traumatol Arthrosc. 2021 Feb;29(2):540–5.

223. Williams DS, Martin AE. Gait modification when decreasing double support percentage. Journal of Biomechanics. 2019 Jul;92:76–83.

224. Shah H, Albanese E, Duggan C, Rudan I, Langa KM, Carrillo MC, et al. Research priorities to reduce the global burden of dementia by 2025. The Lancet Neurology. 2016 Nov;15(12):1285–94.

225. Brunner R, Dreher T, Romkes J, Frigo C. Effects of plantarflexion on pelvis and lower limb kinematics. Gait & Posture. 2008 Jul;28(1):150–6.

226. Imhoff FB, Cotic M, Dyrna FGE, Cote M, Diermeier T, Achtnich A, et al. Dynamic Q-angle is increased in patients with chronic patellofemoral instability and correlates positively with femoral torsion. Knee Surg Sports Traumatol Arthrosc. 2021 Apr;29(4):1224–31.

227. Diamond LE, Devaprakash D, Cornish B, Plinsinga ML, Hams A, Hall M, et al. Feasibility of personalised hip load modification using real-time biofeedback in hip osteoarthritis: A pilot study. Osteoarthritis and Cartilage Open. 2022 Mar;4(1):100230.

228. Nagano H, Tatsumi I, Sarashina E, Sparrow WA, Begg RK. Modelling knee flexion effects on joint power absorption and adduction moment. The Knee. 2015 Dec;22(6):490–3.

229. Watelain E, Dujardin F, Babier F, Dubois D, Allard P. Pelvic and lower limb compensatory actions of subjects in an early stage of hip osteoarthritis. Archives of Physical Medicine and Rehabilitation. 2001 Dec;82(12):1705–11.

230. Valente G, Taddei F, Jonkers I. Influence of weak hip abductor muscles on joint contact forces during normal walking: probabilistic modeling analysis. Journal of Biomechanics. 2013 Sep;46(13):2186–93.

231. Arrebola LS, Smith T, Silva FF, De Oliveira VGC, De Oliveira PR, Wun PYL, et al. Hip and Knee Weakness and Ankle Dorsiflexion Restriction in Individuals Following Lateral

Patellar Dislocation: A Case-Control Study. Clinical Journal of Sport Medicine. 2021 Nov;31(6):e385–91.

232. Ammann E, Meier RL, Rutz E, Studer K, Valderrabano V, Camathias C. Elevated hip adduction angles and abduction moments in the gait of adolescents with recurrent patellar dislocation. Arch Orthop Trauma Surg [Internet]. 2022 Nov 26 [cited 2022 Dec 29]; Available from: https://link.springer.com/10.1007/s00402-022-04703-y

233. Barton CJ, Levinger P, Menz HB, Webster KE. Kinematic gait characteristics associated with patellofemoral pain syndrome: A systematic review. Gait & Posture. 2009 Nov;30(4):405–16.

234. Shelburne KB, Torry MR, Pandy MG. Muscle, Ligament, and Joint-Contact Forces at the Knee during Walking. Medicine & Science in Sports & Exercise. 2005 Nov;37(11):1948–56.

235. Fithian DC, Nomura E, Arendt E. Anatomy of patellar dislocation. Operative Techniques in Sports Medicine. 2001 Jul;9(3):102–11.

236. Iacobescu G, Cirstoiu C, Cursaru A, Anghelescu D, Stanculescu D. Correlation between Patellar Tilt Angle, Femoral Anteversion and Tibial Tubercle Trochlear Groove Distance Measured by Computer Tomography in Patients with non-Traumatic Recurrent Patellar Dislocation. Maedica (Bucur). 2020 Jun;15(2):174–80.

237. Besier TF, Draper CE, Gold GE, Beaupré GS, Delp SL. Patellofemoral joint contact area increases with knee flexion and weight-bearing. J Orthop Res. 2005 Mar;23(2):345–50.

238. Mountney J, Senavongse W, Amis AA, Thomas NP. Tensile strength of the medial patellofemoral ligament before and after repair or reconstruction. J Bone Joint Surg Br. 2005 Jan;87(1):36–40.

239. Lee TQ, Yang BY, Sandusky MD, McMahon PJ. The effects of tibial rotation on the patellofemoral joint: assessment of the changes in in situ strain in the peripatellar retinaculum and the patellofemoral contact pressures and areas. J Rehabil Res Dev. 2001;38(5):463–9.

240. Radler C, Kranzl A, Manner HM, Höglinger M, Ganger R, Grill F. Torsional profile versus gait analysis: Consistency between the anatomic torsion and the resulting gait pattern in patients with rotational malalignment of the lower extremity. Gait & Posture. 2010 Jul;32(3):405–10.

241. Jud L, Hartmann M, Vlachopoulos L, Zimmermann SM, Ackermann J, Fucentese SF. Increased tibial tuberosity torsion has the greatest predictive value in patients with patellofemoral instability compared to other commonly assessed parameters. Knee surg sports traumatol arthrosc. 2024 May;32(5):1179–86.

242. Walton DM, Liu RW, Farrow LD, Thompson GH. Proximal tibial derotation osteotomy for torsion of the tibia: A review of 43 cases. Journal of Children's Orthopaedics. 2012 Mar;6(1):81–5.

243. Arnold AS, Delp SL. Rotational moment arms of the medial hamstrings and adductors vary with femoral geometry and limb position: implications for the treatment of internally rotated gait. Journal of Biomechanics. 2001 Apr;34(4):437–47.

244. Teitge RA. Osteotomy in the Treatment of Patellofemoral Instability: Techniques in Knee Surgery. 2006 Mar;5(1):2–18.

245. Franciozi CE, Ambra LF, Albertoni LJB, Debieux P, Rezende FC, Oliveira MAD, et al. Increased Femoral Anteversion Influence Over Surgically Treated Recurrent Patellar Instability Patients. Arthroscopy: The Journal of Arthroscopic & Related Surgery. 2017 Mar;33(3):633–40.

246. Feller JA, Amis AA, Andrish JT, Arendt EA, Erasmus PJ, Powers CM. Surgical Biomechanics of the Patellofemoral Joint. Arthroscopy: The Journal of Arthroscopic & Related Surgery. 2007 May;23(5):542–53.

247. Skouras AZ, Kanellopoulos AK, Stasi S, Triantafyllou A, Koulouvaris P, Papagiannis G, et al. Clinical Significance of the Static and Dynamic Q-angle. Cureus [Internet]. 2022 May 11 [cited 2024 Oct 18]. Available from: https://www.cureus.com/articles/76097-clinical-significance-of-the-static-and-dynamic-q-angle

248. Alexander N, Brunner R, Cip J, Viehweger E, De Pieri E. Increased Femoral Anteversion Does Not Lead to Increased Joint Forces During Gait in a Cohort of Adolescent Patients. Front Bioeng Biotechnol. 2022 Jun 6;10:914990.

249. Alexander N, Cip J, Brunner RG, De Pieri E. Effect of femoral derotational osteotomy in patients with idiopathic increased femoral anteversion on joint loading and muscular demands. Journal of Children's Orthopaedics. 2024 Aug 11;18632521241269339.

250. Lavikainen J, Stenroth L, Alkjær T, Karjalainen PA, Korhonen RK, Mononen ME. Prediction of Knee Joint Compartmental Loading Maxima Utilizing Simple Subject Characteristics and Neural Networks. Ann Biomed Eng. 2023 Nov;51(11):2479–89.

251. Tsaopoulos DE, Baltzopoulos V, Maganaris CN. Human patellar tendon moment arm length: Measurement considerations and clinical implications for joint loading assessment. Clinical Biomechanics. 2006 Aug;21(7):657–67.

252. Arnold AS, Komallu AV, Delp SL. Internal rotation gait: a compensatory mechanism to restore abduction capacity decreased by bone deformity? Developmental Medicine & Child Neurology. 2008 Sep 26;39(1):40–4.

253. Pirker W, Katzenschlager R. Gait disorders in adults and the elderly: A clinical guide. Wien Klin Wochenschr. 2017 Feb;129(3–4):81–95.

254. Tomasi M, Artoni A, Mattei L, Di Puccio F. On the estimation of hip joint loads through musculoskeletal modeling. Biomech Model Mechanobiol. 2023 Apr;22(2):379–400.

255. Roelker SA, Caruthers EJ, Baker RK, Pelz NC, Chaudhari AMW, Siston RA. Interpreting Musculoskeletal Models and Dynamic Simulations: Causes and Effects of Differences Between Models. Ann Biomed Eng. 2017 Nov;45(11):2635–47.

256. Curreli C, Di Puccio F, Davico G, Modenese L, Viceconti M. Using Musculoskeletal Models to Estimate in vivo Total Knee Replacement Kinematics and Loads: Effect of Differences Between Models. Front Bioeng Biotechnol. 2021 Jul 28;9:703508.

257. Wesseling M, Derikx LC, De Groote F, Bartels W, Meyer C, Verdonschot N, et al. Muscle optimization techniques impact the magnitude of calculated hip joint contact forces. Journal Orthopaedic Research. 2015 Mar;33(3):430–8.

258. Scheys L, Van Campenhout A, Spaepen A, Suetens P, Jonkers I. Personalized MR-based musculoskeletal models compared to rescaled generic models in the presence of increased femoral anteversion: Effect on hip moment arm lengths. Gait & Posture. 2008 Oct;28(3):358–65.

259. Giri S, Tewari RP, Salhi A, Lempereur M, Borotikar B. A Musculoskeletal Model Customized for Sagittal and Frontal Knee Kinematics With Improved Knee Joint Stability. Journal of Biomechanical Engineering. 2022 Jul 1;144(7):071010.

260. Kainz H, Schwartz MH. The importance of a consistent workflow to estimate muscle-tendon lengths based on joint angles from the conventional gait model. Gait & Posture. 2021 Jul;88:1–9.

261. Krähenbühl N, Horn-Lang T, Hintermann B, Knupp M. The subtalar joint: A complex mechanism. EFORT Open Reviews. 2017 Jul;2(7):309–16.

262. Killen BA, Willems M, Jonkers I. An open-source framework for the generation of OpenSim models with personalised knee joint geometries for the estimation of articular contact mechanics. Journal of Biomechanics. 2024 Dec;177:112387.

263. Mosconi D, Bó APL, Siqueira AAG. Predictive Simulations with OpenSim Moco to Investigate the Interaction Between Human and Assistive Exoskeleton. In: 2023 45th Annual International Conference of the IEEE Engineering in Medicine & Biology Society (EMBC) [Internet]. Sydney, Australia: IEEE; 2023 [cited 2025 Jan 29]. p. 1–4. Available from: https://ieeexplore.ieee.org/document/10340617/

264. Morrison T, Su HJ. Gait Prediction for Prosthesis Design Evaluation. In: Volume 7: 46th Mechanisms and Robotics Conference (MR) [Internet]. St. Louis, Missouri, USA: American Society of Mechanical Engineers; 2022 [cited 2025 Jan 29]. p. V007T07A031. Available from: https://asmedigitalcollection.asme.org/IDETC-CIE/proceedings/IDETC-CIE2022/86281/V007T07A031/1150630

265. Veeger DHEJ. 'What if': the use of biomechanical models for understanding and treating upper extremity musculoskeletal disorders. Man Ther. 2011 Feb;16(1):48–50.

266. Pitto L, Kainz H, Falisse A, Wesseling M, Van Rossom S, Hoang H, et al. SimCP: A Simulation Platform to Predict Gait Performance Following Orthopedic Intervention in Children With Cerebral Palsy. Frontiers in Neurorobotics [Internet]. 2019 Jul 17;13. Available from: https://www.frontiersin.org/article/10.3389/fnbot.2019.00054/full

6 Appendix

6.1 Supplementary material 1 – Muscle force scatterplots

Scatterplots between lower limb torsions and changes in muscle forces in loading response. The black line represents a least square fitted line. BW = body weight, Max = maximum, RMS = Root Mean Square. This figure was created by the author of this thesis.

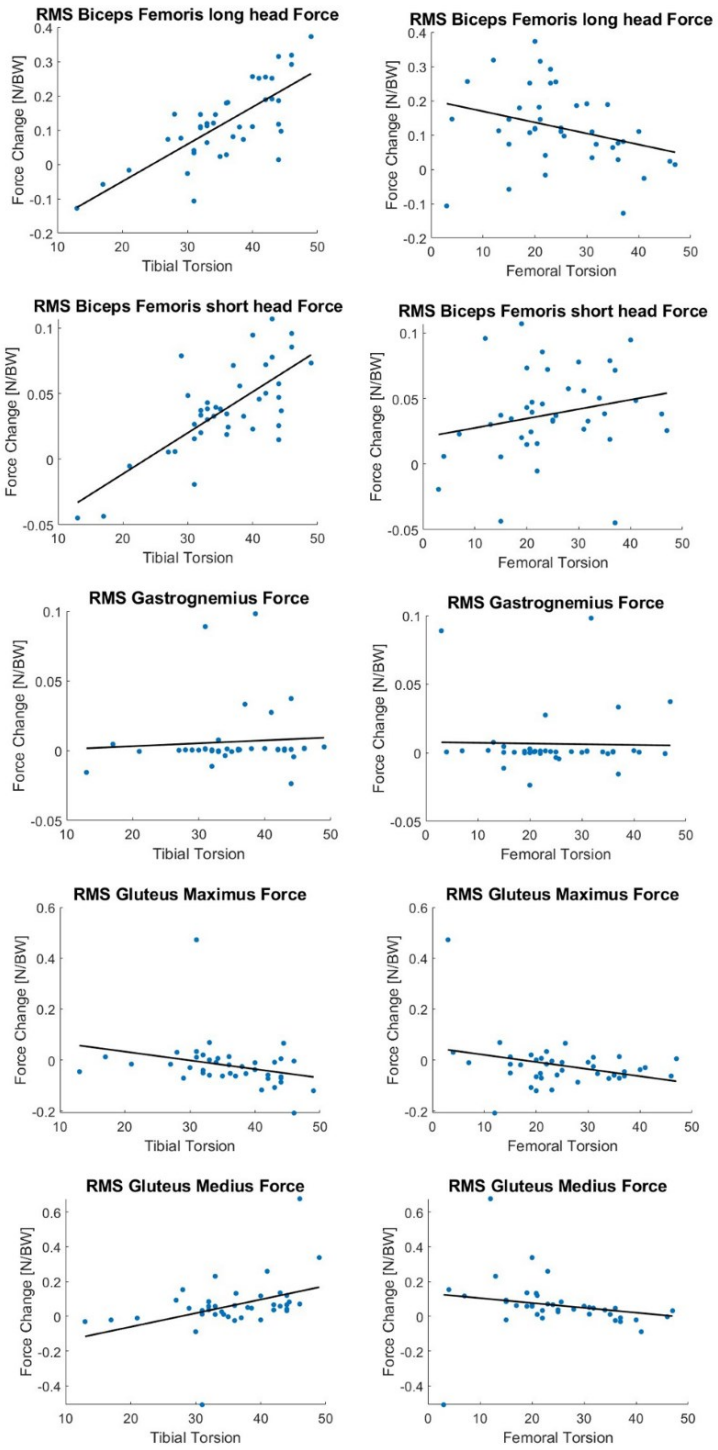

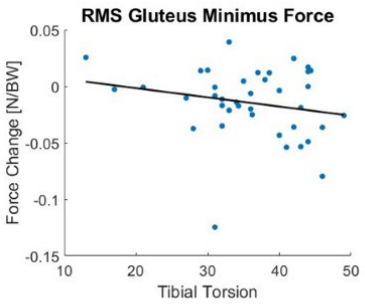
RMS Gluteus Minimus Force
Force Change [N/BW]
Tibial Torsion

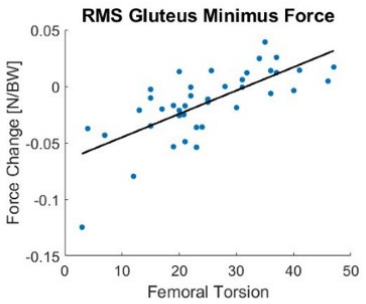
RMS Gluteus Minimus Force
Force Change [N/BW]
Femoral Torsion

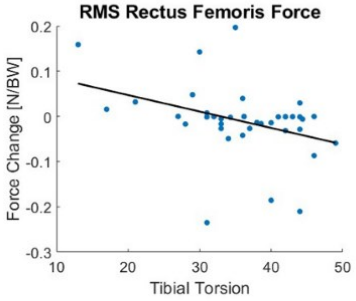
RMS Rectus Femoris Force
Force Change [N/BW]
Tibial Torsion

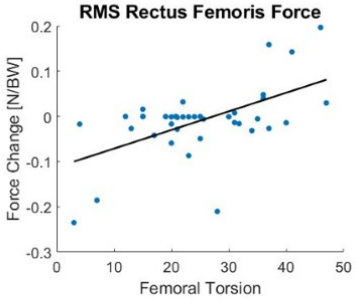
RMS Rectus Femoris Force
Force Change [N/BW]
Femoral Torsion

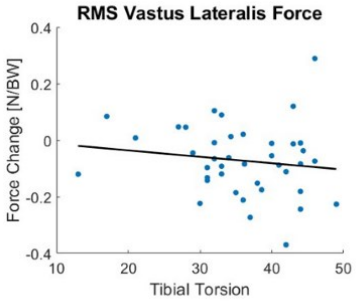
RMS Vastus Lateralis Force
Force Change [N/BW]
Tibial Torsion

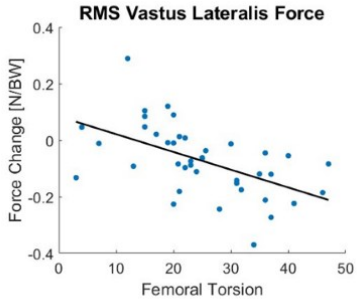
RMS Vastus Lateralis Force
Force Change [N/BW]
Femoral Torsion

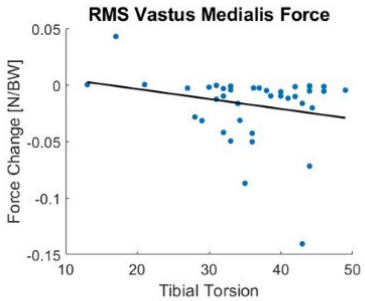
RMS Vastus Medialis Force
Force Change [N/BW]
Tibial Torsion

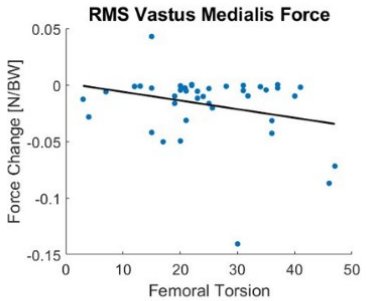
RMS Vastus Medialis Force
Force Change [N/BW]
Femoral Torsion

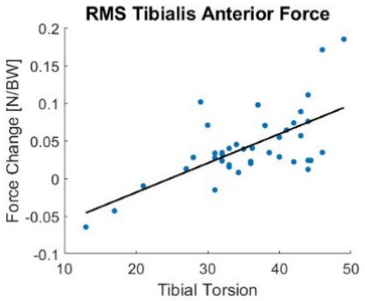
RMS Tibialis Anterior Force
Force Change [N/BW]
Tibial Torsion

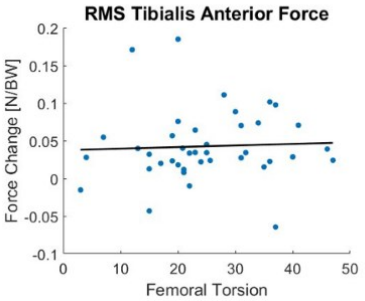
RMS Tibialis Anterior Force
Force Change [N/BW]
Femoral Torsion